

**CHARACTERIZATION AND PESTICIDES
ADSORPTION OF BENTONITE AND
MODIFIED BENTONITE**



**A Thesis Submitted in Partial Fulfillment of the Requirements for the
Degree of Doctor of Philosophy in Chemistry
Suranaree University of Technology
Academic Year 2018**

การวิเคราะห์คุณลักษณะและการดูชั้นสารกำจัดศัตรูพืชของเบนโทไนด์และ
เบนโทไนด์ดัดแปร



นางชุตติมา เป็ลื่องกลาง

วิทยานิพนธ์นี้เป็นส่วนหนึ่งของการศึกษาตามหลักสูตรปริญญาวิทยาศาสตรดุษฎีบัณฑิต

สาขาวิชาเคมี

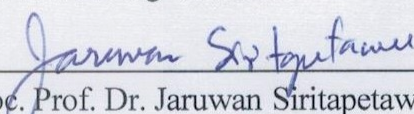
มหาวิทยาลัยเทคโนโลยีสุรนารี

ปีการศึกษา 2561

**CHARACTERIZATION AND PESTICIDES ADSORPTION OF
BENTONITE AND MODIFIED BENTONITE**

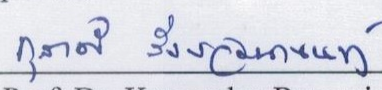
Suranaree University of Technology has approved this thesis submitted in partial fulfillment of the requirements for the Degree of Doctor of Philosophy.

Thesis Examining Committee



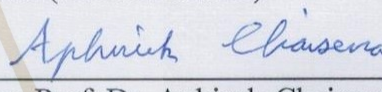
(Assoc. Prof. Dr. Jaruwan Siritapetawee)

Chairperson



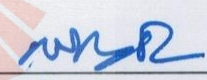
(Asst. Prof. Dr. Kunwadee Rangriwatananon)

Member (Thesis Advisor)



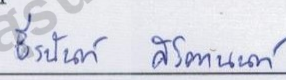
(Assoc. Prof. Dr. Aphiruk Chaisena)

Member



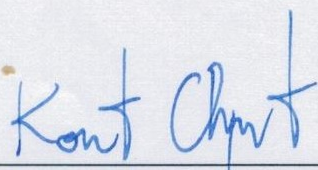
(Assoc. Prof. Dr. Sanchai Prayoonpokarach)

Member



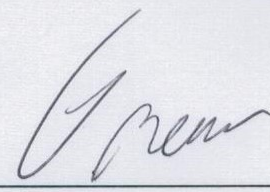
(Asst. Prof. Dr. Theeranun Siritanon)

Member



(Assoc. Prof. Flt. Lt. Dr. Kontorn Chamniprasart)

Vice Rector for Academic Affairs
and Internationalization



(Assoc. Prof. Dr. Worawat Meevasana)

Dean of Institute of Science

ชุตติมา เปลื้องกลาง : การวิเคราะห์คุณลักษณะและการดูดซับสารกำจัดศัตรูพืชของ
เบนโทไนท์และเบนโทไนท์ดัดแปร (CHARACTERIZATION AND PESTICIDES
ADSORPTION OF BENTONITE AND MODIFIED BENTONITE)

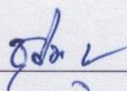
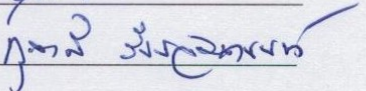
อาจารย์ที่ปรึกษา : ผู้ช่วยศาสตราจารย์ ดร.กฤษดี รังษีวัฒนานนท์, 165 หน้า.

งานวิจัยนี้ได้ทำการดัดแปรเบนโทไนท์ด้วย กรด ความร้อน สารลดแรงตึงผิว และ อัลคาไลน์ เพื่อช่วยเพิ่มความสามารถในการดูดซับสารกำจัดศัตรูพืช ดังนั้นงานนี้จึงมุ่งเน้นไปที่การเตรียมเบนโทไนท์ที่ดัดแปรด้วยกรดร่วมกับความร้อน ออร์กาโน-เบนโทไนท์ (HDTMA และ SDS) และ อัลคาไลน์-เบนโทไนท์ เพื่อกำจัด อะทราซีน ไดยูรอน 2,4-D และ พาราควอต จากสารละลายในน้ำ เบนโทไนท์ดัดแปรด้วยการร่วมกันของกรดและความร้อนซึ่งเริ่มต้นด้วยการเผาที่ 500 องศาเซลเซียส ตามด้วยกรดไฮโดรคลอริก ความเข้มข้น 0.5 โมลาร์ ($BC_{500}A_{0.5}$) ให้ประสิทธิภาพสูงในการกำจัดอะทราซีน ในขณะที่เบนโทไนท์และ ออร์กาโน-เบนโทไนท์ (HDTMA-เบนโทไนท์ และ SDS-เบนโทไนท์) สามารถดูดซับสารกำจัดศัตรูพืชที่ศึกษาจากสารละลายในน้ำได้ แต่ HDTMA-เบนโทไนท์ มีความเป็นไฮโดรโฟบิกมากกว่าเบนโทไนท์ซึ่งทำให้มีประสิทธิภาพที่สูงขึ้นสำหรับการดูดซับ ไดยูรอน 2,4-D และอะทราซีน สำหรับอัลคาไลน์ - เบนโทไนท์ สามารถเตรียมด้วยสารละลายโซเดียมไฮดรอกไซด์ ความเข้มข้น 0.25 และ 0.5 โมลาร์ ณ เวลาในการกระตุ้นต่าง ๆ เบนโทไนท์ดัดแปรที่ความเข้มข้น 0.5 โมลาร์ เป็นเวลา 3 ชั่วโมงเหมาะสมที่สุดสำหรับการกำจัดพาราควอตออกจากสารละลายในน้ำนอกจากนี้ความสามารถในการดูดซับยังขึ้นอยู่กับค่า pH ความเข้มข้นเริ่มต้นของสารกำจัดศัตรูพืช และอุณหภูมิ ความสัมพันธ์ระหว่างคุณสมบัติทางกายภาพเช่น ระยะห่างระหว่างชั้น พื้นที่ผิว BET ขนาดอนุภาค ประจุลบพื้นผิว และอัตราส่วน SiO_2 / Al_2O_3 ของเบนโทไนท์ กับการดูดซับของเบนโทไนท์และเบนโทไนท์ดัดแปรเป็นสิ่งที่สังเกตได้ สำหรับการดูดซับสารกำจัดศัตรูพืชที่อยู่รวมกันในสารละลายในน้ำ พบว่า $BC_{500}A_{0.5}$ และ HDTMA-เบนโทไนท์ ที่ความเข้มข้น 60 มิลลิโมลาร์ HDTMA เป็นตัวดูดซับที่เหมาะสมที่สุดดังนั้นจึงสามารถใช้เป็นตัวดูดซับแบบมัลติฟังก์ชันได้

สาขาวิชาเคมี
ปีการศึกษา 2561

ลายมือชื่อนักศึกษา

ลายมือชื่ออาจารย์ที่ปรึกษา

CHUTIMA PLUANGKLANG : CHARACTERIZATION AND PESTICIDES
ADSORPTION OF BENTONITE AND MODIFIED BENTONITE. THESIS
ADVISOR : ASST. PROF. KUNWADEE RANGSRIWATANANON,
Ph.D. 165 PP.

BENTONITE / COMBINATION ACID AND HEAT / SURFACTANT / ALKALI /
ADSORPTION / PESTICIDES

Modification of bentonite with acid, heat, surfactant and alkali for pesticides adsorption were carried out in this research. The modification provides the adsorbents with enhancement of capability to adsorb pesticides. Therefore, this work focused on preparations of combined heat and acid treated bentonite, organo-bentonite (HDTMA and SDS) and alkali-bentonite for the removal of atrazine, diuron, 2,4-D and paraquat from aqueous solutions. The bentonite modified with combination of acid and heat, firstly calcined at 500 °C following with 0.5 M HCl, (BC₅₀₀A_{0.5}) provides a high efficiency for removal of atrazine. While, bentonite and organo-bentonite (HDTMA-bentonite and SDS-bentonite) are able to uptake the studied pesticides from aqueous solutions but HDTMA-bentonite is more hydrophobic than bentonite leads to a higher efficiency for adsorption of diuron, 2,4-D and atrazine. The alkali-bentonites were prepared with 0.25 M and 0.5 M NaOH at various activation times. Bentonite modified with 0.5 M for 3 hours is most suitable for removal of paraquat from aqueous solutions. Moreover, the adsorption capacities depend on pH, initial concentration of pesticides and temperature. The relations between the physical properties, such as interlayer spacing, BET surface area, particle size, surface negative

charge and $\text{SiO}_2/\text{Al}_2\text{O}_3$ ratio, and the adsorption capacities of the bentonite and modified bentonite are noticed. For simultaneous adsorption of various pesticides, it was found that samples of $\text{BC}_{500}\text{A}_{0.5}$ bentonite modified and organo-bentonite modified with 60 mM HDTMA are the most suitable adsorbent, consequently, they could be used as multifunctional adsorbent.



School of Chemistry

Academic Year 2018

Student's Signature _____

Advisor's Signature _____

ACKNOWLEDGEMENTS

Firstly, I would like to express my sincere gratitude and deepest appreciate to my advisor, Assistant Professor Dr. Kunwadee Rangriwatananon who has given me much knowledge, valuable guidance, and encouragement throughout my graduate study. She showed me different ways to approach a research problem and the need to be persistent to accomplish any goal. My appreciation also goes to my committee members, Assistant Professor Dr. Aphiruk Chaisena, Assistant Professor Dr. Sanchai Prayoonpokarach, Assistant Professor Dr. Theeranun Siritanon and Associate Professor Dr. Jaruwan Siritapetawee for their time and useful suggestion. I would also like to thank all lectures at the School of Chemistry, Suranaree University of Technology for their good attitude and advice.

I would like to thank the staff of the scientific equipment center F2, F10 and F11, Suranaree University of Technology for providing all equipment and glassware. I would also like to thank all of my good friends in the Kunwadee group the School of Chemistry, Suranaree University of Technology for their friendship and all the help, they have provided.

My grateful appreciate is expressed to the Government Officers Development Scholarship, funded by National Science and Technology Agency

(NSTDA), for financial support. I also wish to acknowledge the Nakhon Ratchasima Rajabhat University.

Finally, I would to express my endless gratitude to my dearest family including my father, my mother, my husband and my babies for their infinite love, understanding, encouragement and care throughout my life. I would like to honour to adore Buddha for my life guide though anywhere and time.

Chutima Pluangklang



CONTENTS

	Page
ABSTRACT IN THAI.....	I
ABSTRACT IN ENGLISH.....	II
ACKNOWLEDGEMENTS.....	IV
CONTENTS.....	VI
LIST OF TABLES.....	XII
LIST OF FIGURES.....	XV
LIST OF ABBREVIATIONS.....	XX
CHAPTER	
I INTRODUCTION.....	1
1.1 Significance of study	1
1.2 Research objectives	6
1.3 Scope and limitations of the study.....	7
1.4 Expected results.....	8
1.5 References.....	8
II LITERATRRRE REVIEW	13
2.1 Clay and modified clay	14
2.1.1 Adsorption using acid modified clay.....	16
2.1.2 Adsorption using alkaline modified clay.....	18
2.1.3 Adsorption using heat modified clay	21

CONTENTS (Continued)

	Page
2.1.4 Adsorption using organo-clay	22
2.2 Adsorption of four pesticides by using clay and modified clay	26
2.2.1 Adsorption of atrazine by modified clay	26
2.2.2 Adsorption of paraquat by modified clay	28
2.2.3 Adsorption of diuron by modified clay	31
2.2.4 Adsorption of 2,4-D by modified clay.....	32
2.3 Adsorption.....	33
2.4 References	36
III FACILE METHOD TO ENHANCE PESTICIDES ADSORPTION BY TREATED BENTONITE WITH HEAT AND ACID AS MULTIFUNCTIONAL ADSORBENTS.....	42
3.1 Abstract	42
3.2 Introduction.....	43
3.3 Material and Methods	46
3.2.1 Materials	46
3.2.2 Preparation of Modified Bentonite	46
3.2.3 Characterization.....	47
3.2.4 Batch Adsorption.....	49
3.2.5 Effect of pH	50
3.2.6 Simultaneous adsorption of various pesticides in solutions	50

CONTENTS (Continued)

	Page
3.2.7 Adsorption Isotherm	51
3.2.8 Kinetic Adsorption Study	51
3.4 Results and Discussion	52
3.4.1 Characterization of Bentonite and Modified Bentonite.....	52
3.4.1.1 XRF and CEC analysis.....	52
3.4.1.2 XRD analysis.....	53
3.4.1.3 Thermogravimetric analysis	56
3.4.1.4 FT-IR analysis	58
3.4.1.5 Temperature-programmed desorption of ammonium (NH ₃ -TPD) study.....	61
3.4.1.6 NMR analysis	62
3.4.1.7 Textural properties study.....	63
3.4.1.8 Particle size analysis.....	66
3.4.2 The Effect of pH.....	69
3.4.3 Simultaneous adsorption of various pesticides in solution.....	74
3.4.4 Adsorption Isotherms.....	76
3.4.5 Kinetic Experiments	92
3.5 Conclusion	97
3.6 References	98

CONTENTS (Continued)

	Page
IV EFFECT OF SURFACTANT MODIFIED BENTONITE ON PESTICIDE ADSORPTION	104
4.1 Abstract	104
4.2 Introduction	105
4.3 Experiment	106
4.3.1 Materials	106
4.3.2 Modification of bentonite	106
4.3.2.1 Preparation of organo-bentonite	106
4.3.2.2 Characterization.....	107
4.3.3 Batch adsorption	107
4.3.3.1 Kinetic adsorption	107
4.3.3.2 Effect of surfactant loading	107
4.3.3.3 Optimum contact time and equilibrium time.....	109
4.3.3.4 Effect of pH	109
4.3.4 Adsorption isotherm	109
4.3.5 Simultaneous adsorption of various pesticides in solution.	110

CONTENTS (Continued)

	Page
4.4 Results and discussion	111
4.4.1 Characterization of bentonite and modified bentonite.....	111
4.4.1.1 XRD analysis.....	111
4.4.1.2 FTIR analysis.....	115
4.4.1.3 Thermal analysis of bentonite and modified bentonite ..	119
4.4.1.4 Particle size analysis.....	124
4.4.2 Effect of surfactant loading level on adsorption of pesticides	129
4.4.3 The Effect of pH on adsorption of pesticides	133
4.4.4 Simultaneous adsorption of various pesticides in solution	136
4.4.5 Kinetic Experiments	137
4.5 Conclusions	143
4.6 Reference	144
V THE INFLUENCE OF ALKALI ACTIVATION ON BENTONITE AND MODIFIED BENTONITE FOR ADSORPTION OF PESTICIDES	146
5.1 Abstract	146
5.2 Introduction	147
5.3 Material and Methods	148
5.3.1 Materials	148
5.3.2 Preparation of Modified Bentonite	148

CONTENTS (Continued)

	Page
5.3.3 Characterization.....	148
5.3.4 Batch Adsorption	149
5.4 Results and Discussion	150
5.4.1 Characterization of Bentonite and Modified Bentonite.....	150
5.4.1.1 Chemical composition.....	150
5.4.1.2 XRD analysis.....	151
5.4.1.3 FTIR analysis	152
5.4.1.4 Textural properties study.....	154
5.4.1.5 Surface morphology	155
5.4.2 Effect of alkali-activation on adsorption of pesticides.....	157
5.5 Conclusion	159
5.6 Reference	159
VI CONCLUSION	161
APPENDIX	163
CURRICULUM VITAE	165

LIST OF TABLES

Table	Page
1.1 Top 10 imported pesticide in 2012	2
2.1 Characteristic of desired pesticides	14
3.1 Chemical composition and CEC values for bentonite and modified bentonite samples.	53
3.2 The d-spacing (\AA) of bentonite and modified bentonite changes upon atrazine, diuron, 2,4-D and paraquat adsorption	55
3.3 The water content (%) in bentonite and modified bentonite	58
3.4 Surface area, mean pore diameter and zeta potential of the bentonite and modified bentonite samples	64
3.5 Measurement of particle size distribution	67
3.6 Langmuir and Freundlich atrazine adsorption isotherm constants.....	80
3.7 Langmuir and Freundlich diuron adsorption isotherm constants.....	81
3.8 Langmuir and Freundlich 2,4-D adsorption isotherm constants.....	81
3.9 Langmuir and Freundlich paraquat adsorption isotherm constants.....	82
3.10 Parameters for adsorption of atrazine on bentonite and BC ₅₀₀ A _{0.5}	85
3.11 Parameters for adsorption of diuron on bentonite and BC ₅₀₀	86
3.12 Parameters for adsorption of 2,4-D on bentonite and BA _{0.5} C ₅₀₀	87

LIST OF TABLES (Continued)

Table	Page
3.13 Parameters for adsorption of paraquat on bentonite and BC ₅₀₀	88
3.14 Thermodynamic parameters for adsorption of atrazine on bentonite and BC ₅₀₀ A _{0.5}	89
3.15 Thermodynamic parameters for adsorption of diuron on bentonite and BC ₅₀₀	90
3.16 Thermodynamic parameters for adsorption of 2,4-D on bentonite and BA _{0.5} C ₅₀₀	91
3.17 Thermodynamic parameters for adsorption of paraquat on bentonite and BC ₅₀₀	92
3.18 Kinetic model parameters obtained for the adsorption of atrazine onto bentonite and modified bentonite adsorbents.....	95
3.19 Kinetic model parameters obtained for the adsorption of diuron onto bentonite and modified bentonite adsorbents.....	95
3.20 Kinetic model parameters obtained for the adsorption of 2,4-D onto bentonite and modified bentonite adsorbents.....	96
3.21 Kinetic model parameters obtained for the adsorption of paraquat onto bentonite and modified bentonite adsorbents.....	96
4.1 The d-spacing (Å) of bentonite and modified bentonite changes upon type and concentration of surfactant.....	115
4.2 The percent composition of water and surfactants of bentonite.....	123

LIST OF TABLES (Continued)

Table	Page
4.3 Measurement of particle size distribution of modified bentonite by HDTMA	125
4.4 Measurement of particle size distribution of modified bentonite by SDS	125
4.5 Kinetic model parameters obtained for the adsorption of atrazine (50 ppm) onto bentonite and modified bentonite adsorbents	142
4.6 Kinetic model parameters obtained for the adsorption of diuron (50 ppm) onto bentonite and modified bentonite adsorbents	142
4.7 Kinetic model parameters obtained for the adsorption of 2,4-D (50 ppm) onto bentonite and modified bentonite adsorbents	147
4.8 Kinetic model parameters obtained for the adsorption of paraquat (200 ppm) onto bentonite and modified bentonite adsorbents	143
5.1 Chemical composition for bentonite and modified bentonite samples.....	150
5.2 Surface area, mean pore diameter, particle size and zeta potential of the bentonite and modified bentonite samples	155

LIST OF FIGURES

Figure	Page
1.1 Chemical structure of (a) atrazine (b) paraquat (c) diuron and (d) 2,4-D3
2.1 The different layer structures (A) The 1:1 layer, (B) the 2:1 layer, (C) the 2:1 layer with anhydrous interlayer cations, (D) the 2:1 layer with hydrated interlayer cations and (E) the 2:1 layer with octahedral interlayer sheet.....	15
2.2 Hemimicelle and admicelle formation by cationic surfactants on clay surface.....	24
3.1 XRD patterns for bentonite, BC ₅₀₀ , BC ₅₀₀ A _{0.5} , BA _{0.5} , and BA _{0.5} C ₅₀₀ adsorbents. (Q = quartz; M = montmorillonite; C = cristobalite.).....	55
3.2 TGA/DTG for bentonite, BA _{0.5} , BC ₅₀₀ , BA _{0.5} C ₅₀₀ and BC ₅₀₀ A _{0.5}	56
3.3 Mid FT-IR spectra of bentonite, BC ₅₀₀ , BC ₅₀₀ A _{0.5} , BA _{0.5} and BA _{0.5} C ₅₀₀ samples.	60
3.4 NIR FT-IR spectra of bentonite, BC ₅₀₀ , BC ₅₀₀ A _{0.5} , BA _{0.5} and BA _{0.5} C ₅₀₀ samples.....	60
3.5 NH ₃ -TPD profiles for bentonite and modified bentonite.	61
3.6 ²⁷ Al MAS NMR spectra for bentonite and modified bentonite. (Spinning side-bands are marked with asterisks).	63
3.7 SEM micrographs of bentonite (a), BC ₅₀₀ (b), BA _{0.5} (c), BC ₅₀₀ A _{0.5} (d) and BA _{0.5} C ₅₀₀ (e).....	65

LIST OF FIGURES (Continued)

Figure	Page
3.8 Particle size distributions for bentonite (a), BA _{0.5} (b), BA _{0.5} C ₅₀₀ (c), BC ₅₀₀ (d), and BC ₅₀₀ A _{0.5} (e).....	68
3.9 Adsorption capacity of modified and unmodified bentonite for atrazin(a), diuron (b), 2,4-D (c) and paraquat (d) at various pH at 50 ppm.	72
3.10 Adsorption of single-component pesticide (50 ppm) at pH 6.5±0.5 onto bentonite and modified bentonite.	75
3.11 Adsorption of quaternary-component pesticides (50 ppm) at pH 6.5±0.5 onto bentonite and modified bentonite.	75
3.12 Adsorption of bentonite and modified bentonite samples for atrazine (a), diuron (b), 2,4-D (c) and paraquat (d) at 50 ppm.....	76
3.13 Equilibrium isotherms for adsorption of atrazine onto bentonite and modified bentonite at pH 3 (a) and pH 6 (b)	77
3.14 Equilibrium isotherms for adsorption of diuron onto bentonite and modified bentonite at pH 4 (a) and pH 6 (b)	78
3.15 Equilibrium isotherms for adsorption of 2,4-D onto bentonite and modified bentonite at pH 3 (a) and pH 6 (b).....	78
3.16 Equilibrium isotherms for adsorption of paraquat onto bentonite and modified bentonite at pH 6 (a) and pH 11 (b).....	79
3.17 Adsorption isotherm of pesticide on bentonite and modified bentonite at 303, 313 and 323 K.	84

LIST OF FIGURES (Continued)

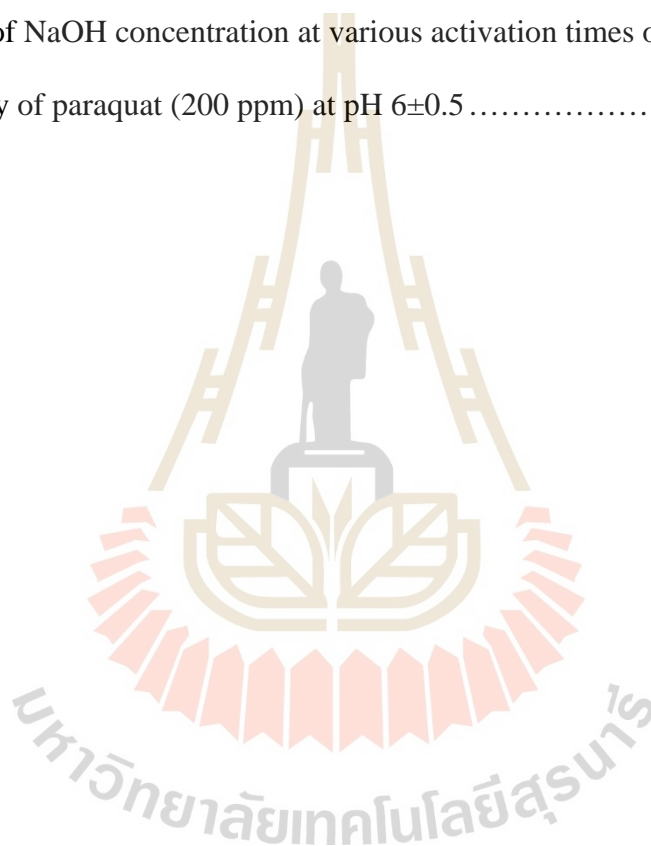
Figure	Page
3.18 pseudo-second order plots of atrazine (a) diuron (b) 2,4-D (c) and paraquat (d) adsorption onto bentonite and modified bentonites.	94
4.4 The XRD patterns of the HDTMA-bentonite with various concentrations of HDTMA (0.5-120 mM).	113
4.5 The XRD patterns of the SDS-bentonite with various concentrations of SDS (5-120 mM).	114
4.6 IR spectra of bentonite modified with 0.5-120 mM HDTMA	117
4.7 IR spectra of bentonite modified with 5-120 mM SDS.....	118
4.8 Thermogravimetric (TG) and differential thermogravimetric (DTG) analyses of Bentonite, BH0.5, BH10, BH60 and BH120	121
4.9 Thermogravimetric (TG) and differential thermogravimetric (DTG) analyses of Bentonite, BS5, BS10, BS80 and BS120	122
4.10 Particle size distribution of Bentonite (a), BH0.5 (b), BH1 (c), BH10 (d), BH60 (e), BH120 (f), BS5 (g), BS10 (h), BS80 (i) and BS120 (j)	126
4.11 Effect of surfactant concentration loading on adsorption capacity of atrazine (a) and diuron (b) on various adsorbent at initial concentration 50 ppm.	130

LIST OF FIGURES (Continued)

Figure	Page
4.12 Effect of surfactant concentration loading on adsorption capacity of 2,4-D (a) and paraquat (b) on various adsorbent at initial concentration 50 and 200 ppm, respectively.....	132
4.13 Effect of pH on adsorption capacity for removal of (a) atrazine (b) diuron (c) 2,4-D and (d) paraquat	134
4.14 Adsorption of quaternary-component pesticides (50 ppm) at pH 6.5±0.5 onto bentonite and modified bentonite.	137
4.15 Effect of the contact time on the adsorption of atrazine (a), diuron (b), 2,4-D (c) and paraquat (d) on bentonite, BH60 and BS80.....	138
4.16 pseudo-second order plots of atrazine (a) diuron (b) 2,4-D (c) and paraquat (d) adsorption onto bentonite and modified bentonites.	140
5.1 XRD patterns for bentonite and modified bentonite with 0.25M (a) and 0.5M NaOH (b) at various activation times. (Q = quartz; M = montmorillonite; C = cristobalite.).....	152
5.2 FT-IR spectra of bentonite and modified bentonite with 0.25M (a) and 0.5M NaOH (b) at various activation times.....	153
5.3 SEM micrographs of bentonite (a) and modified bentonite with 0.5M NaOH 3 h (b) 0.5M NaOH 6 h (c)	156

LIST OF FIGURES (Continued)

Figure	Page
5.4 Effect of NaOH concentration with activation time of 3 hours on adsorption capacity of pesticide (50 ppm) at pH 6±0.5.....	157
5.5 Effect of NaOH concentration at various activation times on adsorption capacity of paraquat (200 ppm) at pH 6±0.5	158

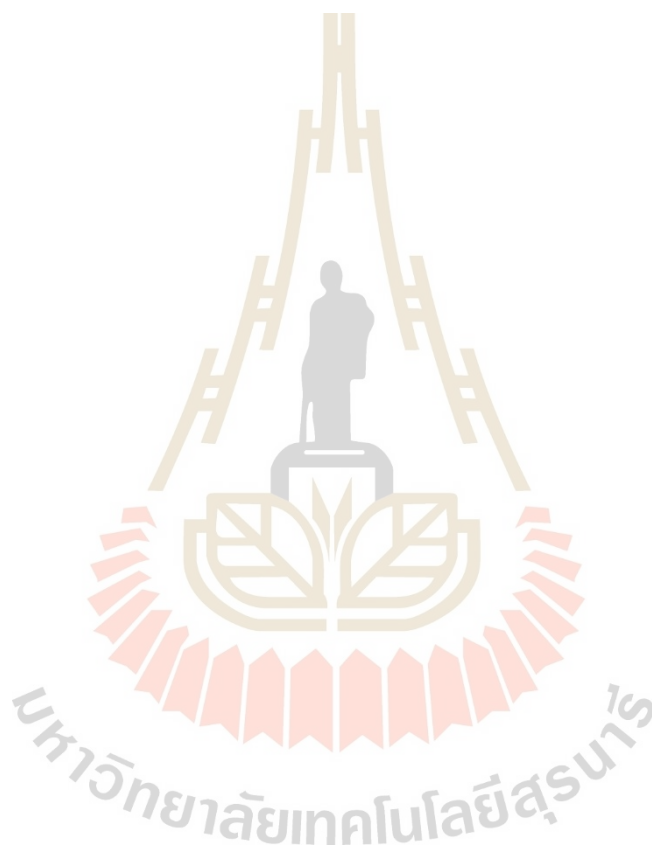


LIST OF ABBREVIATIONS

CEC	cation exchange capacity
cm^{-1}	wavenumber (per centimeter)
cmol	centimole
C_0	concentrations of pesticides in solution at initial
C_e	concentrations of pesticides in solution at equilibrium
FT-IR	Fourier transform infrared
g	gram
K_L	Langmuir constant
M	molar
mg/L	Milligram per Litre
min	minute
mL	milliliter
mM	millimolar
nm	nanometer
q_e	amount of pesticide adsorbed at equilibrium.
q_m	maximum adsorption monolayer capacity
R^2	R-squared
SEM	Scanning electron microscopy
T	temperature
V	volume of the solution.
Å	Angstrom

LIST OF ABBREVIATIONS (Continued)

ΔG°	change in standard Gibbs free energy
ΔH°	change in standard enthalpy
ΔS°	change in standard entropy
μm	micrometer



CHAPTER I

INTRODUCTION

1.1 Significance of study

Within the last 30 years, the use of organic pesticides in agriculture of Thailand has increased continuously. Because of the increasing demand for pesticide products due to economic and population growth, farmers are using chemicals to increase productivity and reduce damage from insects and weeds. As can be seen from the import of pesticides which increased from 80 million tons in 2005, to more than 120 million tons in 2012. The top 10 imported pesticides in 2012 are shown in Table 1.1. It can be seen that most imports are herbicides such as atrazine, paraquat dichloride, diuron and 2,4-dichlorophenoxyacetic acid (2,4-D). The structures of these pesticides are shown in Figure 1.1. Atrazine is one of the main herbicides applied to agricultural soils and has been widely used as a pre- and post-emergent herbicide to control broad leaf weeds in field crops, orchards and non-cropped areas. Due to its widespread use, long-term persistence in soil, greater leaching potential and relatively high solubility in water, there for, atrazine can contaminate in environmental and effect to human health. Recently, atrazine is recognized as an endocrine disruptor for mammals and aquatic life.

Table 1.1 Top 10 imported pesticides in 2012.

No.	Common name	Number of registrations	Type
1	glyphosate isopropylammonium	149	herbicide
2	paraquat dichloride	129	herbicide
3	ametryn	94	herbicide
4	atrazine	85	herbicide
5	abamectin	83	insecticide
6	diuron	63	herbicide
7	2,4-dichlorophenoxyacetic acid (2,4-D)	62	herbicide
8	butachlor	58	herbicide
9	acetochlor	56	herbicide
10	imidacloprid	51	insecticide

Paraquat is widely used in Thailand to eliminate broad-leaved weeds and grasses in variety of crops. Occupational and accidental exposure of paraquat to agriculture workers and children can affect human health. The toxicity of paraquat for humans is manifested in different organs of humans, including liver, brain, kidneys, heart, adrenal glands and muscles (Ait et al., 201).

Diuron is a substituted phenyl urea used as a herbicide to control broad-leaved and grass weeds and as a biocidal antifouling agent. It causes a cancer in rat urinary bladder and is toxic to the reproductive system of oysters, sea urchins and lizards.

Diuron blocks the electron transfer to the photosystem II within the thylakoid membrane of chloroplasts, which inhibits photosynthetic oxygen and energy production in plants and algae (Mirna et al., 2017).

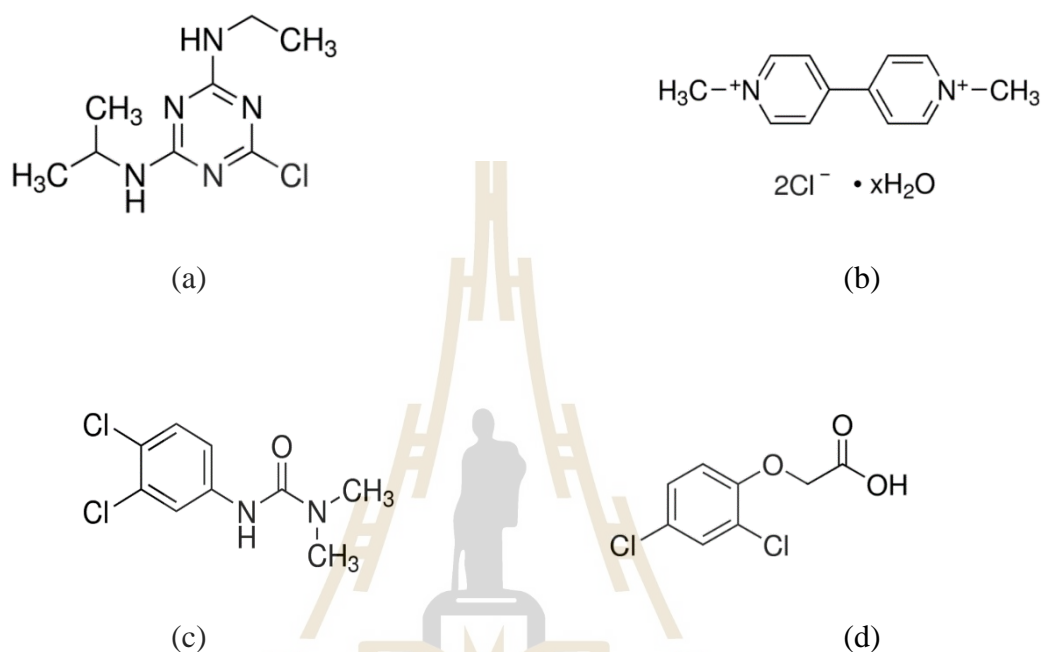


Figure 1.1 Chemical structure of (a) atrazine (b) paraquat (c) diuron and (d) 2,4-D.

2,4-Dichlorophenoxyacetic acid is in the phenoxyacetic acid class of compounds and has been used world widely since 1940s. It works as a herbicide when the concentration is as high as 500 mg.L^{-1} . There are over 1500 herbicide products containing 2,4-D as the main ingredient (Kang et al., 2017). The toxicity of 2,4-D exposure causes serious eye and skin irritation, nausea, weakness, fatigue and in some cases neurotoxic effects including inflammation of nerve ending (Jamil et al., 2011; Leite et al., 2013; RaoChu, 2010; Salman et al., 2011) Therefore, the harmful influence of pesticides on human health, animals and environment has resulted to the imposition of stringent legislation on the purity of drinking water in many countries in

the world. For example, the European Directive Nr. 98/83/CE for drinking water allows $0.1 \mu\text{g L}^{-1}$ for a single pesticide and $0.5 \mu\text{g L}^{-1}$ the total amount of the pesticides (Bouras et al., 2007; Chingombe et al., 2006). The EC Drinking Water Directive (80/778/EC) stipulates the requirement that no single pesticide should exceed 0.1 mg L^{-1} and total pesticides should not exceed five-fold of this level in drinking water from the tap (Pavlovic et al., 2013). As a result of the wide application of pesticides, they have frequently been detected in surface and drinking waters at levels exceeding the permissible limits. Therefore, it is necessary to limit the agrochemical substances discharged into the environment as much as possible, and also to act on removing them completely.

Based on the above data, the popularity of herbicides is widespread and causes environmental problems. Especially, the problem of wastewater contaminated by pesticides that have strong impact for human and aquatic animals. Harmful effects on consumers and on living organisms, both acute and cumulative in the body, can cause future diseases. Therefore, the importance of environmentally-friendly treatment of contaminated toxins in a safe and healthy environment is interest. Various methods have been used for the removal of these substances including Fenton process (Navarro et al., 2011), biological treatment (González et al., 2012), advanced oxidation treatment (Badawy et al., 2006), membrane technologies (PlakasKarabelas, 2012), ion exchange treatment (Humbert et al., 2008), chemical coagulation (Alexander et al., 2012) activated carbon, ozone treatment and adsorption (Chaara et al., 2012; Leite et al., 2013; Salvestrini et al., 2010). It is a challenge to find single method for pesticide removal from surface and ground waters, or for its elimination from contaminated aqueous effluents. Adsorption is a simple and convenient method for removal of the

pesticides compared to other physical, chemical, or biological technologies. Various solid substrates offering good adsorptive properties, for example, clay minerals, zeolites, and activated carbon, are applied to the removal of organic contaminants from waters (Castro et al., 2009; Chen et al., 2009; Jamil et al., 2011; Kovaivos et al., 2011; Salvestrini et al., 2010; Zadaka et al., 2009; Zhang et al., 2012). Bentonite is a clay mainly constituted by the clay mineral montmorillonites. It is abundant and cheap in Thailand and has been reported with appreciable adsorption capacity. Bentonite contains a net negative charge due to isomorphous substitution in the aluminosilicate layers neutralized by inorganic cations, which in aqueous medium are strongly neutralized by inorganic cations, and strongly hydrated and confer the clay surface a hydrophilic character.

Acid, alkaline, thermal and surfactant modification optimises the physical characteristics of bentonite for removal of contaminants by causing structural and textural changes within the clay, so enhancing adsorption capacity. Acid and thermal treatments are low-cost methods that require few chemicals and are simple to apply. Acid activated bentonite is suitable for removal or elimination of impurities; it increases both porous surface area and the numbers of silanol groups present in the clay, which are important for the adsorption of organic compounds (Peter Komadel, 2016; P. KomadelMadejová, 2006). Heat treatment significantly alters the surface properties of bentonite; it improves porosity by increasing mesopore volume, increases the number of surface adsorption sites, and increases the number of siloxane groups present, while it reduces the number of hydroxyl groups present (Bojemueller et al., 2001; Gupta et al., 2015; Heller-Kallai, 2006; Nones et al., 2015; Wu et al., 2005). Alkaline treatment remarkably changes to the surface properties of bentonite;

alkaline first attacks the tetrahedral layer. If the attack is prolonged and severe the mineral structure is destroyed, but 75-85% of the total alumina must be removed from montmorillonite before the structure is completely destroyed. The exposed SiO₂ tetrahedral were attacked by the reagents releasing the Si originally in tetrahedral coordination. NaOH may have removed the silica layer, but the other reagents effected only a partial removal (D.Carroll, 1971) . In addition to these structural changes, acid, alkaline and heat treatments alter textural properties of the clay and improve its dispersibility in water. These treatments can also enhance pesticide adsorption performance as described here, for the sequestration of pesticide. Moreover the adsorption phenomena of organic compound on organo-clay, i. e. surfactant-modified-clay and so far all results published on the different adsorbate-adsorbent interactions have confirmed their high efficiency in adsorption of pesticides pollutants.

This study aims to combine acid, alkaline, heat and surfactant treatments on bentonite to optimise its adsorption capability for removal of these pesticides. Various methods are used to characterize the modified bentonite samples and to investigate changes to their structural and textural properties.

1.2 Research objectives

1.2.1 To find out the different modified methods (acid, alkaline, heat and surfactant) with single and combined step and the optimum condition of the modifications for bentonite.

1.2.2 To characterize the physical and chemical properties of unmodified and modified bentonite samples.

1.2.3 To investigate the capability in the pesticides adsorption of all adsorbents at various pHs.

1.2.4 To investigate the simultaneous adsorption of cationic, basic, acidic pesticide and non-ionic pesticide in solutions.

1.2.5 To investigate the adsorption isotherms and equilibrium parameters of the adsorbed pesticides by unmodified and modified bentonite.

1.3 Scope and limitations of the study

1.3.1 Bentonite has been modified by acid, alkaline, heat and surfactants. The modification was performed by a single step with each modifier (acid, alkaline, heat and surfactants) and combined steps with these modifiers, including in the different sequences of the modification.

1.3.2 Bentonite and the modified bentonite samples were characterized with various techniques such as XRD, XRF, FT-IR spectroscopy, TGA-DTG, BET, TPD, zeta potential, Al and Si NMR and particle size distribution.

1.3.3 Adsorption isotherms and equilibrium parameters of four pesticides selected based on physicochemical properties (paraquat, atrazine, 2,4-D and dinuron that are cationic, basic, acidic and non-ionic pesticides, respectively) by bentonite and modified bentonite samples have been investigated.

1.4 Expected results

1.4.1 The optimum condition to prepare modified bentonite samples with acid, alkaline, surfactant and heat to enhance the removal of each pesticide will be achieved.

1.4.2 The modified bentonite samples will be achieved with the combined method and their physical and chemical properties will be understood.

1.4.3 Adsorbents that are low cost and provide highly efficient adsorption of each pesticide will be obtained.

1.5 References

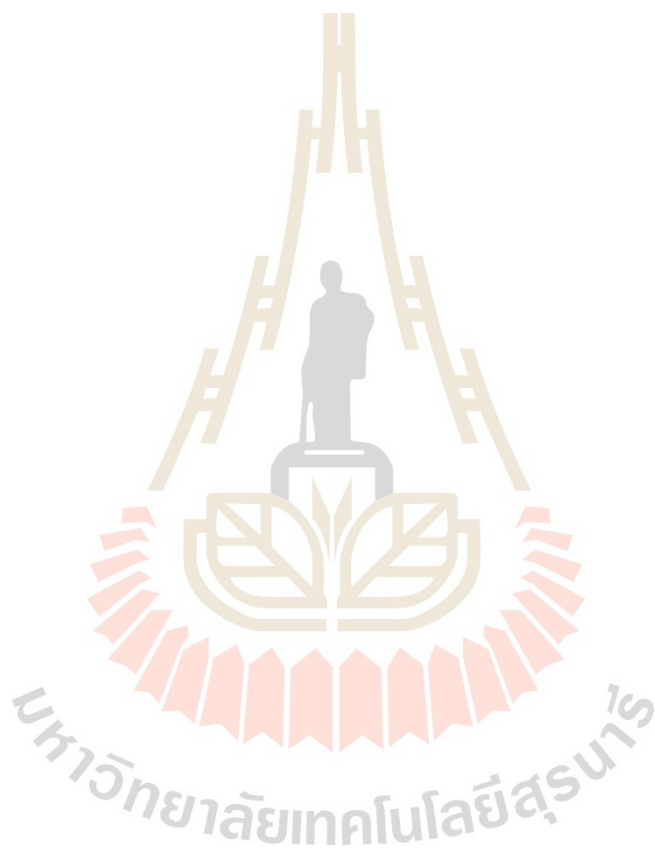
- Ait Sidhoum, D., Sociás-Viciana, M. M., Ureña-Amate, M. D., Derdour, A., González-Pradas, E., and Debbagh-Boutarbouch, N. (2013). Removal of paraquat from water by an Algerian bentonite. **Applied Clay Science**. 83-84: 441-448.
- Alexander, J. T., Hai, F. I., and Al-aboud, T. M. (2012). Chemical coagulation-based processes for trace organic contaminant removal: Current state and future potential. **Journal of Environmental Management**. 111: 195-207.
- Badawy, M. I., Ghaly, M. Y., and Gad-Allah, T. A. (2006). Advanced oxidation processes for the removal of organophosphorus pesticides from wastewater. **Desalination**. 194: 166-175.
- Bojemueller, E., Nennemann, A., and Lagaly, G. (2001). Enhanced pesticide adsorption by thermally modified bentonites. **Applied Clay Science**. 18: 277-284.

- Bouras, O., Bollinger, J.-C., Baudu, M., and Khalaf, H. (2007). Adsorption of diuron and its degradation products from aqueous solution by surfactant-modified pillared clays. **Applied Clay Science**. 37: 240-250.
- Castro, C. S., Guerreiro, M. C., Goncalves, M., Oliveira, L. C. A., and Anastacio, A. S. (2009). Activated carbon/iron oxide composites for the removal of atrazine from aqueous medium. **J Hazard Mater**. 164: 609-614.
- Chara, D., Bruna, F., Draoui, K., Ulibarri, M. A., Barriga, C., and Pavlovic, I. (2012). Study of key parameters affecting adsorption of the herbicide Linuron on organohydrotalcites. **Applied Clay Science**. 58: 34-38.
- Chen, G. C., Shan, X. Q., Zhou, Y. Q., Shen, X. E., Huang, H. L., and Khan, S. U. (2009). Adsorption kinetics, isotherms and thermodynamics of atrazine on surface oxidized multiwalled carbon nanotubes. **J Hazard Mater**. 169: 912-918.
- Chingombe, P., Saha, B., and Wakeman, R. J. (2006). Sorption of atrazine on conventional and surface modified activated carbons. **Journal of Colloid and Interface Science**. 302: 408-416.
- González, A. J., Gallego, A., Gemini, V. L., Papalia, M., Radice, M., Gutkind, G., and Korol, S. E. (2012). Degradation and detoxification of the herbicide 2,4-dichlorophenoxyacetic acid (2,4-D) by an indigenous *Delftia* sp. strain in batch and continuous systems. **International Biodeterioration & Biodegradation**. 66: 8-13.
- Gupta, V. K., Sharma, M., and Vyas, R. K. (2015). Hydrothermal modification and characterization of bentonite for reactive adsorption of methylene blue: An ESI-MS study. **Journal of Environmental Chemical Engineering**. 3: 2172-2179.

- Heller-Kallai, L. (2006). Chapter 7.2 Thermally Modified Clay Minerals. In B. K. G. T. Faïza Bergaya & L. Gerhard (Eds.), **Developments in Clay Science** (Vol. Volume 1, pp. 289-308): Elsevier.
- Humbert, H., Gallard, H., Suty, H., and Croué, J.-P. (2008). Natural organic matter (NOM) and pesticides removal using a combination of ion exchange resin and powdered activated carbon (PAC). **Water Research**. 42: 1635-1643.
- Jamil, T. S., Gad-Allah, T. A., Ibrahim, H. S., and Saleh, T. S. (2011). Adsorption and isothermal models of atrazine by zeolite prepared from Egyptian kaolin. **Solid State Sciences**. 13: 198-203.
- Komadel, P. (2016). Acid activated clays: Materials in continuous demand. **Applied Clay Science**. 131: 84-99.
- Komadel, P., and Madejová, J. (2006). Chapter 7.1 Acid Activation of Clay Minerals. In B. K. G. T. Faïza Bergaya & L. Gerhard (Eds.), **Developments in Clay Science** (Vol. Volume 1, pp. 263-287): Elsevier.
- Kovaios, I. D., Paraskeva, C. A., and Koutsoukos, P. G. (2011). Adsorption of atrazine from aqueous electrolyte solutions on humic acid and silica. **J Colloid Interface Sci**. 356: 277-285.
- Leite, M. P., dos Reis, L. G. T., Robaina, N. F., Pacheco, W. F., and Cassella, R. J. (2013). Adsorption of paraquat from aqueous medium by Amberlite XAD-2 and XAD-4 resins using dodecylsulfate as counter ion. **Chemical Engineering Journal**. 215-216: 691-698.
- Navarro, S., Fenoll, J., Vela, N., Ruiz, E., and Navarro, G. (2011). Removal of ten pesticides from leaching water at pilot plant scale by photo-Fenton treatment. **Chemical Engineering Journal**. 167: 42-49.

- Nones, J., Nones, J., Riella, H. G., Poli, A., Trentin, A. G., and Kuhnen, N. C. (2015). Thermal treatment of bentonite reduces aflatoxin b1 adsorption and affects stem cell death. **Mater Sci Eng C Mater Biol Appl.** 55: 530-537.
- Pavlovic, I., González, M. A., Rodríguez-Rivas, F., Ulibarri, M. A., and Barriga, C. (2013). Caprylate intercalated layered double hydroxide as adsorbent of the linuron, 2,4-DB and metamitron pesticides from aqueous solution. **Applied Clay Science.** 80-81: 76-84.
- Plakas, K. V., and Karabelas, A. J. (2012). Removal of pesticides from water by NF and RO membranes -A review. **Desalination.** 287: 255-265.
- Rao, Y. F., and Chu, W. (2010). Degradation of linuron by UV, ozonation, and UV/O₃ processes-Effect of anions and reaction mechanism. *Journal of Hazardous Materials.* 180: 514-523.
- Salman, J. M., Njoku, V. O., and Hameed, B. H. (2011). Adsorption of pesticides from aqueous solution onto banana stalk activated carbon. **Chemical Engineering Journal.** 174: 41-48.
- Salvestrini, S., Sagliano, P., Iovino, P., Capasso, S., and Colella, C. (2010). Atrazine adsorption by acid-activated zeolite-rich tuffs. **Applied Clay Science.** 49: 330-335.
- Wu, P., Wu, H., and Li, R. (2005). The microstructural study of thermal treatment montmorillonite from Heping, China. **Spectrochim Acta A Mol Biomol Spectrosc.** 61: 3020-3025.
- Zadaka, D., Nir, S., Radian, A., and Mishael, Y. G. (2009). Atrazine removal from water by polycation-clay composites: effect of dissolved organic matter and comparison to activated carbon. **Water Res.** 43: 677-683.

Zhang, C., Yan, J., Zhang, C., and Yang, Z. (2012). Enhanced adsorption of atrazine from aqueous solution by molecularly imprinted TiO₂ film. **Solid State Sciences**. 14: 777-781.



CHAPTER II

LITERATURE REVIEW

In this study we are interested in using the adsorbents such as; bentonite (B), acid activated bentonite (BA), alkaline activated (B_NaOH), thermal treated bentonite (BC), combined treated with acid/heat (BAC, BCA) and organo-bentonite (HDTMA; BH and SDS; BS) and for adsorptions of four different classes of pesticides (atrazine, paraquat, diuron and 2,4-dichlorophenoxyacetic acid (2,4-D)) in aqueous solutions. The characteristics of these pesticides are shown in the **Table 2.1**. A property of contaminant in water is dependent on which class of the pesticide. Adsorption process is challenge to modify adsorbent to possess high effective for removing pesticides. Various techniques have been used to characterize modified bentonite samples in order to investigate the change of their structures, textural and surface properties. Numerous researches attempt to develop new proper adsorbent. Following sections provide detailed reviews of the modification of different adsorbents for removal of pesticides in water.

Table 2.1 Characteristic of desired pesticides.

Pesticide	Molecular weight (g mol ⁻¹)	Width (Å)	Length (Å)	pK _a	Log K _{ow}	Solubility at 25°C (mg L ⁻¹)
Atrazine	215.68	11.2	~3	1.7	2.5	30
Paraquat	257.16	13.4	~3	6.6	- 4.5	7 x 10 ⁵
Diuron	233.09	4.87	~9	13.5	2.68	42
2,4-D	221.04	9.6	~6	3.1	2.8	900

2.1 Clay and modified clay

Bentonite is named after Fort Benton near Rock River, Wyoming, USA, from where it was originally found by W.C. Knight in 1898. The mineral is a natural clay belonging to the smectite group; it was formed by devitrification of submerged volcanic ash. Raw bentonite is composed of diverse mineral substances, including quartz, cristobalite, feldspars, and several varieties of clay mineral. The major component of bentonite is montmorillonite, a dioctahedral smectite. Montmorillonite is a porous clay mineral consisting of a 2:1-layered structure, with alternating layers of exchangeable cations. The layers consist octahedral alumina sheets that are sandwiched by two tetrahedral silica sheets. Substituting Al³⁺ for Si⁴⁺ in the silica tetrahedral sheets and Mg²⁺ for Al³⁺ in the alumina octahedral sheets produces a net negative charge, which is usually balanced by adsorbed cations (**Figure 2.1**). These cations are easily replaced by either organic or inorganic cations, accounts for the unique hydrophilic, tumescent, and adsorption properties of montmorillonite (Park et

al., 2016). Bentonite clay minerals are available in Thailand; they are an important low-cost source of montmorillonite and exhibit excellent adsorption capacities. Bentonite minerals have complex surface morphologies and provide a unique combination of properties, including thixotropic gel formation with water, good water adsorption capacity, large surface area, a layered structure, and high cation exchange capability (CEC) (Choo and Bai, 2016; Murray, 2006).

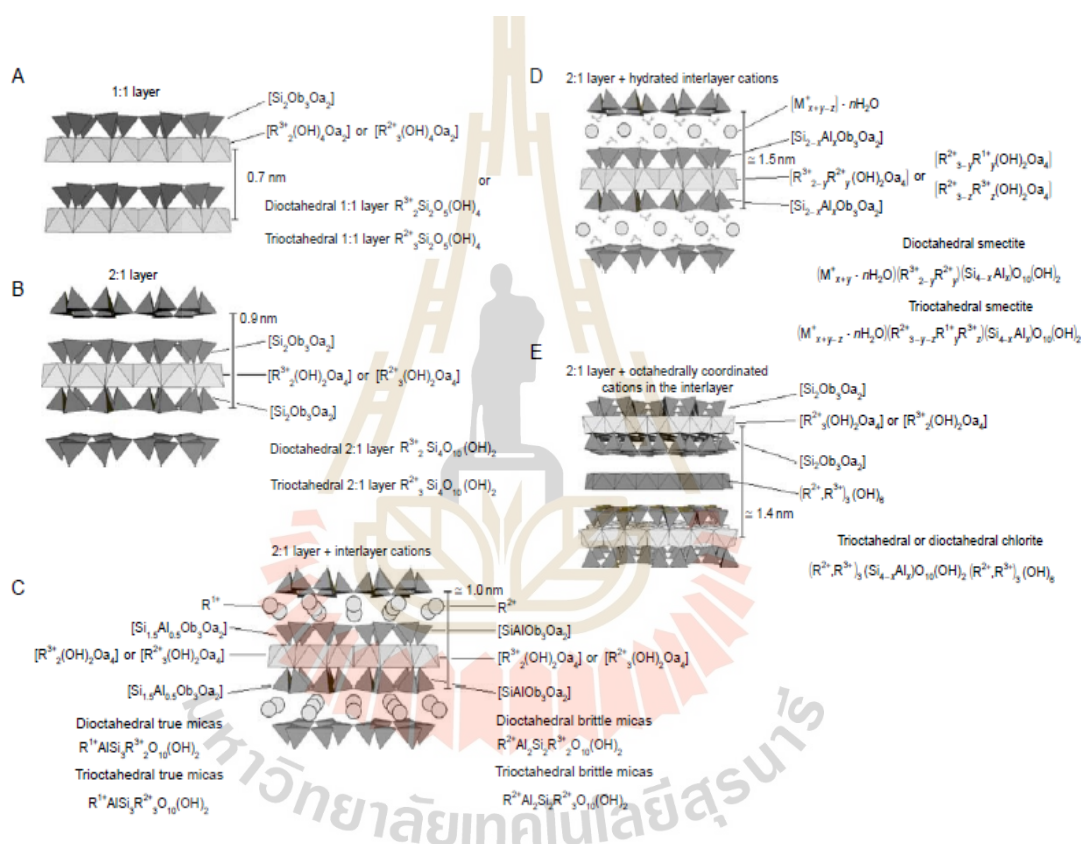


Figure 2.1 The different layer structures (A) The 1:1 layer, (B) the 2:1 layer, (C) the 2:1 layer with anhydrous interlayer cations, (D) the 2:1 layer with hydrated interlayer cations and (E) the 2:1 layer with octahedral interlayer sheet.

2.1.1 Adsorption using acid modified clay

High surface area, porosity and acid site on the surface clay have significantly increased adsorption by using acid modified clay. Bentonite has always a multitude of markets, and acid activated bentonite has been a standard product for many decades. Usually a Ca^{2+} -bentonite is treated with inorganic acids to replace divalent with monovalent hydrogen ion and remove mineral impurities and dealuminate Al from the O sheet, thus altering the clay layers and increasing the specific surface area, porosity and acid site. For example, Tong et al. (2014), reported the acid-activated montmorillonite, the results showed that the acid treatment of montmorillonite improved the specific surface area and the amount of acid site SiOH_2^+ on the surface. From this process, the structure and properties change. However, the strength, type of acid and times of acid activation also affect its structure and properties. Which corresponds the other reports, such as, Gates et al. (2002), described about the acid modified bentonite with HCl, with prolonged acid treatment (24 h) led to a breakdown in the structure of this component, and caused a precipitation of hydrous silica phases. Structural decomposition was accomplished by a release into solution of octahedrally coordinated Mg, Fe and Al. These were also substantial losses to solution of Na and Ca. The precipitate of hydrous silica was enriched with time of acid treatment. A substantial amount of Al was retained within the solid reaction product, most likely as a constituent of impurities that were resistant to acid attack. Biesiki et al. (2013), describes the acid treatment of natural montmorillonite clay.

Three different acids (HCl, HNO_3 and H_2SO_4) were tested, and HCl and H_2SO_4 were more efficient for removing Fe from the clay. The results indicate that HCl better preserves the material structure because less Al is removed. Combination

of HCl acid solution concentration and temperature, such as 4 M/50°C and 1M/75°C, assured that Fe was removed with less damage to the structure. It can be seen that, mild acid concentrations and low temperature, less damaged the structure of clay. This change in properties has been shown to improve the absorption of toxic substances, which is consistent with many researches. Such as, Javed et al. (2018), who reported the activation of bentonite clay using different acids (1M of Phosphoric acid, Acetic acid, Citric acid and Oxalic acid) and activated at 60°C for 24 h. This report uses mild conditions to modify the clay so that the structure can be maintained and increase the efficiency of Red 73 adsorption from textile wastewater. Pawar et al. (2016), report about acid activation of bentonite using high bentonite content (6% w/v) and 6 N sulfuric acid at 65°C for 10 h. The separation of fine spent sorbents from treated water after remediation is a major difficulty associated with phosphate wastewater treatment technology. A novel aluminium-pillared acid activated bentonite powder (Al-ABn) and alginate immobilized aluminium-pillared acid activated bentonite beads (Al-ABn-AB) were synthesized and used for the removal of aqueous phosphate. Moreover, Rezaei et al. (2018), studied two modified bentonite adsorbents, namely acid-activated (H-Be) (0.2 and 0.4M H₂SO₄ and HCl) and aluminum pillared (Al-Be) bentonite, synthesized and used for the removal of the residual xanthate (potassium amyl xanthate) from the synthetic and real solutions. Al-Be was found superior to H-Be in terms of adsorption performance and under optimum conditions (adsorbent dosage: 7500 mg.L⁻¹; xanthate concentration: 2000 mg.L⁻¹; pH = 12.2; time = 45 min) and more than 99% of the residual xanthate was removed. Pentrak et al. (2012), reported the modified with HCl treatment on various type of clay to improve the structure and physicochemical properties which then increases surface area, and enhance its

adsorption capacity for adsorbed methylene blue. Decreasing values of CEC upon HCl attacked. The changes in the SDS of smectites-clay showed increasing rate of their dissolution in HCl with rising substitution for octahedral Al. The MB spectra of SWy-2 revealed heterogeneity of layer charge distribution in this montmorillonite. Formation of MB monomers confirmed that smectite/illite was more stable in HCl than illite despite of its higher content of swelling layers. So the MB adsorption is a very sensitive tool for characterization of layer charge of different clay minerals modified upon acid treatment.

2.1.2 Adsorption using alkaline modified clay

The effect of alkali activation on the physiochemical properties of clay and zeolite were reported by Yujiro et al. (2005). They reported that the structure of natural zeolite such as mordenite and clinoptilolite after treatment with 3.0M NaOH solution at 150°C was changed to phillipsite and by this type of modification the amount of ammonium removal from solution by modified zeolite was two-fold greater (1.92 mmol g⁻¹) than that taken up by the starting material. In another study, Cuevas et al. (2006), reported that Spanish reference benonite (FEBEX) was modified with alkaline solution (mixture of NaOH, KOH and Ca(OH)₂ with pH in the range of 12-13. The solid/alkaline solution ratio was 1/3 or 80 g of bentonite and 240 ml of solution and time of contact was from 7 days up to 365 days at 35, 60 and 90°C. The aim of their work was to clarify the effect of the alkaline plume induced by concrete on bentonite. By their of modification, they observed that the pH of solution was decreased after two months of contact and concluded that one of the most important observations made during the interaction between alkaline solutions and bentonite was that montmorillonite can be considered as an important buffer agent of the pH in the

bentonite. The pH decrease is mainly due to the dissolution of montmorillonite and the deprotonation of aqueous silica (i.e. $\text{H}_4\text{SiO}_4 \longrightarrow \text{H}_2\text{SiO}_4^{2-} + 2\text{H}^+$), and also to the incorporation of OH^- in the structure of newly-formed minerals or the retention of OH^- in the external surface of smectite may play a significant role". Also they reported that the change in structure of bentonite was dependent on temperature and contact time and it can be resulted that the cation exchange capacity of alkaline modified bentonite was greater than raw bentonite. There are a little previous reports that provide information about adsorption using alkaline-clay, such as Bentonite, biotite, illite, kaolin, vermiculite and zeolite were acidified or alkalinized with hydrochloric acid or sodium hydroxide at concentrations of 0.1, 1.0 and 5.0 mole dm^3 at room temperature for two weeks. In acid treatments, dissolution of Al prevailed over Si and the opposite was observed in alkali treatments. The XRD patterns showed severe alteration of the crystal structure after acid treatments, whereas sharpening of the XRD peaks after alkali treatments was observed. Illite and kaolin were most resistant to acid attack. With a few exceptions, the surface areas of the minerals computed from both water and nitrogen adsorption isotherms increased with acid and alkali treatments. With increasing reagent concentration, the nitrogen surface area increased faster than the water surface area. Well-defined trends were not noted in either changes of average water or nitrogen adsorption energies or in relative amounts of adsorption sites, indicating that the effects of acid and alkali attack are controlled by the individual character of the minerals (Jozefaciuk, 2002). The adsorption of bixin in aprotic solvents onto acid- and alkali-treated kaolinite was investigated. Kaolinite was treated three times, for 6 h each, with 8 M HCl or 5 M KOH. The adsorbents were characterized by XRD, FT-IR, EDS, and BET- N_2 . The effects of contact time and dye

concentration on adsorption capacity and kinetics, electronic transition of bixin before and after adsorption, and also mechanism of bixin-kaolinite adsorption were investigated. Dye adsorption followed pseudo-second order kinetics and was faster in acetone than in dimethyl carbonate. The best adsorption results were obtained for KOH-treated kaolinite. In both of the solvents, the adsorption isotherm followed the Langmuir model and adsorption capacity was higher in dimethyl carbonate ($q_m = 0.43$ mg/g) than in acetone (0.29 mg/g). The adsorption capacity and kinetics of KOH-treated kaolinite ($q_m = 0.43$ mg/g, $k_2 = 3.27$ g/mg·min) were better than those of HCl-treated kaolinite ($q_m = 0.21$ mg/g, $k_2 = 0.25$ g/mg·min) and natural kaolinite ($q_m = 0.18$ mg/g, $k_2 = 0.32$ g/mg·min). There are shift in the band position of maximum intensity of bixin after adsorption on this adsorbent. Adsorption in this system seemed to be based essentially on chemisorption due to the electrostatic interaction of bixin with the strong basic and reducing sites of kaolinite (Winda et al., 2018). The adsorption of monovalent organic cationic dye, methylene blue, on the natural and modified with hydrochloric acid and sodium hydroxide Latvian clay samples from water solutions has been studied. It was established, that alkali and acidic treatment of Latvian clay samples changes their sorption characteristics. It was found that increasing concentration of hydrochloric acid from 5 mass% until 15 mass%, decreases adsorption of clay samples proportionally to the acid concentration. Increasing concentration of sodium hydroxide from 5 mass% to 15 mass%, BET specific surface area of the modified clay samples is lower than BET specific surface area of the natural clay sample. The studies have proven that adsorption ability of Latvian clays is sufficient for using them in waste water purification from admixtures of organic dyes (Lakevics et al., 2014).

2.1.3 Adsorption using heat modified clay

Heat treatment can lead to the dehydration and dehydroxylation, and even the movements of octahedral cations within the O sheet (Heller-Kallai, 2006). Heat treatment significantly alters the surface properties of bentonite; it improves porosity by increasing mesopore volume, increases the number of surface adsorption sites, and increases the number of siloxane groups present, while it reduces the number of hydroxyl groups present (Bojemueller et al., 2001; Gupta et al., 2015; Heller-Kallai, 2006; Nones et al., 2015; Wu et al., 2005). On the other hand, heat treatment may also change the textural properties. These changes were suggested to be able to enhance the adsorption capacity of the resulting pesticide adsorption. For example, Bojemueller et al. (2001), reported the Wyoming bentonite was calcined at 350-550°C for 1, 3 and 12 h, dispersed in water and freeze-dried. Calcination at 350-450°C for 12 h decreased the specific surface area strongly. At higher calcination temperatures, the surface area became similar to the value of the uncalcined bentonite (24 m²/g). The micropore (diameter < 2 nm) volume of the calcined samples was very small (<0.2 μl). In contrast, the mesopore (diameter 2-50 nm) volume increased sharply when the bentonite was calcined at > 450°C. The Wyoming bentonite used in these experiments adsorbed considerable amounts of metolachlor from aqueous solutions, and the adsorption was enhanced by calcinating the bentonite with interact with aluminum ions or oligomeric hydroxoaluminum cation on the edges of clay. M.D. Ureña-Amate et al. (2005), reported the effect of ionic strength and temperature on adsorption of atrazine by heat treated kerolite clay at 600°C. It was found that the adsorption experiment also showed that the lower temperature, the more effective the adsorption of atrazine from both, pure water and 0.1 M KCl solutions. Maqueda et al. (2013),

suggested that Al cation liberated by the thermal treatment were bound to the external surfaces and edges of TMT, which could increase the uptake of diuron.

2.1.4 Adsorption using organo-clay

Clays contain a net negative charge due to isomorphous substitution in layers of clay neutralized by inorganic cations, which are strongly hydrated and confer the clay surface a hydrophilic character. The negative charge on the surface of bentonite, facilitates to change surface properties. One of the modification method widely employed is to use organic surfactants. Surfactants are long-chain molecules that contain both hydrophilic and hydrophobic moieties. Depending on their origin, surfactants are either biosurfactants or synthetic, and they can be classified as ionic and nonionic, according to their hydrophilic moiety. A general model of adsorption of ionic surfactants on a solid surface is the formation of a monolayer or “hemomicelle” at the solid-aqueous interface via strong coulombic or ionic interaction at surfactant concentration is equal or less than below its critical micelle concentration (CMC). If the surfactant concentration in solution exceeds the CMC, the hydrophobic tails of the surfactant molecules associate to form a bilayer or “admicelle” as shown in **Figure 2.2** (Gangula et al., 2010). The application of a cationic surfactant on clays causes the change of the clay surface from hydrophilic to hydrophobic and from negatively to positively charged, due to the sorption of the molecule onto its external surface and into the interlayer spacing and exposure of new sorption sites of clays. The series of cationic surfactants: tetramethylammonium chloride (TMA), hexadecyl trimethylammonium bromide (HDTMA), hexadecyl benzyl dimethylammonium chloride (HDBDMA) and dioctodecyl dimethylammonium bromide (DDDMA); removal of organic matter dissolved in water by the adsorption-flocculation process.

Quaternary ammonium cations are the most frequently used surfactants for preparing clays, with an excellent hydrophobicity and high efficiency for metals and organic contaminants recovery. According to Azejjel et al. (2009), The capacities of two Moroccan clays, one of them swelling and the other non-swelling, as sorbents of three ionisable pesticides: terbutryn (basic), dicamba (anionic) and paraquat (cationic) were studied. Sorption was studied on natural and modified clays with three quaternary alkyl ammonium cations of different long-chains, octadecyltrimethylammonium (ODTMA), octyltrimethylammonium (OTMA) and tetramethylammonium (TMA). Freundlich or Langmuir models were used to obtain sorption parameters. Sorption of terbutryn and dicamba by ODTMA-clays was always higher than by natural clays. Distribution coefficients (K_d) of these modified clays increased 55-128-fold (terbutryn), and 1.4-8.6-fold (dicamba) respect to the natural clays. In contrast, sorption of terbutryn by the TMA-clays and of dicamba by TMA- and OTMA-clays was lower than for natural clays. Sorption coefficients of paraquat by natural clays were similar or higher than those obtained with modified clays.

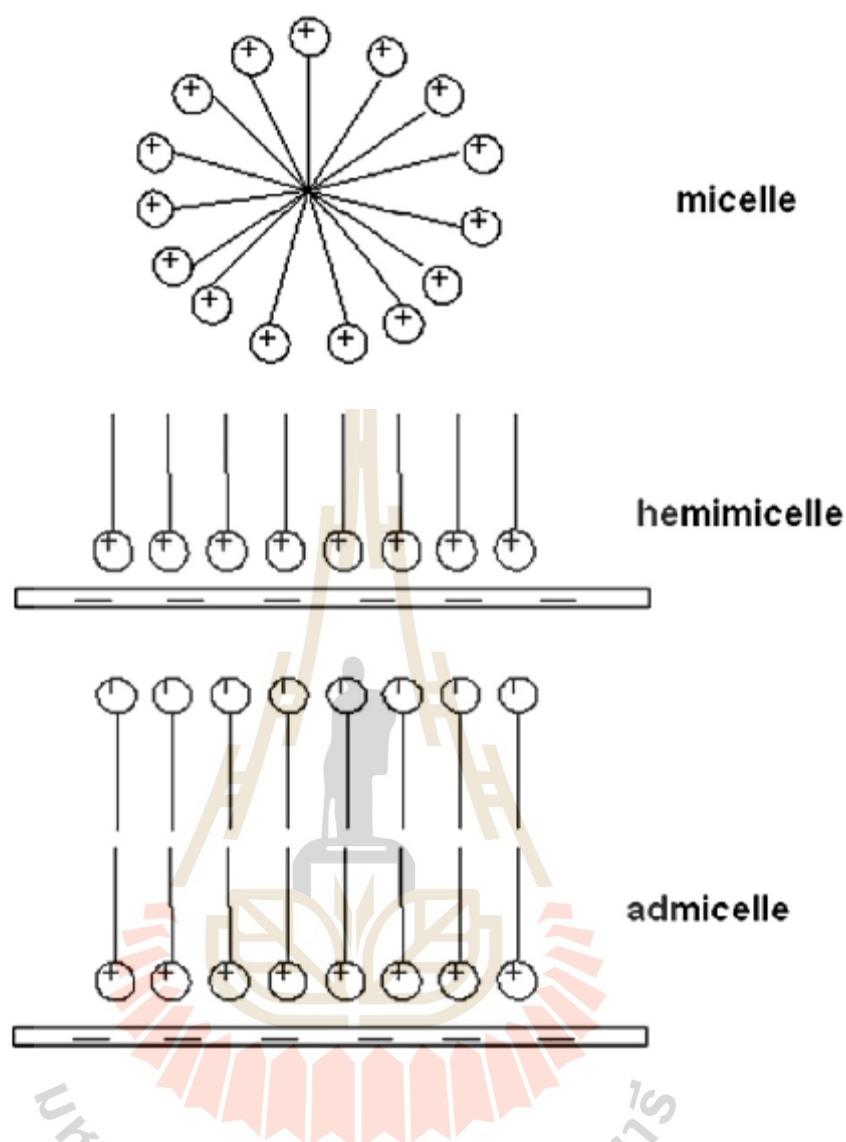


Figure 2.2 Hemimicelle and admicelle formation by cationic surfactants on clay surface.

In general, the sorption of herbicides was higher by swelling clay than by non-swelling clay. The results point out that the Moroccan clays studied may be used as sorbents of cationic pesticides in their natural form and of basic or even anionic herbicides when modified with long-chain organic cations in barrier technologies to enhance the immobilization of herbicides and to prevent the contamination of surface and ground water. Bouras et al. (2007) studied the adsorption of the herbicide diuron

and its three degradation products: 3-(3,4-dichlorophenyl) -1-methylurea, 1-(3,4-dichlorophenyl) urea and 2,4-dichloroanilin on three organo–inorgano-clay minerals. These surfactant-modified pillared clays (SMPC) were prepared by intercalation of polycations of aluminum(III), iron(III) or titanium(IV) into the interlamellar space of a montmorillonite, followed by co-adsorption of cetyl trimethylammonium bromide. The adsorption capacity of these new microporous solids was considerably enhanced especially with Ti- or Fe-SMPC. The adsorption isotherms of diuron and its derivatives at different pHs were performed on each SMPC. These isotherms are typically S-type curves and suggested a hydrophobic adsorption mechanism. A comparative study of adsorption of the four compounds on each SMPC adsorbent shows the high adsorption capacity of diuron in comparison with its degradation products. This new generation of adsorbents could thus be considered as powerful competitors to activated carbon for the water treatment of industrial effluents in acidic medium. These reports have shown that montmorillonite/ bentonite particularly important roles in this family of adsorbents and have been most extensively studied. Li et al. (2009) reported that the inorganic–organic bentonites were prepared by co-adsorption of cetyl trimethylammonium (CTMA) ions onto bentonites intercalated by poly(hydroxo aluminum) or poly(hydroxo iron) cations. The inorganic–organic bentonites adsorbed much more anionic herbicide 2,4-D than the inorganic and organic bentonites. For bentonites modified with poly(hydroxo iron) and CTMA ions, the enhancement may be attributed not only to the van der Waals interaction between 2,4D and the organic cations, but also to the strong bonding of 2,4-D on the inorganic cations, which was confirmed by desorption studies, XRD measurements and FTIR analysis. The inorganic–organic bentonites did not show higher adsorption of

acetochlor compared to the organo-bentonite. For such a nonionic herbicide, the van der Waals interaction dominated the adsorption, and the inorganic modification did not make an obvious contribution to the adsorption.

2.2 Adsorption of four pesticides by clay and modified clay

Besides, some other approaches (e. g., acid activation, heat treatment and surfactant) have been applied to modify the surface structure and physicochemical properties of bentonite, such as surface area, swelling ability, cation exchange capacity (CEC) or layer charge, which then may enhance the adsorption capacity of bentonite.

2.2.1 Adsorption of atrazine by modified clay

Ulrich et al. (2001), reported the adsorption of atrazine on clay minerals, such as kaolinite, illite and montmorillonite. The adsorption isotherms are linear at pH 5.8 in the low concentration range studied. The adsorption constant K_d is proportional to the external surface in Na^+ layer silicates. This implies that atrazine molecules do not intercalate even in swelling Na^+ clay minerals. González-Pradas (2003) interested the adsorption of 6-chloro-N2-ethyl-N4-isopropyl-1,3,5-triazine-2,4-diamine (atrazine) on heat treated kerolite samples at 110°C (K-110), 200°C (K-200), 400°C (K-400) and 600°C (K-600) from aqueous solution at 25°C. The evolution of surface properties of kerolite samples such as specific surface area and porosity after heat treatment was analysed. The adsorption experimental data points have been fitted to the Freundlich equation in order to calculate the adsorption capacities (K_f) of the samples; K_f values range from 468 mg kg⁻¹ for the K-110 sample up to 2291 mg kg⁻¹ for the K-600 sample. The values obtained for the removal efficiency (percentage of pesticide removed), ranged from 48% for K-110 up to 78% for K-600. The adsorption

experiments showed that the stronger heat treatment, the most effective adsorption of atrazine, so, as this type of clay is relatively plentiful, these activated samples might be used in order to remove this pesticide from water. Zadaka et al. (2009) reported the atrazine removal from water by two polycations pre-adsorbed on montmorillonite. Batch experiments demonstrated that the most suitable composite poly (4-vinylpyridine-co-styrene)-montmorillonite (PVP-co-S90% -mont.) removed 90–99% of atrazine (0.5–28 ppm) within 20–40 min at 0.367% w/w. Calculations employing Langmuir's equation could simulate and predict the kinetics and final extents of atrazine adsorption. Column filter experiments (columns 20_ 1.6 cm) which included 2 g of the PVP co-S90%-mont composite mixed with excess sand removed 93–96% of atrazine (800 ppb) for the first 800 pore volumes, whereas the same amount of granular activated carbon (GAC) removed 83–75% . In the presence of dissolved organic matter (DOM; 3.7 ppm) the efficiency of the GAC filter to remove atrazine decreased significantly (68–52% removal), whereas the corresponding efficiency of the PVP-co-S90%-mont. filter was only slightly influenced by DOM. Thus, the PVP-co-S90%-mont. composite is a new efficient material for the removal of atrazine from water. Zheng (2011) suggested that the organobentonite (CTMA-Bent) was prepared from Na⁺ saturated bentonite (Na-Bent) by intercalation with cetyltrimethylammonium bromide (CTMA), and used as a carrier of nanoscale zero valent iron (NZVI) for the removal of atrazine. The NZVI/CTMA-Bent composite was characterized by X-ray diffraction (XRD) and transmission electron microscope (TEM), and good dispersion of nanoscale iron particles on the carrier was observed. The removal efficiency of atrazine by this composite was compared with that by commercial iron powder and NZVI itself. For both treatments by NZVI and NZVI/CTMA-Bent, the removal

efficiency increased as the pH of the solution decreased, and the removal percentage of atrazine by NZVI/CTMA-Bent reached 63.5% at initial pH = 5.0 after 120 min. It is not only much higher than that (26.6%) by NZVI containing the same amount of iron, but also superior to the sum (32.1%) of reduction by NZVI plus adsorption by CTMA-Bent (5.5%). Besides, the NZVI/CTMA-Bent has a good long-term stability, and the carrier CTMA-Bent could prevent the iron ions (the byproduct of dechlorination) from leaching into the solution. Liu et al. (2014) studies the preparation, characterization and adsorption capacity for atrazine with magnetic mesoporous clay (sepiolite). They described about the Fe₃O₄/sepiolite magnetic composite (MSEP) was prepared by chemical co-precipitation method in air and used as adsorbent to remove atrazine from aqueous solution. The results show that the specific surface area, average pore diameter and pore volume were increasing. The adsorption experiments of atrazine onto MSEP show that the adsorption process followed the Langmuir isotherm model and the maximum adsorption capacity can reach 15.9 µg per unit BET surface area of adsorbent.

2.2.2 Adsorption of paraquat by modified clay

The surface properties of mineral clays include the presence of negative charge. As such mineral clays are good adsorbents owing to their high cation exchange capacity (CEC). So it is suitable to absorb the positively charged substances such as paraquat. The risk of contaminate by paraquat is enhanced by its high water solubility (7×10^5 mg.L⁻¹) (**Table 4.1**), and it has been detected in surface and drinking water. Thus, the necessity to reduce the concentration of paraquat in water is a worldwide challenge as far as water pollution is concerned. So, many researchers are interested to remove paraquat from water. For instance, Rytwo et al. (2002) reported the adsorption

of the divalent organic cations paraquat (PQ), diquat (DQ) and methyl green (MG) on sepiolite. The largest amounts of DQ, PQ and MG adsorbed were between 100% and 140% of the cation exchange capacity (CEC) of sepiolite. In previous experiments with monovalent organic cations (dyes), the largest amounts of these dyes adsorbed were about 400% of the CEC of sepiolite. Consequently, it was proposed that most of this adsorption was to neutral sites of the clay. The large differences between the adsorption of these divalent organic cations and the monovalent dyes may indicate that there is almost no interaction between DQ, PQ and MG and the neutral sites of sepiolite. Adsorption results were compared with calculations of an adsorption model that combines the Gouy–Chapman solution and specific binding in a closed system. The model considers cation adsorption on neutral sites of the clay, in addition to adsorption to mono- or divalent negatively charged sites, forming neutral or charged complexes. The model could adequately simulate the adsorption of the divalent organic cations DQ and PQ when added alone, and could yield good fit for the competitive adsorption experiment between the monovalent dye methylene blue and DQ. In competitive adsorption experiments, when total cationic charges exceeded the CEC, monovalent organic cations were preferentially adsorbed on the clay at the expense of the divalent cations. Seki and Yurdakoc (2005), reported the clays were compared with organoclays for the sorption of paraquat from aqueous solution. Sepiolite (S), bentonite (B), and illite (I) were used as clay samples. Organoclays were prepared by the modification of the clays with nonyl- and dodecylammonium chlorides. The adsorption data indicated that illite and modified illite with nonylammonium chlorides are the most effective adsorbents among these clays and organoclay samples, respectively. Tsai et al. (2003), described the effect of particle

size on the process of paraquat adsorption from aqueous solution onto an activated clay surface at 25°C and initial pH 11.0. The effect of the particle size of the clay adsorbent on the adsorption kinetics was found to be of considerable significance; namely, the rate constant (k) of paraquat adsorption by the clay adsorbent decreased with increasing particle size. Ait Sidhoum et al. (2013), reported the sorption-desorption of the paraquat on a bentonite from Maghnia (Algeria) desiccated at 110°C (M), and calcined at 400°C (M400) and 600°C (M600) from aqueous solution at 25°C has been studied using batch experiments. The results show that the sorption capacity of the calcined samples greatly decreased with heat treatment. On the other hand, the sorption process is hardly affected by the working temperature, whereas the higher electrolyte concentration, the lower sorption of this pesticide. Etcheverry et al. (2017), describes the beads of alginate montmorillonite have been used for the first time as sorbent of the cationic pesticide paraquat (PQ). They are a green material because they are formed by a biopolymer and a clay mineral, and because they allow using an energy efficient process to separate the beads after PQ adsorption. The general characterization of the beads, with montmorillonite contents ranging from 0% to 70%, has been carried out by elemental composition. PQ adsorption was studied with adsorption isotherms from aqueous solutions, and maximum adsorption capacities (Q_{\max}) were 0.093, 0.146, 0.187 and 0.278 mmol.g⁻¹ for montmorillonite contents of 0, 5, 30 and 70%, respectively. Q_{\max} varied linearly with the clay content. The results show that montmorillonite is practically the only PQ sorbent, with alginate acting mainly as support of the clay particles, but playing a very important role allowing an effortless handling of the material and the adsorbed pollutant.

2.2.3 Adsorption of diuron by modified clay

Bouras et al. (2007), present the results on the adsorption of diuron, a widely used herbicide, and its degradation products, on a series of three synthesized surfactant modified pillared montmorillonites, intercalated initially by Al(III), Fe(III) or Ti(IV) polycations and modified by co-adsorption with cetyl trimethylammonium bromide (CTAB). A comparative study of adsorption of the four compounds on each SMPC adsorbent shows the high adsorption capacity of diuron in comparison with its degradation products. This new generation of adsorbents could thus be considered as powerful competitors to activated carbon for the water treatment of industrial effluents in acidic medium.

Undabeytia et al. (2012), reported the slow release formulations of the herbicide diuron designed to reduce the risk of water pollution resulting from conventional formulations. The new formulations were based on herbicide incorporation in phosphatidylcholine (PC) vesicles that were adsorbed on the clay mineral montmorillonite. The active ingredient contents of the formulations reached up to 28% w/w. Thermal analysis revealed that the closely packed arrangement of PC on the clay enhanced diuron sorption by disrupting the interactions among PC molecules. Adsorption experiments using diuron were performed in soils with different physico-chemical properties to evaluate the relationship between the sorption and the mobility of the herbicide. In soil column experiments with sandy soil, the herbicide in PC-clay-based formulations mainly accumulated in the top soil, and there was a one-third reduction in leaching compared to the commercial formulation. The differences in leaching (compared to the commercial formulation) were lower when using loam soil due to its higher sorption of the herbicide and hysteresis effects. In the

sandy soil, bioassay experiments showed a higher herbicidal activity in the top-soil layer for the PC–clay formulations than for the commercial formulation. Therefore, PC–clay formulations of this herbicide can be used at lower doses than recommended, thereby reducing the environmental risks associated with the application of diuron formulations

2.2.4 Adsorption of 2,4-D by modified clay

Li et al. (2009), reported that inorganic–organic bentonites were prepared by co-adsorption of cetyl trimethylammonium (CTMA) ions onto bentonites intercalated by poly(hydroxo aluminum) or poly(hydroxo iron) cations. The inorganic–organic bentonites adsorbed much more of the anionic herbicide 2,4-D than the inorganic and organic bentonites. For bentonites modified with poly(hydroxo iron) and CTMA ions, the enhancement may be attributed not only to the van der Waals interaction between 2,4-D and the organic cations, but also to the strong bonding of 2,4-D on the inorganic cations. The inorganic–organic bentonites did not show higher adsorption of acetochlor compared to the organo-bentonite. For such a nonionic herbicide, the van der Waals interaction dominated the adsorption, and the inorganic modification did not make an obvious contribution to the adsorption. Bakhtiary et al. (2013) described about preparing, characterizing and examining the potentials of modified bentonite and zeolite in adsorption and release of 2,4-dichlorophenoxyacetic acid (2,4-D) herbicide. 2,4-D sorption of the N-cetylpyridinium (NCP) -modified bentonites and zeolites were much higher than those of unmodified substrates. The 2,4-D adsorption capacity of the organo-minerals increased with increasing surfactant loading. Desorption isotherms of 2,4-D did not coincide with their corresponding sorption isotherms showing hysteresis. The proportion of 2,4-D released from the

organo-minerals after seven desorption cycles varied between 29% and 50% of the total retained herbicide. The sorbed 2,4-D on the adsorbents showed a gradual release pattern with time. The release pattern of 2,4-D from NCP modified bentonite and zeolite, make these synthetic organo-minerals suitable candidates for slow release formulation of 2,4-D.

2.3 Adsorption

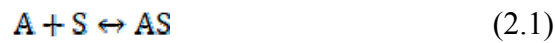
Adsorption is the phenomenon of accumulation of large number of molecular species at the surface of liquid or solid phase in comparison to the bulk (Hameed *et al.* 2007). One can find in the literature several models describing process of adsorption, namely Langmuir isotherm and Freundlich isotherm.

Langmuir's isotherm

Langmuir's isotherm describing the adsorption of adsorbate (A) onto the surface of the adsorbent (S) requires three assumptions:

- The surface of the adsorbent is in contact with a solution containing an adsorbate which is strongly attracted to the surface.
- The surface has a specific number of sites where the solute molecules can be adsorbed.
- The adsorption involves the attachment of only one layer of molecules to the surface, i.e. monolayer adsorption. The chemical reaction for monolayer adsorption.

The chemical reaction for monolayer adsorption can be represented as follows:



where A represents the adsorbate of interest in solution, S is an empty surface site, and AS is the surface species responsible for the adsorption. The equilibrium constant K_{ads} for this reaction is given by:

$$K_{ads} = \frac{[AS]}{[A][S]} \quad (2.2)$$

[A] denotes the concentration of A, while the other two terms [S] and [AS] are two-dimensional analogs of concentration and are expressed in units such as mol.cm⁻². The principle of chemical equilibrium holds with these terms. The complete form of the Langmuir isotherm considers Eq. (2.2) in terms of surface coverage θ which is defined as the fraction of the adsorption sites to which a solute molecule has become attached. An expression for the fraction of the surface with unattached sites is therefore (1 - θ). Given these definitions, thus rewrite the term [AS]/[S] as

$$\frac{[AS]}{[S]} = \frac{\theta}{(1-\theta)} \quad (2.3)$$

Express [A] as C and rewrite Eq. (2) as:

$$K_{ads} = \frac{\theta}{C(1-\theta)} \quad (2.4)$$

Rearranging, that obtain the final form of the Langmuir adsorption isotherm:

$$\theta = \frac{K_{ads}C}{1+K_{ads}C} \quad (2.5)$$

If we define Y as the amount of adsorption in units of moles adsorbate per mass adsorbent, and Y_{max} as the maximal adsorption, then:

$$\theta = \frac{Y}{Y_{max}} \quad (2.6)$$

and the isotherm can be expressed as:

$$\frac{C}{Y} = \frac{1}{K_{ads}Y_{max}} + \frac{C}{Y_{max}} \quad (2.7)$$

Where K_{ads} is the equilibrium constant, C is concentration of solute molecule at equilibrium, Y is the amount of mole of adsorbate per mass of adsorbent and Y_{max} is the maximal adsorption corresponding to complete monolayer coverage on the adsorbent surface.

Freundlich isotherm

Freundlich isotherm is an empirical model used to describe the adsorption in aqueous systems. This is commonly used to describe the adsorption characteristics for the heterogeneous surface, in which it is characterized by the heterogeneity factor $1/n$. Hence, the empirical equation can be written

$$q_e = K_F C_e^{1/n} \quad (2.8)$$

Where q_e is the solid phase adsorbate concentration in equilibrium (mg.g^{-1}), C_e the equilibrium liquid phase concentration (mg.L^{-1}), K_F the Freundlich constant (mg.g^{-1}) (L.mg^{-1})^{1/n} and $1/n$ is the heterogeneity factor. A linear form of the Freundlich expression can be obtained by taking logarithms of Eq. (2.9):

$$\ln q_e = \ln K_F + \frac{1}{n} \ln C_e \quad (2.9)$$

Therefore, a plot of $\ln q_e$ versus $\ln C_e$ enables the constant K_F and exponent $\frac{1}{n}$ to be determined.

2.4 References

- Ait Sidhoum, D., Socías-Viciana, M. M., Ureña-Amate, M. D., Derdour, A., González-Pradas, E., and Debbagh-Boutarbouch, N. (2013). Removal of paraquat from water by an Algerian bentonite. **Applied Clay Science**. 83-84: 441-448.
- Azejjel, H., Del Hoyo Martínez, C., Draoui, K., Rodriguez-Cruz, S., and Sánchez-Martín, M. (2009). Natural and modified clays from Morocco as sorbents of ionizable herbicides in aqueous medium. **Desalination**. 249: 1151-1158.
- Bakhtiary, S., Shirvani, M., and Shariatmadari, H. (2013). Adsorption-desorption behavior of 2,4-D on NCP-modified bentonite and zeolite: implications for slow-release herbicide formulations. **Chemosphere**. 90: 699-705.
- Bieseki, L., Treichel, H., Araujo, A. S., and Pergher, S. B. C. (2013). Porous materials obtained by acid treatment processing followed by pillaring of montmorillonite clays. **Applied Clay Science**. 85: 46-52.
- Bojemueller, E., Nennemann, A., and Lagaly, G. (2001). Enhanced pesticide adsorption by thermally modified bentonites. **Applied Clay Science**. 18: 277-284.
- Bouras, O., Bollinger, J.-C., Baudu, M., and Khalaf, H. (2007). Adsorption of diuron and its degradation products from aqueous solution by surfactant-modified pillared clays. **Applied Clay Science**. 37: 240-250.
- Choo, K. Y., and Bai, K. (2016). The effect of the mineralogical composition of various bentonites on CEC values determined by three different analytical methods. **Applied Clay Science**. 126: 153-159.

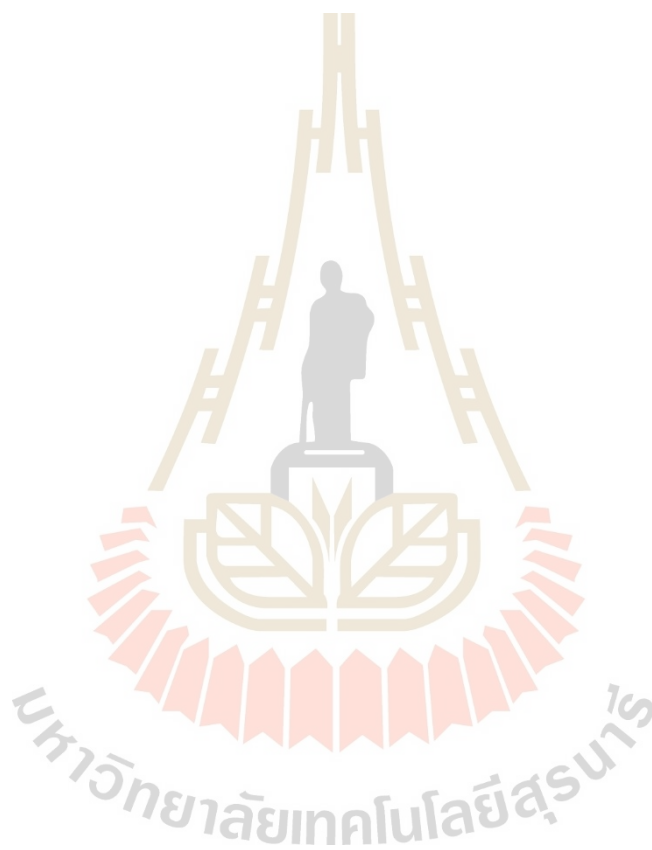
- Cuevas, J., Vigil de la Villa Mencía, R., Ramírez, S., Sánchez, L., Fernández, R., and Leguey, S. (2013). The alkaline reaction of FEBEX bentonite: a contribution to the study of the performance of bentonite/concrete engineered barrier system. **Journal of Iberian Geology**, 2006. 32: 147-169.
- Etcheverry, M., Cappa, V., Trelles, J., and Zanini, G. (2017). Montmorillonite-alginate beads: Natural mineral and biopolymers based sorbent of paraquat herbicides. **Journal of Environmental Chemical Engineering**. 5: 5868-5875.
- Gangula, S., Suen, S.-Y., and Conte, E. D. (2010). Analytical applications of admicelle and hemimicelle solid phase extraction of organic analytes. **Microchemical Journal**, 95, 2-4.
- Gates W. P., Anderson J. S., Raven M. D., and Churchman G. J. (2002). Mineralogy of a bentonite from Miles, Queensland, Australia and characterisation of its acid activation products. **Applied Clay Science**. 20: 189-197.
- González-Pradas, E. (2003). Adsorption of atrazine from aqueous solution on heat treated kerolites. **Chemosphere**. 51: 85-93.
- Gupta, V. K., Sharma, M., and Vyas, R. K. (2015). Hydrothermal modification and characterization of bentonite for reactive adsorption of methylene blue: An ESI-MS study. **Journal of Environmental Chemical Engineering**. 3: 2172-2179.
- Heller-Kallai, L. (2006). Chapter 7.2 Thermally Modified Clay Minerals. In B. K. G. T. Faïza Bergaya and L. Gerhard (Eds.), **Developments in Clay Science**. (Vol. Volume 1, pp. 289-308): Elsevier

- Javed, S. H., Zahir, A., Khan, A., Afzal, S., and Mansha, M. (2018). Adsorption of Mordant Red 73 dye on acid activated bentonite: Kinetics and thermodynamic study. **Journal of Molecular Liquids**. 254: 398-405.
- Jozefaciuk, G. (2002). Effect of acid and alkali treatments on surface-charge properties of selected minerals. **Clays and Clay Minerals - CLAYS CLAY MINER.** 50: 647-656.
- Lakevics, V., Stepanova, V., Skuja, I., Jurgelane, I., and Ruplis, A. (2014). Influence of Alkali and Acidic Treatment on Sorption Properties of Latvian Illite Clays. **Key Engineering Materials**. 604: 71-74.
- Li, J., Li, Y., and Lu, J. (2009). Adsorption of herbicides 2,4-D and acetochlor on inorganic–organic bentonites. **Applied Clay Science**. 46: 314-318.
- Liu, H., Chen, W., Liu, C., Liu, Y., and Dong, C. (2014). Magnetic mesoporous clay adsorbent: Preparation, characterization and adsorption capacity for atrazine. **Microporous and Mesoporous Materials**. 194: 72-78.
- Maqueda, C., dos Santos Afonso, M., Morillo, E., Torres Sánchez, R. M., Perez-Sayago, M., and Undabeytia, T. (2013). Adsorption of diuron on mechanically and thermally treated montmorillonite and sepiolite. **Applied Clay Science**. 72: 175-183.
- Murray, H. H. (2006). Chapter 2 Structure and Composition of the Clay Minerals and their Physical and Chemical Properties. In H. M. Haydn (Ed.), **Developments in Clay Science** (Vol. Volume 2, pp. 7-31): Elsevier
- Nones, J., Nones, J., Riella, H. G., Poli, A., Trentin, A. G., and Kuhnen, N. C. (2015). Thermal treatment of bentonite reduces aflatoxin b1 adsorption and affects

- stem cell death. **Materials science and engineering. C, Materials for biological applications.** 55: 530-537.
- Park, J.-H., Shin, H.-J., Kim, M. H., Kim, J.-S., Kang, N., Lee, J.-Y., and Kim, D.-D. (2016). Application of montmorillonite in bentonite as a pharmaceutical excipient in drug delivery systems. **Journal of Pharmaceutical Investigation.** 46: 363-375.
- Pentrák, M., Czímerová, A., Madejová, J., and Komadel, P. (2012). Changes in layer charge of clay minerals upon acid treatment as obtained from their interactions with methylene blue. **Applied Clay Science.** 55: 100-107.
- Pawar, R. R., Gupta, P., Lalhmunsiana, Bajaj, H. C., and Lee, S. M. (2016). Al-intercalated acid activated bentonite beads for the removal of aqueous phosphate. **The Science of the total environment.** 572: 1222-1230.
- Rezaei, R., Massinaei, M., and Zeraatkar Moghaddam, A. (2018). Removal of the residual xanthate from flotation plant tailings using modified bentonite. **Minerals Engineering.** 119: 1-10.
- Rytwo, G., Tropp, D., and Serban, C. (2002). Adsorption of diquat, paraquat and methyl green on sepiolite: experimental results and model calculations. **Applied Clay Science.** 20: 273-282.
- Seki, Y., and Yurdakoc, K. (2005). Paraquat adsorption onto clays and organoclays from aqueous solution. **Journal of colloid and interface science.** 287: 1-5.
- Tong, D. S., Zheng, Y. M., Yu, W. H., Wu, L. M., and Zhou, C. H. (2014). Catalytic cracking of rosin over acid-activated montmorillonite catalysts. **Applied Clay Science.** 100: 123-128.

- Tsai, W. T., Lai, C. W., and Hsien, K. J. (2003). The effects of pH and salinity on kinetics of paraquat sorption onto activated clay. **Colloids and Surfaces A: Physicochemical and Engineering Aspects**. 224: 99-105.
- Ulrich Herwig, Erwin Klumpp, Hans-Dieter Narres, Milan J. Schwuger (2001). Physicochemical interactions between atrazine and clay minerals. **Applied Clay Science**. 18: 211-222.
- Undabeytia, T., Recio, E., Maqueda, C., Sánchez-Verdejo, T., and Balek, V. (2012). Slow diuron release formulations based on clay–phosphatidylcholine complexes. **Applied Clay Science**. 55: 53-61.
- Ureña-Amate, M., Socías-Viciana, M. d. M., Gonzalez-Pradas, E., and Saifi, M. (2005). Effects of ionic strength and temperature on adsorption of atrazine by a heat treated kerolite. **Chemosphere**. 59: 69-74.
- Winda R., Jean-François, F., Thamrin, U., and Ze'phirin, M. (2018). Adsorption Characteristics of Bixin on Acid- and Alkali-Treated Kaolinite in Aprotic Solvents. **Bioinorganic Chemistry and Applications**. 1-9.
- Wu, P., Wu, H., and Li, R. (2005). The microstructural study of thermal treatment montmorillonite from Heping, China. **Spectrochimica acta. Part A, Molecular and biomolecular spectroscopy**. 61: 3020-3025.
- Yujiro, W., Hirohisa, Y., Junzo, T., and Yuzuke, M. (2005). Hydrothermal modification of natural zeolites to improve uptake of ammonium ions. **Journal of Chemical Technology & Biotechnology**. 80: 376-380.
- Zadaka, D., Nir, S., Radian, A., and Mishael, Y. G. (2009). Atrazine removal from water by polycation-clay composites: effect of dissolved organic matter and comparison to activated carbon. **Water research**. 43: 677-683.

Zhang, Y., Li, Y., and Zheng, X. (2011). Removal of atrazine by nanoscale zero valent iron supported on organobentonite. **The Science of the total environment.** 409: 625-630.



CHAPTER III

FACILE METHOD TO ENHANCE PESTICIDES ADSORPTION BY TREATED BENTONITE WITH HEAT AND ACID AS MULTIFUNCTIONAL ADSORBENTS

3.1 Abstract

The efficiency of combined heat and acid for modification of bentonite as multifunctional adsorbents, for removal of pesticides (atrazine, diuron, 2,4-D and paraquat) from aqueous solution was investigated. Bentonite was modified with single step as BA_{0.5} (with HCl 0.5M) and BC₅₀₀ (calcined at 500°C) and combined steps of heat and acid with different sequences (BA_{0.5}C₅₀₀ and BC₅₀₀A_{0.5}). These adsorbents were characterised by XRD, XRF, FT-IR ²⁷Al MAS NMR, BET, NH₃-TPD, SEM, TGA, HPLC and particle size analysis. Atrazine, diuron, 2,4-D and paraquat adsorptions were performed in aqueous solution at various pesticide concentrations, contact times and pH levels. It was found that the sequence of the treatment affects the atrazine adsorption significantly. The maximum atrazine adsorption is at pH 2.0 and the adsorption capability is in the order of BC₅₀₀> BC₅₀₀A_{0.5}> BA_{0.5}> BA_{0.5}C₅₀₀> Bentonite, but at a broad pH range of 3.0 to 9.0 BC₅₀₀A_{0.5} exhibits the highest efficiency on the atrazine adsorption. The maximum atrazine adsorption of BC₅₀₀A_{0.5}

is at pH 6.0 and its adsorption efficiency is about 12 times greater than that of the other adsorbents under the initial atrazine concentration of 50 mg.L^{-1} . The adsorption of diuron on all modified bentonites shows a similarly high capacity compared to unmodified bentonite and the adsorption decreases with an increase in pH. The greatest adsorption of 2,4-D prefers to BA_{0.5}C₅₀₀, occurred at pH 2-4. Additionally, adsorption of paraquat increases with an increase in pH. All adsorbents can absorb paraquat quite well except BA_{0.5}C₅₀₀. Additionally, adsorption of paraquat increased with increasing pH. All adsorbents can absorb paraquat well except BA_{0.5}C₅₀₀. For simultaneous adsorption of various pesticides, it was found that BC₅₀₀A_{0.5} is the most suitable adsorbent, consequently, it could be used as multifunctional adsorbent. In addition, the adsorption process of these pesticides on the adsorbents fitted well with Langmuir adsorption isotherm and pseudo-second order kinetics model.

3.2 Introduction

The agricultural use of organic pesticides has increased continuously over the past 30 years, and this has resulted in pesticide residue and metabolite contamination of soils and ground water (Ghimire and Woodward, 2013; Grovermann et al., 2013). Atrazine, diuron, 2,4-D and paraquat are one of the main pesticides used in agriculture, and there are many recent reports of studies into the absorption of four pesticides (Bouras et al., 2007; Castro et al., 2009; Chen et al., 2009; Kovaivos et al., 2011; Zadaka et al., 2009; Zhang et al., 2012.). Atrazine, diuron, 2,4-D and paraquat are widely used as a pre- and post-emergent herbicide to control and eliminate broad leaf weeds and grasses in field crops, orchards, and non-cropped areas (Velki et al., 2017). There are recent reports of the absorption of atrazine, diuron, 2,4-D and

paraquat, an endocrine disruptor for mammalian and aquatic life, by organisms. The toxicity of four pesticides for humans is manifested in different organs of humans (Jamil et al., 2011; Leite et al., 2013; Li et al., 2017; Rao and Chu, 2010; Salman et al., 2011). Due to four pesticides widespread application, long-term persistence in soil, significant leaching potential, and relatively high solubility in water, They are frequently detected in ground, surface, and drinking waters (Amaral et al. , 2014; Tomkins and Ilgner, 2002) . Therefore, it is necessary to limit the agrochemical substances discharged into the environment as much as possible, and also to act on removing them completely.

It is a challenge to find single method for atrazine diuron 2,4-D and paraquat removal from surface and ground waters, or for its elimination from contaminated aqueous effluents. Adsorption is a simple and convenient method for removal of the compound compared to other physical, chemical, or biological technologies. Various solid substrates offering good adsorptive properties, including clay minerals, zeolites, and activated carbon, are applied to the removal of organic contaminants from waters (Castro et al. , 2009; Chen et al. , 2009; Jamil et al. , 2011; Kovaivos et al. , 2011; Salvestrini et al. , 2010; Zadaka et al. , 2009; Zhang et al. , 2012). Raw bentonite is composed of diverse mineral substances, including quartz, cristobalite, feldspars, and several varieties of clay mineral. The major component of bentonite is montmorillonite, a dioctahedral smectite. Montmorillonite is a porous clay mineral consisting of a 2:1-layered structure, with alternating layers of exchangeable cations. The layers consist octahedral alumina sheets that are sandwiched by two tetrahedral silica sheets. Substituting Al^{3+} for Si^{4+} in the silica tetrahedral sheets and Mg^{2+} for Al^{3+} in the alumina octahedral sheets produces a net negative charge, which is usually

balanced by adsorbed cations. These cations are easily replaced by either organic or inorganic cations, accounts for the unique hydrophilic, tumescent, and adsorption properties of montmorillonite (Park et al., 2016). Bentonite clay minerals are available in Thailand; they are an important, low-cost source of montmorillonite and exhibit excellent adsorption capacities. Bentonite minerals have complex surface morphologies and provide a unique combination of properties, including thixotropic gel formation with water, good water adsorption capacity, large surface area, a layered structure and high cation exchange capability (CEC) (Choo and Bai, 2016; Murray, 2006).

Acid and thermal modification optimises the physical characteristics of bentonite for removal of contaminants by causing structural and textural changes within the clay, so enhancing adsorption capacity. Acid and thermal treatments are low-cost methods that require few chemicals and are simple to apply. Acid activated bentonite is suitable for removal or elimination of impurities; it increases both porous surface area and the numbers of silanol groups present in the clay, which are important for the adsorption of organic compounds (Komadel, 2016; Komadel and Madejová, 2006). Heat treatment significantly alters the surface properties of bentonite; it improves porosity by increasing mesopore volume, increases the number of surface adsorption sites, and increases the number of siloxane groups present, while it reduces the number of hydroxyl groups present (Bojemueller et al., 2001; Gupta et al., 2015; Heller-Kallai, 2006; Nones et al., 2015; Wu et al., 2005). In addition to these structural changes, both acid and heat treatments alter textural properties of the clay and improve its dispersibility in water. As mentioned above, the use of heat and acid for the treatments can promote pesticide adsorption performance. Thus, we are interested to

combined heat and acid in the modification of bentonite to optimise active sites for adsorption of different types of pesticides such as atrazine (basic), diuron (non-ionic), 2,4-D (acidic) and paraquat (cation) in aqueous media, including the investigation of simultaneous adsorption of these pesticides to evaluate the potentiality of these adsorbents for application as multifunctional adsorbents.

3.3 Material and Methods

3.2.1 Materials

Bentonite (B) was purchased from Thai Nippon Chemical Industry Co., Ltd. **Tables 3.1** and **3.4** list chemical and physical properties of bentonite. Reagent grade atrazine (2-chloro-4-ethylamino-6-isopropylamine-5-triazine), diuron (1,2-dimethyl-3,5-diphenylpyrazolium methyl sulfate), 2,4-D (2,4-dichlorophenoxy acetic acid) and paraquat (1,1'-dimethyl-4,4-bipyridinium dichloride) were obtained from Sigma-Aldrich.

3.2.2 Preparation of Modified Bentonite

Bentonite was sieved with 63 μm mesh and dried overnight at 110°C before using in the modification. Single-step modified bentonite (modified by either acid or heat) and two-step modified samples (modification with both acid and heat) were prepared by the following procedures;

Acid treatment

Bentonite (4 g) were activated by immersion in 100 mL HCl at various concentrations ($x = 0.1\text{--}3\text{ M HCl}$) at 100°C for 6 h (BA_x). Next, the mixture was centrifuged and washed with deionised-water (DI water) to ensure the removal of

chloride ions, then dried in an oven overnight at 110°C. The BA_x samples were stored in a desiccator

Heat treatment

Bentonite (4 g) were calcined at various temperatures ($y = 300\text{--}600^\circ\text{C}$) for 12 h. (BC_y), then cooled in a desiccator.

Combined acid and heat treatments

The obtained BA_x and BC_y samples were tested for atrazine, diuron, 2,4-D and paraquat adsorption. The sample activated with 0.5 M HCl (BA_{0.5}) and the 500°C heat-treated sample (BC₅₀₀) exhibited the best pesticide adsorption (data not shown). Therefore, BA_{0.5} and BC₅₀₀ were selected for combined acid and heat treatment. The BA_{0.5}BC₅₀₀ sample was prepared by calcination of BA_{0.5} (4 g) at 500°C for 12 h. BC₅₀₀BA_{0.5} was prepared following the same procedure, but using BC₅₀₀ in place of bentonite.

3.2.3 Characterization

The chemical compositions of the major elements in bentonite and modified bentonite were determined by energy dispersive XRF (EDS Oxford Instrument ED 2000) using an Rh X-ray tube with a vacuum medium. The CEC was determined by a standard method (Ross and Ketterings, 2011) in which all adsorbed cations in a bentonite sample are replaced by a common ion, such as NH₄⁺, and then the amount of adsorbed common ion is determined. The interlayer spacing of the samples were determined by X-Ray diffraction patterns obtained from back-pressed powder samples recorded on a Bruker, D5005 Cu K α radiation, scanning from 3°–50° at a rate of 0.05°/s at 35 mV and 35 mA. The framework and OH groups were confirmed by FT-IR spectroscopy (Spectrum GX, Perkin-Elmer) as KBr discs, over

the range 4000–400 cm^{-1} and near-IR diffuse reflection (DRIFT) in the range 8000–4000 cm^{-1} . The DRIFT technique is especially appropriate in this region because no sample dilution is required. Specific surface and pore size distributions were evaluated by nitrogen gas adsorption at -196°C using automated volumetric equipment (Autosorb 1-Quantachrome). All samples were characterised by solid state ^{27}Al CP/MAS NMR (JEOL JNM-ECA600), with a static 11 T magnetic field at a spin rate of 11 kHz. The ^{27}Al CP/MAS NMR spectra were recorded at a frequency of 130 MHz. The NMR reference used was $\text{Al}(\text{NO}_3)_3 \cdot 9\text{H}_2\text{O}$ with a chemical shift of 0.00 ppm. The particle size distributions (PDS) of all samples were analysed by a Horiba laser-scattering particle-size-distribution analyser (LA-950). Active site was determined using NH_3 temperature-program desorption (TPD) apparatus (BEL Japan, model BELCAT-B). Samples were pre-treated at 300°C for 2 h and then exposed to a flow of NH_3/He at 100°C for 30 min. Weakly adsorbed NH_3 was removed by flushing with He gas at 100°C for 30 min. The NH_3 TPD profile was obtained over the range 100° to 600°C at a heating rate of $10^\circ\text{C}/\text{min}$. Desorbed NH_3 was detected using a thermal conductivity detector. Scanning electron micrographs (SEM) were taken on a ZEISS, model AURIGA. The samples were deposited on a sample holder with an adhesive carbon foil and sputtered with gold. TGA curves are obtained by heating the sample in a alumina70 cell from 30 to 800°C at heating rate of $10^\circ\text{C min}^{-1}$ under an air atmosphere using a thermogravimetric analyzer (TGA-DSC, METTLER). TGA is a technique that measures changes in weight in relation to changes in temperature. The measured weight loss curve gives information on changes in sample composition and thermal stability. A derivative weight loss curve can be used to tell the point at which weight loss is most apparent. Atrazine, diuron, 2,4-D and paraquat concentration were

determined using UV-visible spectrophotometry at 223, 247, 283 and 257 nm, respectively (T80+UV-Vis spectrophotometer PG instruments). The mixture solution of atrazine, diuron, 2,4-D and paraquat concentration were determined using HPLC (Hewlett Packard series 1100). All experimental measurements were made in duplicate. The quantity of adsorbed atrazine, diuron, 2,4-D and paraquat by bentonite and modified bentonite was calculated from the difference between initial and final pesticide concentrations using the mass balance equation (3.1)

$$q_e = \frac{V(C_i - C_e)}{M} \quad (3.1)$$

Where, q_e is the adsorbed pesticide remaining on adsorbents (mg.g^{-1}) and C_i and C_e are the initial and final pesticide concentrations (mg.L^{-1}), respectively. M is the mass of adsorbent (g), and V is the volume of the pesticide solution (L).

3.2.4 Batch Adsorption

All adsorbents were dried overnight at 110°C prior to commencing the adsorption study. Adsorption experiments were performed by a batch adsorption procedure, using 20 mg of bentonite or modified bentonite added to 10 mL of pesticide solution, and then kept in a shaker bath at 30°C for 24 h. The stock solution were prepared in methanol solutions, final methanol concentrations were less than 0.5% (v/v) to avoid co-solvent effects (Xiang Li, 2016). Suspensions were centrifuged at 3500 rpm then filtered. Either pesticides concentration in filtrates was determined by UV-Vis spectroscopy.

3.2.5 Effect of pH

The effect of pH on the adsorption of atrazine, diuron, 2,4-D and paraquat by bentonite and modified bentonite was investigated over the pH range 2.0–12.0. Pesticide solutions were prepared by dissolving the samples in distilled water. The adsorbents were exposed to the pesticide solution at a solid/ liquid ratio of 20 mg/10 mL. The solution pH was adjusted by adding 0.1 or 0.01 M of HCl or NaOH solution, as appropriate. The mixture was placed on a shaker at 30°C until it reached equilibrium, then centrifuged to separate the filtrate from the solid phase. The filtrate was analysed for residual pesticide concentration. Duplicate tests were performed in all cases.

3.2.6 Simultaneous adsorption of various pesticides in solutions

The aqueous adsorbate solutions used in the adsorption study were: i) each pesticide ii) a quaternary-component solution of atrazine, diuron, 2,4-D and paraquat. The initial concentration of each adsorbate in all solutions was 50 ppm. The initial pH value was unadjusted (6.5 ± 0.5). The experiments were realized at room temperature and using equal volumes of adsorbate solutions, $V = 10.0$ mL. The mass of adsorbent in all the adsorption studies was 20.0 mg. The adsorption experiments were performed in a shaker, and then kept in a shaker for 24 h. Suspensions were centrifuged at 3500 rpm then filtered. Either pesticides concentration in filtrates was determined by UV-Vis spectroscopy. The quaternary-component solution containing all the investigated pesticides (atrazine, diuron, 2,4-D and paraquat) was determined by HPLC (Hewlett Packard series 1100) with diode array detector and UV detector. The ZORBAX Eclipse ODS C18 column (250 mm \times 4.6 mm, particle size 5 μ m) was equipped with HPLC system and the UV detector wavelength was set at 201, 223, 254

and 283 nm. Acetonitrile (A) and water pesticide (2% phosphoric acid) (B) used as mobile phases. The gradient program of HPLC was as follows: 0–13 min 100% B, 3–15 min 60% A and 40% B, 15–18 min 100%(A) and 20–30 min 100%A. The flow rate was set as 0.9 mL min⁻¹

3.2.7 Adsorption Isotherm

Adsorption isotherms for atrazine, diuron, 2,4-D and paraquat were acquired by batch equilibration using 20 mg of bentonite or modified bentonite in 10 mL of aqueous pesticide solution at various concentrations (10-120 ppm) at pH 3.0, 4.0 and 6.0±0.5. After equilibration, solid and liquid phases were separated by centrifugation. Atrazine, diuron, 2,4-D and paraquat concentration were determined spectrophotometrically by measuring absorbance at 223, 247, 283 and 257 nm, respectively. Data obtained from the adsorption tests were used to calculate adsorption capacity, q_e (mg. g⁻¹). The adsorption isotherms were evaluated by applying the Langmuir and Freundlich model.

3.2.8 Kinetic Adsorption Study

Kinetic adsorption experiments were performed at 30°C by contacting the adsorbents with pesticide solutions at a solid/liquid ratio of 20 mg/10 mL. In the first phase of the study, the mixtures were shaken and supernatants collected at the following times 2, 4, 6, 8, 10, 30, 60, 90, 120, 180, 240, 360, 720, 1,080 and 1,440 min, afterwards, supernatants were centrifugated and measured with spectrophotometrically at 223, 247, 283 and 257 nm. All of the batch tests were performed in duplicate and average values were used in the calculation. Deviations are less than 2%.

3.4 Results and Discussion

3.4.1 Characterization of Bentonite and Modified Bentonite

3.4.1.1 XRF and CEC analysis

Table 3.1 shows the effects of acid and heat treatment on the chemical and CEC properties of adsorbents. Acid treatment has a significant effect on chemical composition. The weight percentage of cations (Na^+ , Mg^{2+} , K^+ , Ca^{2+} , and Fe^{3+}) and of Al_2O_3 significantly decreases during both single-step and two-step treatments. For example, observe differences between $\text{BA}_{0.5}$, $\text{BC}_{500}\text{A}_{0.5}$, and $\text{BA}_{0.5}\text{C}_{500}$ that result from the effects of acid leaching. When comparing $\text{SiO}_2/\text{Al}_2\text{O}_3$ ratios for $\text{BC}_{500}\text{A}_{0.5}$ and $\text{BA}_{0.5}\text{C}_{500}$, we see that $\text{BA}_{0.5}\text{C}_{500}$, the sample receiving acid treatment prior to heat treatment, has a greater ratio because of the loss of Al_2O_3 (Table 1). This may be due to larger mean particle sizes of the calcined sample.

There are various methods available to determine CEC. Most approaches involve complete exchange of the naturally occurring cations in a clay mineral with a cationic species such as ammonium ion, followed by the removal of excess substitution ion and determination of the amount retained in the clay interlayer (Choo and Bai, 2016). It was found that CEC values for acid and heat-treated samples are lower than that for bentonite.

Table 3.1 Chemical composition and CEC values for bentonite and modified bentonite samples.

Sample	Chemical (%weight)											CEC	
	Na ₂ O	MgO	Al ₂ O ₃	SiO ₂	P ₂ O ₅	K ₂ O	CaO	TiO ₂	MnO	Fe ₂ O ₃	SiO ₂ / Al ₂ O ₃	(cmol. %LOI kg ⁻¹)	
Bentonite	0.079	0.607	9.472	78.543	1.347	1.703	2.813	0.788	0.045	4.239	8.29	67.62	13.04
BC ₅₀₀	0.058	0.760	9.426	78.914	1.308	1.693	2.750	0.805	0.044	4.021	8.37	47.21	4.98
BC ₅₀₀ A _{0.5}	ND	0.664	8.982	83.001	1.301	0.963	0.825	0.758	0.024	3.342	9.24	44.15	8.69
BA _{0.5}	ND	0.505	7.705	85.236	1.279	0.838	0.530	0.740	ND	2.957	11.06	43.45	9.43
BA _{0.5} C ₅₀₀	ND	0.642	7.355	85.001	1.274	0.832	0.558	0.740	0.020	2.687	11.56	19.11	4.29

The decrease in CEC value with acid treatment results from cationic leaching, while low CEC values resulting from heat treatment may be explained by charge reduction as a result of migration of small-radii cations into vacant octahedral sites and formation of covalent bonds after heating (Chorom and Rengasamy, 1996). Another explanation is that during calcination, the cation becomes more strongly bound to the surface, so that the exchange by NH₄⁺ becomes more difficult. However, the extent of charge reduction depends on the nature of the cation and the heating temperature.

3.4.1.2 XRD analysis

The swelling of bentonite is a consequence of its hydrated structure, in which cations are located in the interlayer space and solvated by water molecules adsorbed from atmosphere (Chorom and Rengasamy, 1996). XRD patterns

of bentonite (**Figure 3.1**) show characteristic diffraction peaks at $2\theta = 6.30, 19.77$ and 34.98 . Quartz (Q) and critobalite (C) impurities are observed in the patterns. The d_{001} reflection at $2\theta = 6.30$ corresponds to $d\text{-spacing} = 14.02 \text{ \AA}$, which is an interlayer comprising mono- and bi-layers of water molecules (Lee and Kim, 2002; Zaghouane-Boudiaf et al., 2014). A decrease in $d\text{-spacing}$ from calcination causes from removal of interlayer water and migration of exchangeable cation (Chorom and Rengasamy, 1996), and $d\text{-spacing}$ decreases from acid treatment results from removal of some cations. BC_{500} shows $d\text{-spacing} = 9.65 \text{ \AA}$, while $BA_{0.5}$ shows $d_{001} = 13.00 \text{ \AA}$ as shown in **Table 3.2** indicating that heat treatment effects basal spacing significantly. The small changes in $d\text{-spacing}$ were observed for all adsorbents after pesticide adsorptions, except BC_{500} , suggesting that the pesticides probably mainly bind to the active sites of face and edge, whereas the pesticides adsorptions may also involve the interlayer space for BC_{500} . In the case of $d\text{-spacing}$ for cationic pesticide (paraquat), it shows a similar value ($12.05\text{-}12.38 \text{ \AA}$), except $BA_{0.5}C_{500}$, suggesting that hydrated paraquat possibly exchange in the interlayer space with smaller size compare to interlayer water.

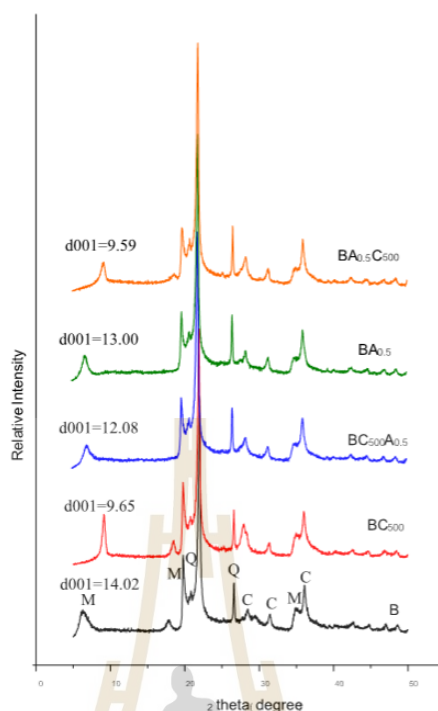


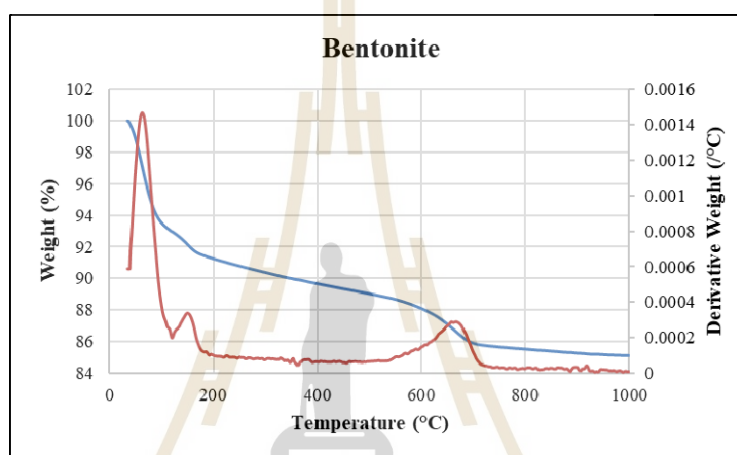
Figure 3.1 XRD patterns for bentonite, BC₅₀₀, BC₅₀₀A_{0.5}, BA_{0.5}, and BA_{0.5}C₅₀₀ adsorbents. (Q = quartz; M = montmorillonite; C = cristobalite.).

Table 3.2 The d-spacing (Å) of bentonite and modified bentonite changes upon atrazine, diuron, 2,4-D and paraquat adsorption.

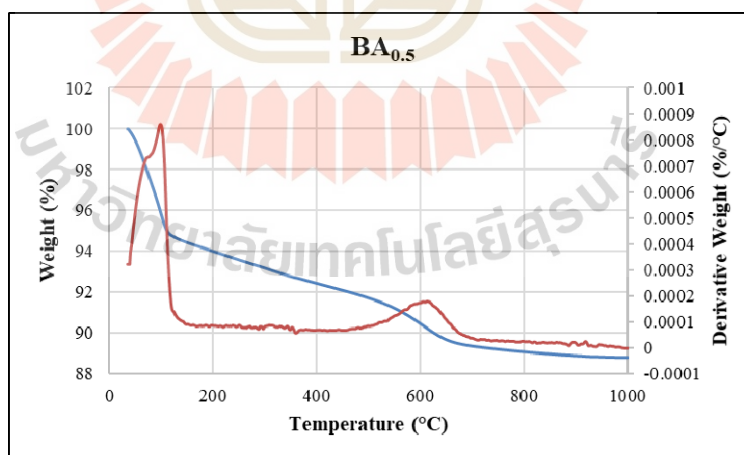
Samples	d-spacing (Å)				
	No adsorption	atrazine	diuron	2,4-D	paraquat
Bentonite	14.02	14.59	14.01	14.21	12.27
BC ₅₀₀	9.65	12.38	12.29	12.90	12.05
BA _{0.5}	13.00	13.71	12.47	13.36	12.16
BC ₅₀₀ A _{0.5}	12.08	12.76	12.17	12.54	12.38
BA _{0.5} C ₅₀₀	9.59	9.51	9.32	9.21	9.70

3.4.1.3 Thermogravimetric analysis

Figure 3.2 shows TGA and DTA thermograms of bentonite and modified bentonite. The weight loss observed between 50°C and 150°C and between 150°C and 400°C is due to the evaporation of water adsorbed on the adsorbents and probably due to hydrate water bound tightly to cations, respectively, and the amounts of water contained are shown in Table 3.3.



(a)



(b)

Figure 3.2 TGA/DTG for bentonite (a), BA_{0.5} (b), BC₅₀₀ (c), BA_{0.5}C₅₀₀ (d) and BC₅₀₀A_{0.5} (e).

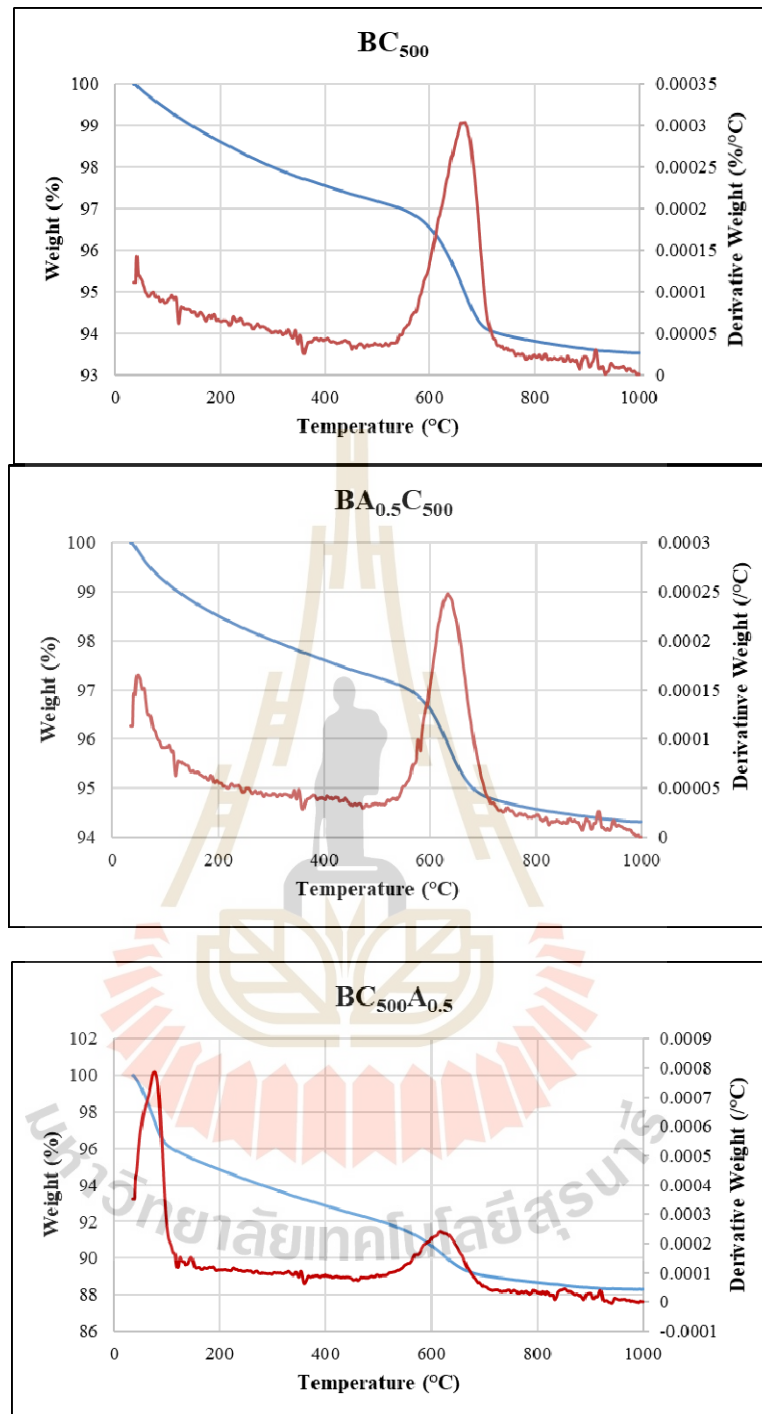


Figure 3.2 (Continued) TGA/DTG for bentonite (a), BA_{0.5} (b), BC₅₀₀ (c), BA_{0.5}C₅₀₀ (d) and BC₅₀₀A_{0.5} (e).

This results show that BC₅₀₀ and BA_{0.5}C₅₀₀ possesses low hydrophilic property due to low water contains. Above 500°C, the weight loss is traceable to dehydration of some trapped water molecules in the interstices of the clay layers and that due to dehydroxylation of the mineral, which is accompanied by a change in the crystal structure (Salawudeen T. Olalekan et al., 2010)

Table 3.3 The water content (%) in bentonite and modified bentonite.

Adsorbents	Weight loss (%)		
	50 - 150°C	150-400°C	500 – 800°C
B	7.83	2.50	5.75
BA _{0.5}	5.56	2.01	4.92
BC ₅₀₀	1.03	1.41	4.17
BA _{0.5} C ₅₀₀	1.18	1.21	2.97
BC ₅₀₀ A _{0.5}	4.59	2.54	4.28

3.4.1.4 FT-IR analysis

The middle-IR and near-IR spectra of adsorbents are shown in **Figures 3.3** and **3.4**, respectively. A characteristic bentonite stretching band at 3626 cm⁻¹ is attributed to OH-dioctahedral smectite. These spectra confirm that the modified bentonite samples are still characteristic of bentonite. Bands at 3420 cm⁻¹ and 1636 cm⁻¹ correspond to stretching and bending vibrations of hydrogen bonded water molecules (Komadel and Madejová, 2013) . After calcination, the spectra show decreases in the intensities of the Al-Al-OH band at 913–920 cm⁻¹ and the Al-Mg-OH

band at 840 cm^{-1} for BC_{500} and $\text{BA}_{0.5}\text{C}_{500}$ samples respectively, suggesting the occurrence of dehydroxylation during calcination (Heller-Kallai, 2006) and partial leaching of octahedral Al cations in acid treated samples (Tong et al., 2014). Changes in the tetrahedral sheets are reflected in the position and shape of the Si-O stretching band (Komadel and Madejová, 2013).; there is a slight decrease in the tetrahedral Si-O band intensity at 1039 cm^{-1} for modified samples. We assigned this to Si-O vibrations within a three-dimensional amorphous phase formed during the acid and thermal treatments (Komadel and Madejová, 2013). Two bands at 520 and 469 cm^{-1} correspond to bending vibrations of Al-O-Si and Si-O-Si, respectively. The band at 520 cm^{-1} is the most sensitive band to the presence of any remaining Al^{3+} species in the octahedral sheets (Erdogan Alver and Alver, 2012) and two samples of $\text{BA}_{0.5}$ and $\text{BA}_{0.5}\text{C}_{500}$ show those with more broad band obviously. The band at 622 cm^{-1} results from coupled Al-O and Si-O out-of-plane vibrations (Eren and Afsin, 2008).

NIR spectra were recorded to determine Si-OH groups in the adsorbent (**Figure 3.4**). The band at 4533 cm^{-1} and 7078 cm^{-1} are assigned to combination mode and first overtones ($2\nu_{\text{OH}}$) of structural OH groups, respectively, and the band at 5240 cm^{-1} corresponds to combination mode of water molecules (Heller-Kallai, 2006; Komadel and Madejová, 2006). $\text{BA}_{0.5}$, $\text{BA}_{0.5}\text{C}_{500}$ and $\text{BC}_{500}\text{A}_{0.5}$ show a new band at 7319 cm^{-1} assigned to the first overtone for silanol ($2\nu_{\text{Si-OH}}$), confirming formation of Si-OH groups during treatment with acid (Komadel and Madejová, 2013).

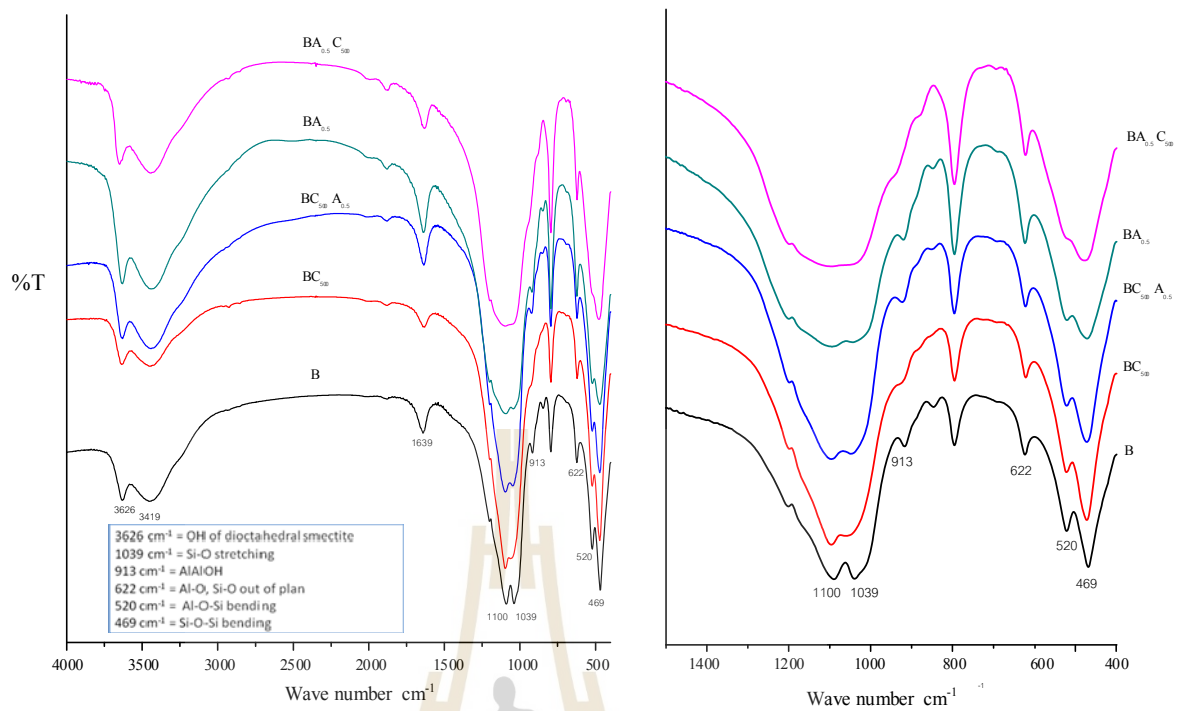


Figure 3.3 Mid FT-IR spectra of bentonite, BC₅₀₀, BC₅₀₀A_{0.5}, BA_{0.5} and BA_{0.5}C₅₀₀ samples.

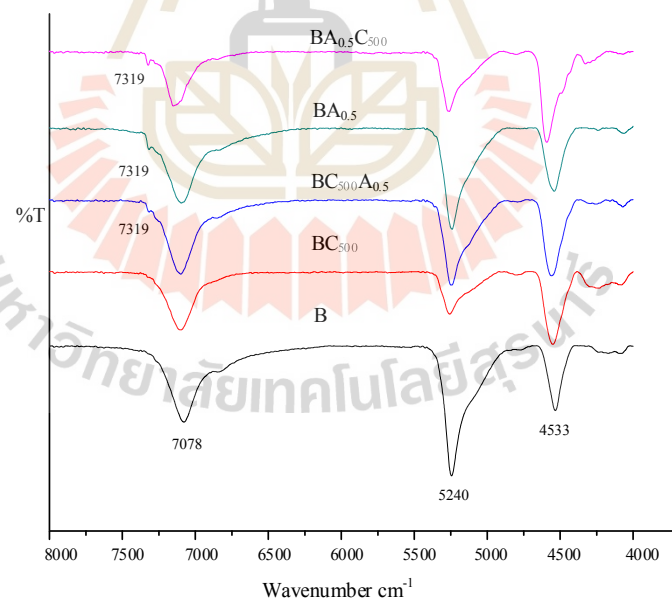


Figure 3.4 NIR FT-IR spectra of bentonite, BC₅₀₀, BC₅₀₀A_{0.5}, BA_{0.5} and BA_{0.5}C₅₀₀ samples.

3.4.1.5 Temperature-programmed desorption of ammonium (NH₃-TPD) study

The NH₃-TPD profile provides information on the strength and density of adsorbent surface acid sites. The NH₃-TPD profile of pristine bentonite shows three discrete desorption maximal peaks in the low-temperature region (50–200°C), medium temperature region (200–420°C), and the high-temperature region (420–800°C), which are attributed to weak, medium, and strongly acidic sites, respectively. **Figure 3.5** shows NH₃-TPD plots for bentonite and modified bentonite. All adsorbents exhibit a peak in the high-temperature region, corresponding to a strongly Lewis-acid site. We attribute this to desorption of NH₃ from Al on the surface of the adsorbent. The greatest density (3.071 mmol/g) of these acid sites are seen for BC₅₀₀A_{0.5}. The NH₃-TPD profiles for acid-activated adsorbents show additional peaks in the mid-temperature region (400–475°C) that can be ascribed to medium acidic Si-OH₂⁺ sites (Tong et al., 2014).

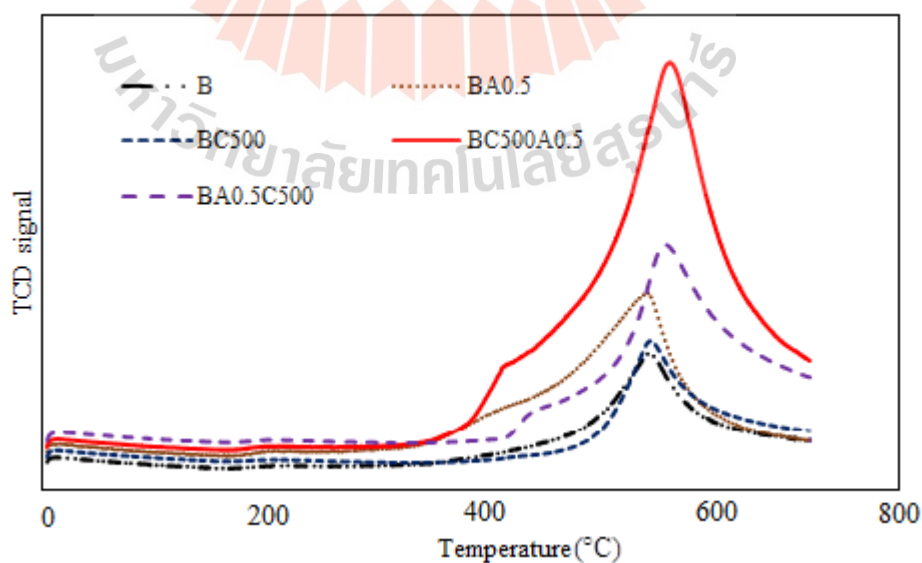


Figure 3.5 NH₃-TPD profiles for bentonite and modified bentonite.

3.4.1.6 NMR analysis

Figure 3.6 shows ^{27}Al MAS NMR spectra for all adsorbents. A major peak at 3.73 ppm in the spectrum for bentonite arises from 6-coordinated Al (Al(VI)), indicating that much of the aluminium is located in octahedral environments. It is notable that the octahedral peak is split in acid treatment performed in the final step. The two minor peaks at 68.25 Al(IV)a and 55.76 Al(IV)b are attributed to the four-coordinate, tetrahedral Al $\text{Q}^3(3\text{Si})$ and $\text{Q}^4(4\text{Si})$ core units, respectively (Brus et al., 2015; Takahashi et al., 2007). This minor peak area decreased after modification with acid. The result suggests that four-coordinate tetrahedral Al is easily removed. In the case of calcination (BC_{500}), the observed decrease in Al(IV) peak may result from some Al in the bentonite tetrahedral sheets probably substituted by other cations, such as Mg^{2+} and Ca^{2+} due to cation migration which are corresponded to elsewhere reports (Calvet and Prost, 1971; Heller-Kallai, 2006). In summary, these arguments account for the disappearance of two minor peaks of tetrahedral Al. The observe peak high for $\text{BA}_{0.5}\text{C}_{500}$ and $\text{BA}_{0.5}$ in these regions are similar, indicating that calcination following acid treatment does not affect the coordination of Al(IV). A small increase in Al(IV) peak hight for $\text{BC}_{500}\text{A}_{0.5}$ may result of Al adopting a tetrahedral site. Based on the NH_3 -TPD results indicate the adsorbents containing Al Lewis-acid sites (three-coordinate Al), although this is not apparent from ^{27}Al NMR spectra, consistent with literature reports (Brus et al., 2015).

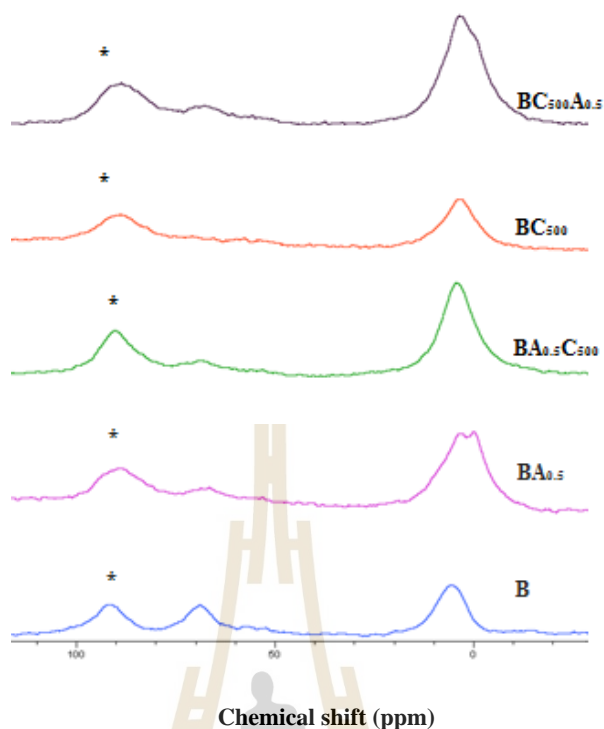


Figure 3.6 ^{27}Al MAS NMR spectra for bentonite and modified bentonite. (Spinning side-bands are marked with asterisks).

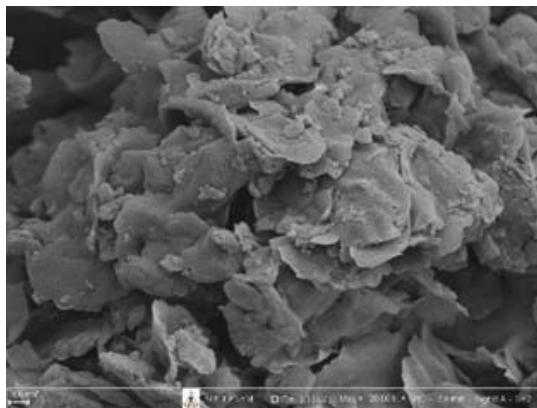
3.4.1.7 Textural properties study

Table 3.4 shows specific surface area, pore surface area, pore volume, mean pore volume and mean pore diameter, for all adsorbents. With the exception of particle size, the BC_{500} sample shows little change in these properties. Whereas, the samples treated with acid either in a single step or in combination with heat treatment ($\text{BA}_{0.5}$, $\text{BA}_{0.5}\text{C}_{500}$ and $\text{BC}_{500}\text{A}_{0.5}$) see increases in specific surface area and pore volume; these increases may result from larger cations such as Na^+ , Mg^{2+} , K^+ , Ca^{2+} and Fe^{3+} , including Al^{3+} being replaced by very small H^+ cations. Based on the results of XRD (**Figure 3.1**) and FT-IR spectra (**Figure 3.3**). The SEM micrographs of the bentonite and modified bentonite are shown in **Figure 3.7**. Bentonite exhibits a typical layered structure with a smooth surface and leafy

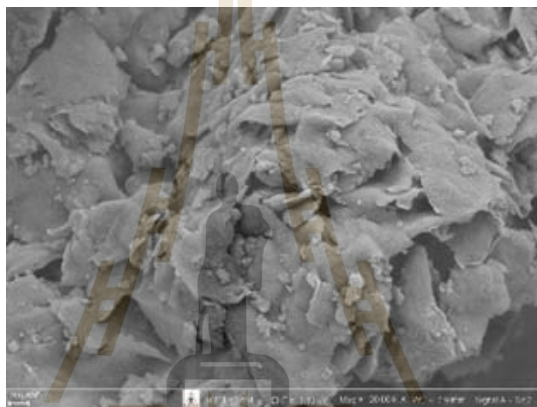
appearance. After modified under mild acid treatment, the layer structure was only slightly broken, suggesting that acid attacks the layer at the edges and surface faces. For thermal activation at 500°C BC₅₀₀ shows a similar layered structure of bentonite but its layer seems to be more firmly pack. Moreover, when combined with heat and acid (BA_{0.5}C₅₀₀, BC₅₀₀A_{0.5}) it shows closely packed texture of BA_{0.5}C₅₀₀ probably due to agglomeration in the face-to-face or face-to-edge contacts. If combination with acid after calcination like BC₅₀₀A_{0.5}, the texture appeared to be more flakes.

Table 3.4 Surface area, mean pore diameter and zeta potential of the bentonite and modified bentonite samples.

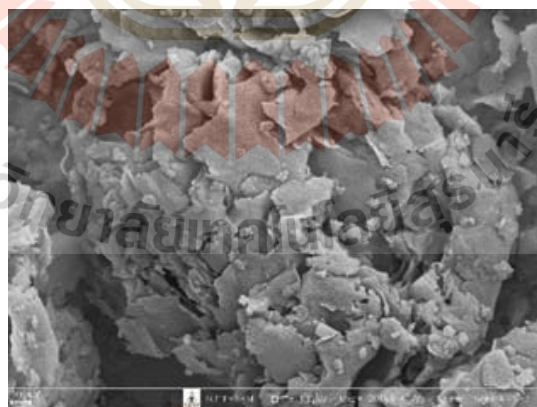
Main Characteristics	B	BC ₅₀₀	BC ₅₀₀ A _{0.5}	BA _{0.5}	BA _{0.5} C ₅₀₀
Specific surface area (m ² /g)	31.76	32.19	67.86	77.12	80.09
Pore surface area (m ² g ⁻¹)	30.901	31.301	55.354	64.704	69.154
Pore volume (cm ³ g ⁻¹)	0.1246	0.1247	0.1750	0.2281	0.2456
Zeta potential (mV)	-35.5	-22.5	-5.55	-11.4	4.83



(a)

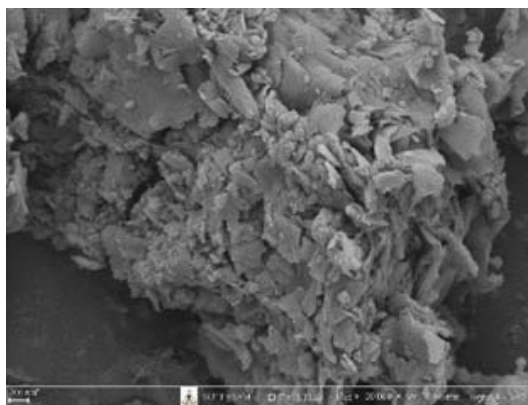


(b)

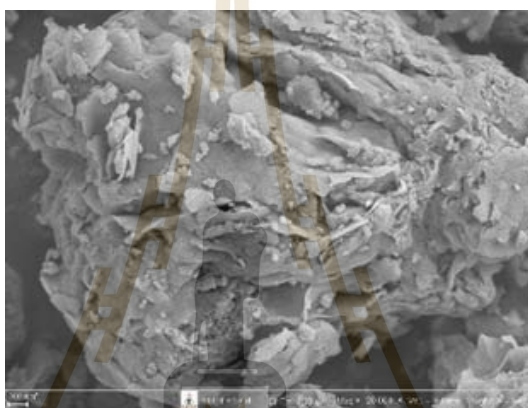


(c)

Figure 3.7 SEM micrographs of bentonite (a), BC₅₀₀ (b), BA_{0.5} (c), BC₅₀₀A_{0.5} (d) and BA_{0.5}C₅₀₀ (e).



(d)



(e)

Figure 3.7 (Continued) SEM micrographs of bentonite (a), BC₅₀₀ (b), BA_{0.5} (c), BC₅₀₀A_{0.5} (d) and BA_{0.5}C₅₀₀ (e).

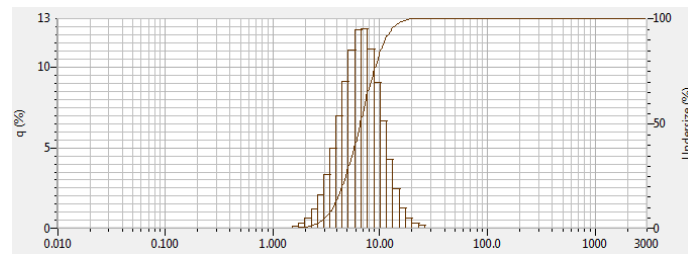
3.4.1.8 Particle size analysis

The particle size distributions and mean particle sizes are shown in **Figure 3.8** and **Table 3.5**, respectively. Samples treated first with acid, BA_{0.5}C₅₀₀ and BA_{0.5} show a bimodal particle-size-distribution. The BA_{0.5} sample has the maxima at approximately 11 μm (74.73%) and 25 μm (25.27%) (**Figure 3.8b**). The large particle size seen for BA_{0.5} may be due to formation of a stable aggregate via hydrogen bonding between silanol groups, while BA_{0.5}C₅₀₀ exhibits the maxima at approx. 13

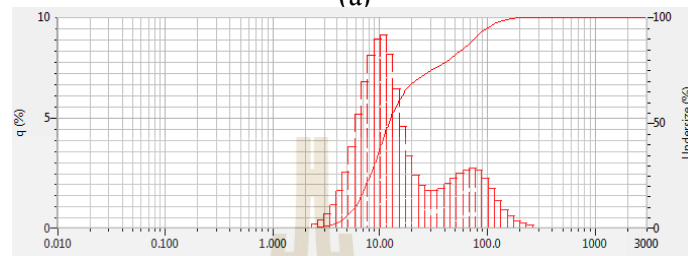
μm (58.39%) and 229 μm (41.61%) (**Figure 6c**). The larger particle size may result from an occurrence of dehydroxylation between aggregated particles due to calcination. On the other hand, the particle size distributions for BC₅₀₀A_{0.5} and BC₅₀₀ show only monomodal distributions, with maxima at about 9 and 11 μm , respectively (**Figure 3.8d, e**). The BC₅₀₀A_{0.5} particle size is smaller than that for BC₅₀₀ due to acid erosion.

Table 3.5 Measurement of particle size distribution.

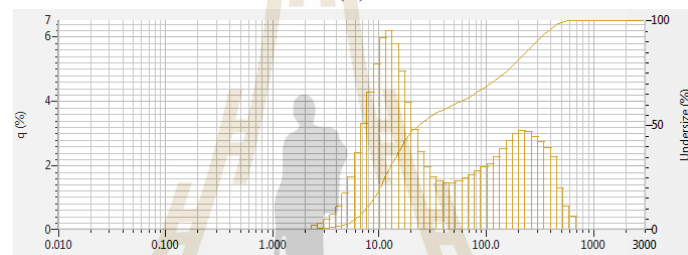
	Monomodal			Bimodal			
	B	BC ₅₀₀	BC ₅₀₀ A _{0.5}	BA _{0.5}	BA _{0.5} C ₅₀₀		
Diameter (μm)				Node 1	Node 2	Node 1	Node 2
				11.56	25.27	13.25	229.08
Undersize (%)				74.73	25.27	58.39	41.61
Mean particle Size (μm)	7.15	11.50	8.71	27.36		97.08	



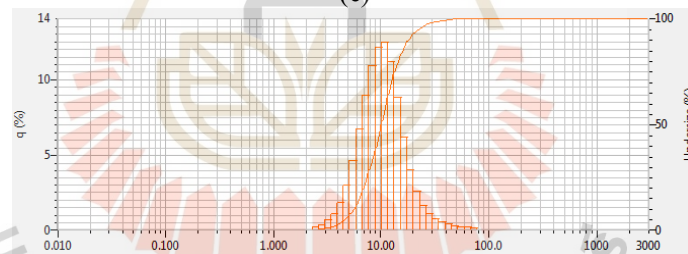
(a)



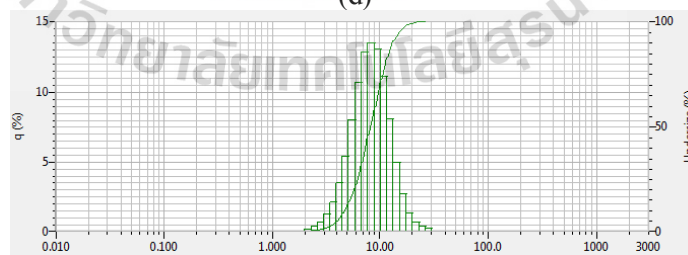
(b)



(c)



(d)



(e)

Diameter (micrometer)

Figure 3.8. Particle size distributions for bentonite (a), BA_{0.5}(b), BA_{0.5}C₅₀₀(c), BC₅₀₀(d), and BC₅₀₀A_{0.5} (e).

3.4.2 The Effect of pH

The changes in pH of the solution affect the speciation of adsorbent species, the adsorbent surface charge, and the degree of pesticide ionization (Moradi, 2014; Nejati, Davary and Saati, 2013). Bentonite can adsorb pesticides through two different mechanisms such as cation exchange and adsorption. (Nithya, K.M, 2010). Both mechanisms are pH dependent because during acid conditions most silanol and aluminol groups are protonated (Batchelor, 1998). The condition of the experiment was varied by adjusting pH ranging from 2.0-12.0 resulting in the change of surface charge of bentonite shown as the following equations (Deutsch, W.J., 1997).

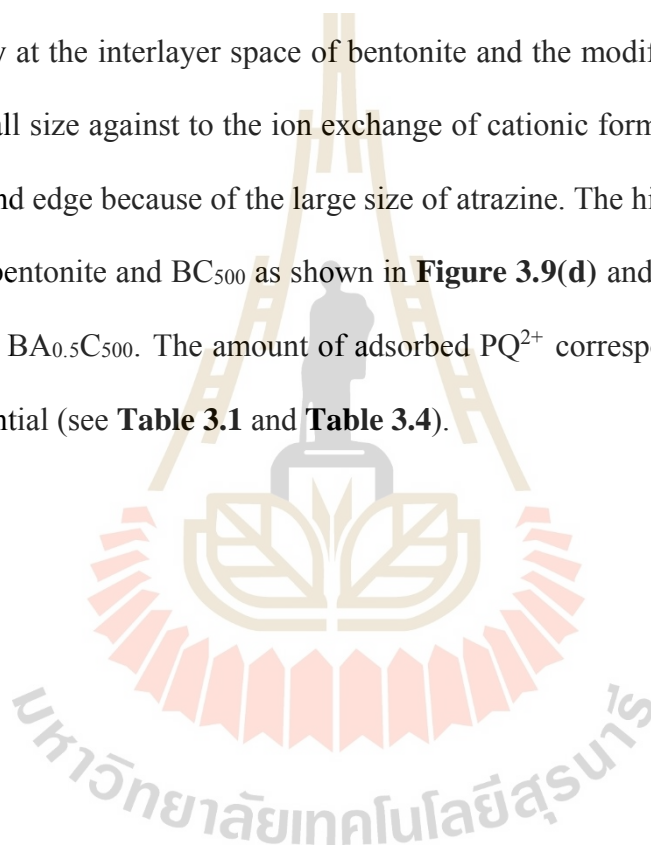


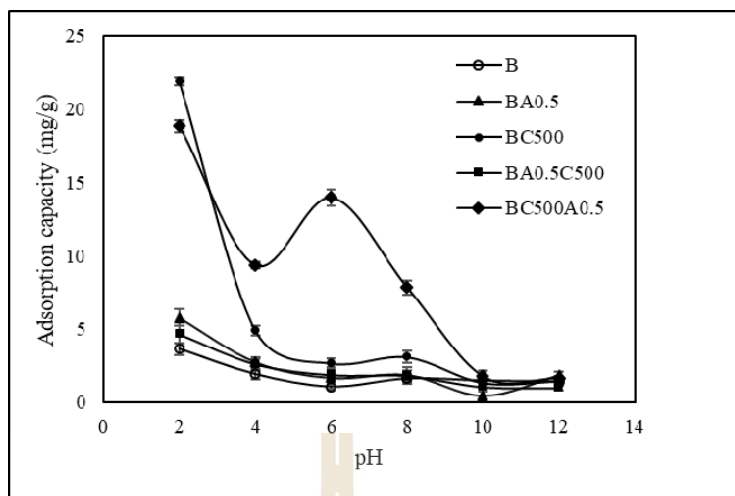
(M = Si or Al)

Figure 3.9 shows the effect of pH all pesticides adsorption by bentonite and modified bentonite. **Figure 3.9(a)** shows the effect of pH on atrazine adsorption by bentonite and modified bentonite. Atrazine is possible in either protonated or neutral form depending on solution pH. At pH values close to the pKa of atrazine (pKa = 1.7), both protonated and neutral forms are present in the solution. Protonated atrazine preferentially adsorbs by cation exchange, while the un-protonated tends to adsorb at adsorbent active sites. Based on the result of adsorption at pH 4-8, neutral form of atrazine seems to most preferential to BC₅₀₀A_{0.5}, because it shows the highest atrazine adsorption capacity. At pH 2.0 BC₅₀₀ sample exhibits the greatest atrazine adsorption capacity. It suggests that at pH 2, BC₅₀₀ removes atrazine mainly through ion exchange. At this pH the removal of atrazine would be through ion exchange and

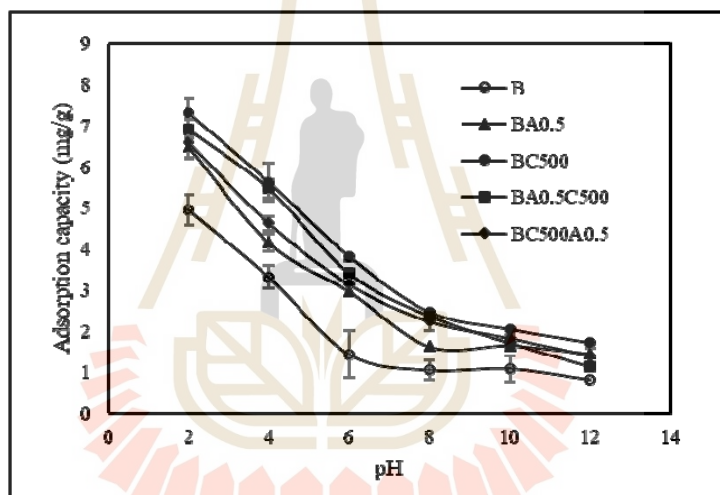
adsorption mechanism due to the existence of both form of atrazine. Even though, it has a lower CEC than bentonite indicating that ion exchange process of cationic atrazine occurs excellently on BC₅₀₀ at edge and face. This may be result from BC₅₀₀ holding more exchangeable cations at edge and face due to calcination. Thus, the cationic atrazine exchange occurs at these sites more easily than the interlayer space of bentonite. In the case of adsorbents activated with acid (BA_{0.5}C₅₀₀, BA_{0.5} and BC₅₀₀A_{0.5}), some partial cations are removed, so these adsorbents show lower CEC values compared to bentonite and BC₅₀₀ suggesting that this would cause a reduction in ion exchange. However, these adsorbents contain high specific surface areas and feature of Al Lewis-acid site, Si-OH and Si-OH₂⁺ groups which are available for both forms of atrazine to bind. However, BC₅₀₀A_{0.5} shows very high adsorption capacity compared to the other adsorbents, despite it having a smaller specific surface area (**Table 3.5**). Atrazine may bind to BC₅₀₀A_{0.5} through both ion exchange and by adsorption process. This may be result form its small particle size with highly active sites at edge and face positions enhancing the adsorption of atrazine. The interactions of neutral atrazine and the adsorbents are probably surface complex of atrazine and Al Lewis-acid and formation of hydrogen bonds with Si-OH and Si-OH₂⁺ groups. The adsorptions of diuron are shown in **Figure 3.9(b)**. Diuron exists a half of neutral form and a half of cationic form at around pH 4 (Bouras, 2007). According to the data, the high adsorption capacity of all adsorbents at low pH may be occurred mainly by ion exchange. The adsorption capacity of atrazine and diuron decreases with increasing pH, possibly due to competition between excess OH⁻ and adsorbate to interact with active sites. However, the high adsorption of diuron with BC₅₀₀ and BA_{0.5}C₅₀₀ compared to the others may cause from and increase in hydrophobicity of both

adsorbents for adsorption of neutral form. Considering the case of 2,4-D adsorption (**Figure 3.9(c)**), it has a pKa of 3.55; it can exist in both neutral and anionic form. At pH 3-6 anionic forms appear as around 22%-99.5% in aqueous solution (Ding, Lu et al., 2012). The lower adsorption capacity of 2,4-D with an increase in pH is probably due to more negative charge of the adsorbents. In contrast to the case of cationic pesticides (paraquat; PQ^{2+}), PQ^{2+} attaches to the active site through ion exchange arising mostly at the interlayer space of bentonite and the modified bentonite samples due to its small size against to the ion exchange of cationic form of atrazine occurring well at face and edge because of the large size of atrazine. The high adsorption of PQ^{2+} appeared on bentonite and BC₅₀₀ as shown in **Figure 3.9(d)** and the lowest adsorption of PQ^{2+} is on BA_{0.5}C₅₀₀. The amount of adsorbed PQ^{2+} corresponds the value of CEC and zeta potential (see **Table 3.1** and **Table 3.4**).



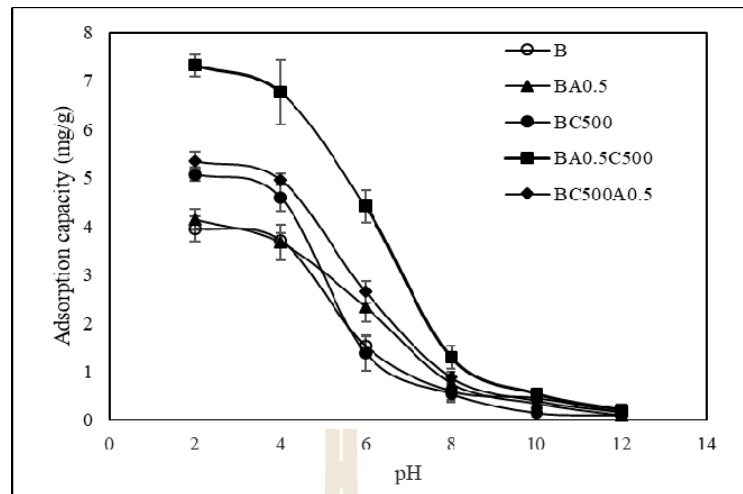


(a)

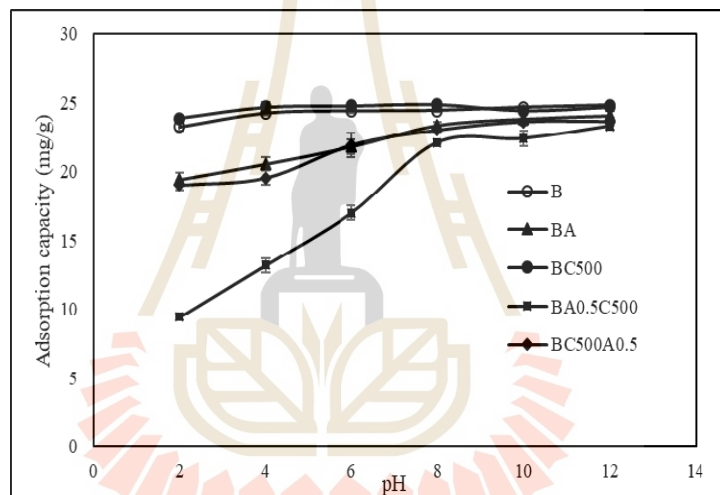


(b)

Figure 3.9 Adsorption capacity of modified and unmodified bentonite for atrazine (a), diuron (b), 2,4-D (c) and paraquat (d) at various pH at 50 ppm.



(c)



(d)

Figure 3.9 (Continued) Adsorption capacity of modified and unmodified bentonite for atrazine (a), diuron (b), 2,4-D (c) and paraquat (d) at various pH at 50 ppm.

3.4.3 Simultaneous adsorption of various pesticides in solutions

The results of each pesticides adsorption and simultaneous adsorptions of the pesticides (atrazine, diuron, 2,4-D and paraquat) from aqueous solution onto all adsorbents at ambient temperature and at initial pH of solution (6.5 ± 0.5) without pH adjustment are shown in **Figure 3.10 and 3.11**, respectively. Atrazine removal efficiencies for BC₅₀₀ ($3.16 \text{ mg} \cdot \text{g}^{-1}$), BA_{0.5} ($4.2 \text{ mg} \cdot \text{g}^{-1}$), and BA_{0.5}C₅₀₀ ($4.12 \text{ mg} \cdot \text{g}^{-1}$) shown in **Figure 3.10** are all of similar magnitude, while BC₅₀₀A_{0.5} provides the greatest removal efficiency with $14.65 \text{ mg} \cdot \text{g}^{-1}$. It is obvious that the removal efficiencies of atrazine for BA_{0.5}C₅₀₀ and BC₅₀₀A_{0.5} very different we can appreciate the importance of the sequencing of treatments.

The maximum total values of pesticides removed from aqueous belongs to BC₅₀₀A_{0.5}. This value confirms that BC₅₀₀A_{0.5} is the most suitable for removal various pesticides simultaneously, consequently, it could be regarded as an efficient multifunctional adsorbent for the investigated types of the pesticides.

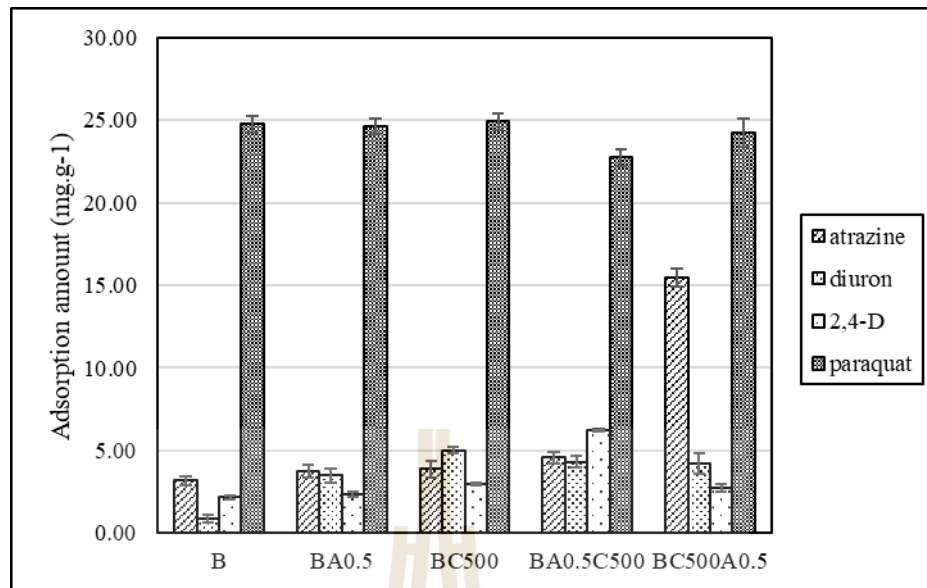


Figure 3.10 Adsorption of single-component pesticide (50 ppm) at pH 6.5±0.5 onto bentonite and modified bentonite.

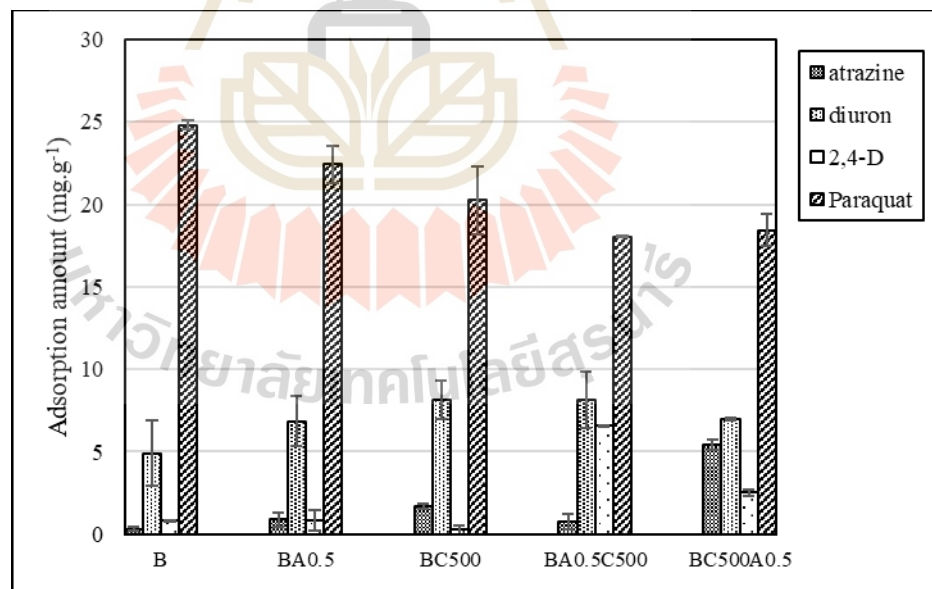


Figure 3.11 Adsorption of quaternary-component pesticides (50 ppm) at pH 6.5±0.5 onto bentonite and modified bentonite.

3.4.4 Adsorption Isotherms

The adsorption of atrazine, diuron, 2,4-D and paraquat as a function of contact time was first evaluated and an example of these data is shown in **Figure 3.12**. As it can be observed, the adsorption kinetics has similar trends and the pesticides adsorption can reach more than 90% in the initial 120 min and apparent equilibrium is reached within 12 h.

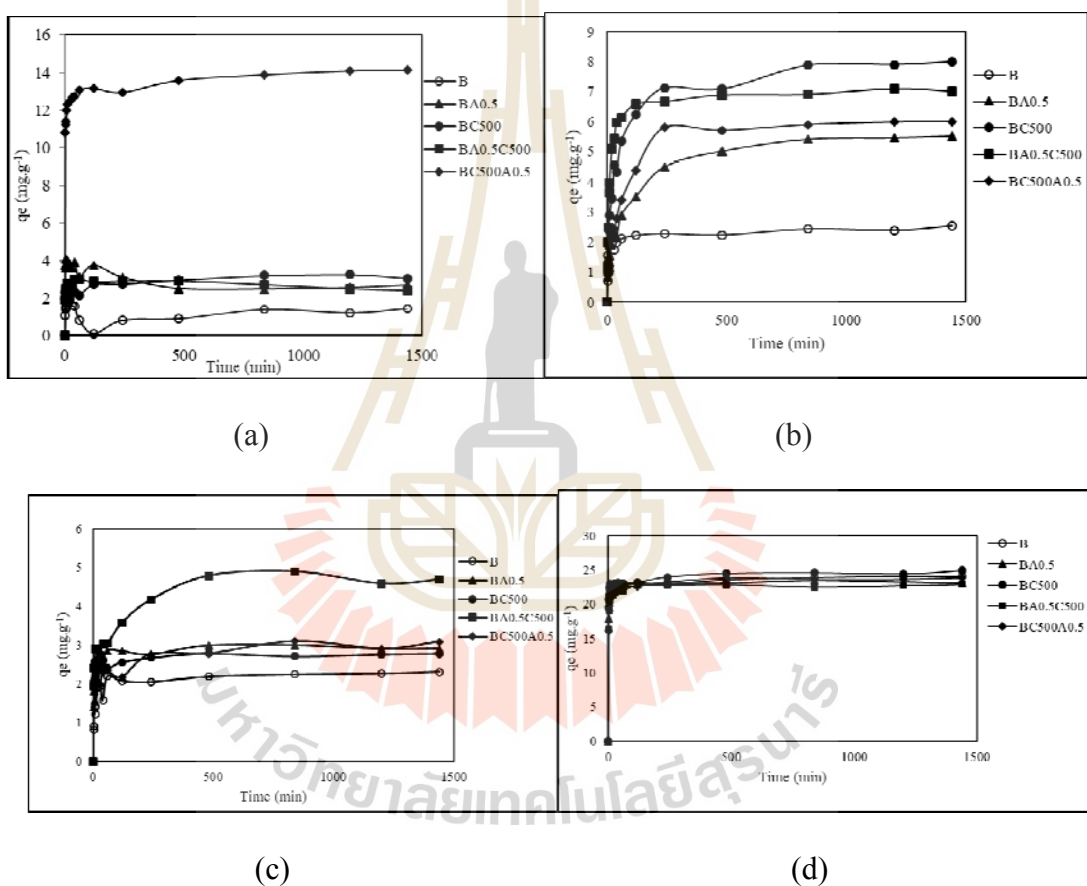


Figure 3.12 Adsorption of bentonite and modified bentonite samples for atrazine (a), diuron (b), 2,4-D (c) and paraquat (d) at 50 ppm.

Figure 3.13-3.16 show adsorption isotherms of bentonite and the modified bentonite samples at 30°C. The figure reveals that increased pesticides concentrations cause an increase in adsorption capacity. Optimal adsorption of atrazine, diuron and 2,4-D occurs at low pH but paraquat at high pH. Pesticides adsorption data were evaluated with Langmuir and Freundlich isotherm models. The Langmuir isotherm is used to determine monolayer and homogeneous adsorption on a surface (Zaghouane-Boudiaf et al., 2014). The Freundlich isotherm is an empirical equation that assumes the adsorption surface being heterogeneous during the course of the adsorption process or multilayer sorption (Ng et al., 2002).

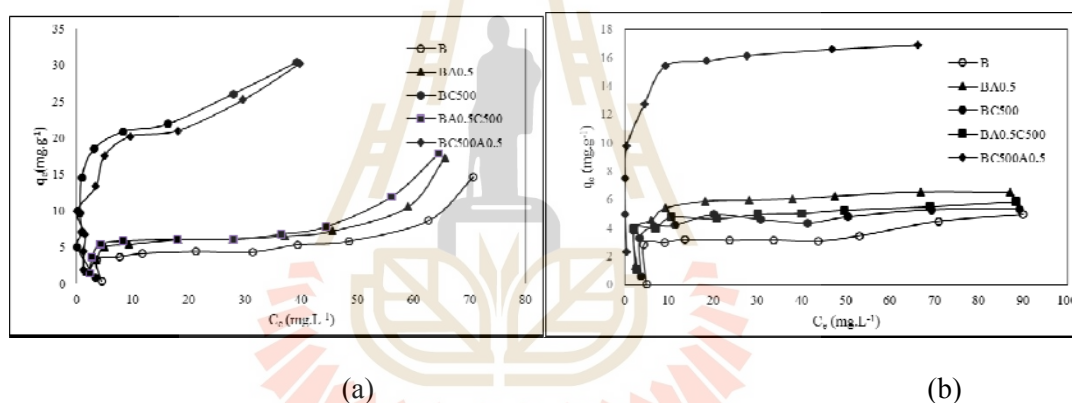
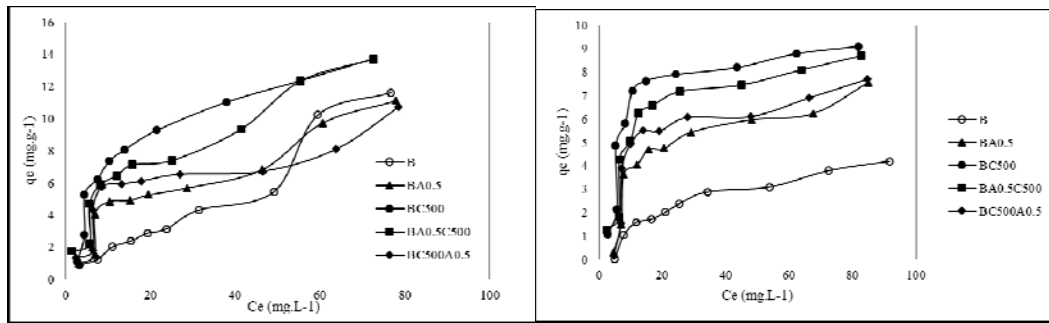


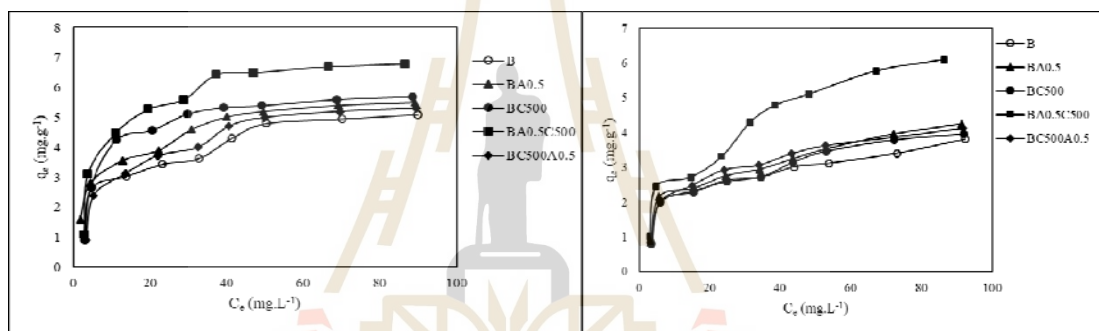
Figure 3.13 Equilibrium isotherms for adsorption of atrazine onto bentonite and modified bentonite at pH 3 (a) and pH 6 (b)



(a)

(b)

Figure 3.14 Equilibrium isotherms for adsorption of diuron onto bentonite and modified bentonite at pH 4 (a) and pH 6 (b)



(a)

(b)

Figure 3.15 Equilibrium isotherms for adsorption of 2,4-D onto bentonite and modified bentonite at pH 3 (a) and pH 6 (b)

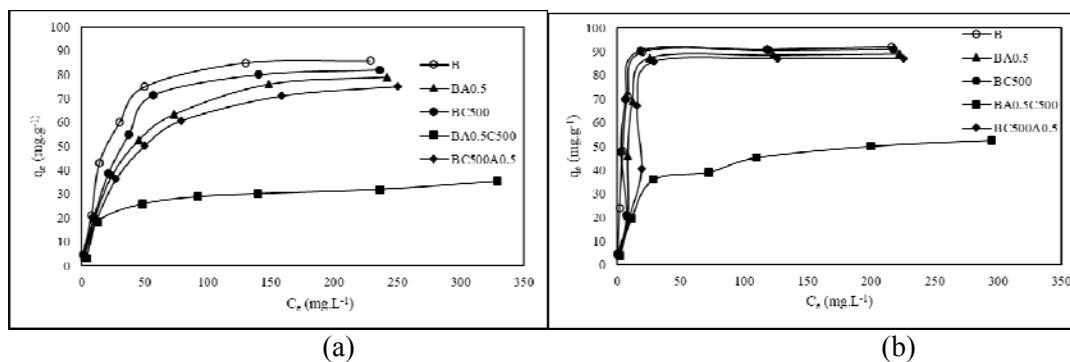


Figure 3.16 Equilibrium isotherms for adsorption of paraquat onto bentonite and modified bentonite at pH 6 (a) and pH 11 (b)

The linear forms of the Langmuir and Freundlich adsorption isotherms shown in Equations (3.3) and (3.4), respectively, were applied to quantitatively evaluate sorption performance.

$$\frac{C_e}{q_e} = \frac{C_e}{q_m} + \frac{1}{q_m K_L} \quad (3.3)$$

Where, C_e is the equilibrium concentration of pesticide in the bulk solution (mg.L^{-1}), q_e is the amount of pesticide adsorbed per unit mass of adsorbent at equilibrium (mg.g^{-1}), q_m is the maximum adsorption capacity (mg.g^{-1}), and K_L is the Langmuir constant (L.mg^{-1}).

$$\log q_e = \log K_F + \frac{1}{n} \log C_e \quad (3.4)$$

Where, K_F (units: $(\text{mg.g}^{-1}) (\text{L.mg}^{-1})^{1/n}$) is the Freundlich constant, characteristic of the system. The constant is indicative of the relative adsorption capacity of an adsorption, while the term $1/n$ represents adsorption intensity. The

detailed parameters of these different isotherm equations are also listed in **Table 3.6-3.9**. All correlation coefficients (R^2) exceed 0.9, suggesting that all models fit the experimental results well.

Table 3.6 Langmuir and Freundlich atrazine adsorption isotherm constants.

Samples	Langmuir			Freundlich		
	q_m (mg.g^{-1})	K_L (L.mg^{-1})	R^2	K_F (mg.g^{-1}). (L.mg^{-1}) ^{1/n}	n	R^2
Atrazine adsorption at pH 3						
B	1.71	3.52	0.5492	1.67	2.68	0.6572
BA _{0.5}	1.10	10.17	0.9209	2.25	2.74	0.7178
BC ₅₀₀	23.64	0.98	0.6046	11.15	3.67	0.8927
BA _{0.5} C ₅₀₀	1.00	13.34	0.7000	2.70	3.02	0.6798
BC ₅₀₀ A _{0.5}	4.87	9.55	0.9359	5.86	2.07	0.8867
Atrazine adsorption at pH 6						
B	3.18	1.01	0.9970	0.38	2.52	0.9822
BA _{0.5}	6.37	0.52	0.9993	0.28	1.99	0.9563
BC ₅₀₀	4.52	2.05	0.9920	0.36	2.38	0.9795
BA _{0.5} C ₅₀₀	5.22	0.53	0.9982	0.31	2.14	0.9651
BC ₅₀₀ A _{0.5}	15.87	3.64	0.9970	0.31	2.04	0.9902

Table 3.7 Langmuir and Freundlich diuron adsorption isotherm constants.

Samples	Langmuir			Freundlich		
	q_m (mg.g^{-1})	K_L (L.mg^{-1})	R^2	K_F (mg.g^{-1}). (L.mg^{-1}) ^{1/n}	n	R^2
Diuron adsorption at pH 4						
B	0.32	16.45	0.9263	2.71	1.45	0.9802
BA _{0.5}	1.44	4.75	0.9095	2.57	4.06	0.9571
BC ₅₀₀	2.05	5.70	0.9674	3.26	2.97	0.9961
BA _{0.5} C ₅₀₀	1.45	7.23	0.9980	1.80	2.10	0.9531
BC ₅₀₀ A _{0.5}	1.86	4.11	0.8283	2.92	3.86	0.8254
Diuron adsorption at pH 6						
B	0.17	31.71	0.9820	0.39	1.87	0.9703
BA _{0.5}	0.88	8.01	0.9327	2.08	3.61	0.9668
BC ₅₀₀	1.92	5.05	0.9541	4.01	5.08	0.8312
BA _{0.5} C ₅₀₀	1.24	7.41	0.9715	3.01	4.04	0.8983
BC ₅₀₀ A _{0.5}	1.19	6.38	0.9262	2.82	4.55	0.8886

Table 3.8 Langmuir and Freundlich 2,4-D adsorption isotherm constants.

Samples	Langmuir			Freundlich		
	q_m (mg.g^{-1})	K_L (L.mg^{-1})	R^2	K_F (mg.g^{-1}). (L.mg^{-1}) ^{1/n}	n	R^2
2,4-D adsorption at pH 3						
B	0.49	10.91	0.9956	1.68	4.06	0.9315
BA _{0.5}	1.28	4.12	0.9825	1.56	3.31	0.9526
BC ₅₀₀	1.25	4.73	0.9452	2.11	4.15	0.8880
BA _{0.5} C ₅₀₀	0.44	24.18	0.9843	2.37	3.92	0.9581
BC ₅₀₀ A _{0.5}	0.32	21.99	0.9962	1.46	3.34	0.9784
2,4-D adsorption at pH 6						
B	0.32	12.19	0.9968	1.26	4.32	0.9701
BA _{0.5}	0.31	14.74	0.9976	0.96	3.06	0.9906
BC ₅₀₀	0.28	15.24	0.9972	1.17	3.06	0.9479
BA _{0.5} C ₅₀₀	0.39	16.57	0.9925	0.58	1.80	0.9842
BC ₅₀₀ A _{0.5}	0.31	14.74	0.9986	1.22	3.70	0.9946

Table 3.9 Langmuir and Freundlich paraquat adsorption isotherm constants.

Samples	Langmuir			Freundlich		
	q_m (mg.g^{-1})	K_L (L.mg^{-1})	R^2	K_F (mg.g^{-1}). (L.mg^{-1}) ^{1/n}	n	R^2
paraquat adsorption at pH 6						
B	4.76	18.77	0.9972	6.69	1.81	0.8977
BA _{0.5}	1.75	100.39	0.9966	3.54	1.56	0.9266
BC ₅₀₀	3.58	23.26	0.9983	5.12	1.71	0.9101
BA _{0.5} C ₅₀₀	0.85	52.63	0.9987	11.83	5.26	0.9726
BC ₅₀₀ A _{0.5}	2.11	43.90	0.9986	2.44	1.43	0.8715
paraquat adsorption at pH 10						
B	32.36	2.40	0.9972	18.52	2.55	0.8977
BA _{0.5}	3.13	103.13	0.9966	8.57	1.87	0.9266
BC ₅₀₀	20.37	6.06	0.9983	16.49	2.50	0.9101
BA _{0.5} C ₅₀₀	2.39	25.03	0.9987	4.64	2.09	0.9726
BC ₅₀₀ A _{0.5}	2.14	155.80	0.9986	5.59	1.63	0.8715

The atrazine adsorption at pH 6 is fit well to Langmuir model more than Freundlich model and the calculated maximum monolayer (q_m) of adsorbed atrazine on BC₅₀₀A_{0.5} is higher than the other adsorbents. Additionally, at pH 3 the data fitted well to both the Langmuir and the Freundlich model for bentonite. Considering the R^2 values of BC₅₀₀, the Freundlich isotherm was found to be satisfactory for describing the adsorption surface becomes heterogeneous during the course of the ion exchange and adsorption process or multilayer sorption for cation and neutral atrazine. Therefore, BC₅₀₀ has a maximum adsorbed atrazine at low pH corresponding to the effect of pH on the adsorption as mention above. While BA_{0.5}, BC₅₀₀A_{0.5} and BA_{0.5}C₅₀₀ fitted to Langmuir isotherm better than Freundlich isotherm. The data of cationic and neutral diuron adsorption at pH 4 are fit to both Langmuir and Freundlich isotherm model for all adsorbents, indicating that adsorption sites on bentonite and the modified

bentonite are uniform and share the same adsorption energy and monolayer adsorption takes place and another position occurred multilayer sorption. Moreover, neutral diuron adsorption at pH 6 shows the best fit to Langmuir model more than Freundlich isotherm model for BC₅₀₀, BA_{0.5}C₅₀₀ and BC₅₀₀A_{0.5}. Therefore, diuron at pH 6 is preferentially adsorbed on bentonite and the modified bentonite surfaces via monolayer adsorption. In the case of bentonite and BA_{0.5} for diuron adsorption at pH 6, it is fit both the Langmuir and the Freundlich isotherm model. In the case of anion and cation pesticides would be described with 2,4-D and paraquat pesticide, respectively. The R² values of the data of neutral and anion 2,4-D adsorption at pH 3, are fit to both the Langmuir and the Freundlich isotherm model for all adsorbents. In addition, at pH 6 the adsorption is only anion 2,4-D and The R² value confirms the adsorption equilibrium data fitted well with Langmuir model. The q_m of 2,4-D adsorbed on BA_{0.5}C₅₀₀ is higher than that on the other adsorbents in this experiment. Moreover, the adsorption isotherm for removal of paraquat from aqueous solution, the R² values from Langmuir isotherm of all adsorbents are closed to 1 indicating that the surface of each adsorbent is unique for paraquat adsorption in monolayer adsorption. **Figure 3.17.** shows the adsorption isotherms of bentonite and the modified bentonite at 303, 313 and 323 K. The results indicate that atrazine, diuron and 2,4-D adsorptions increase with higher temperatures as being the cause of increased pesticides diffusion rates into active site of the adsorbents, but a little bit significant effect for paraquat adsorption.

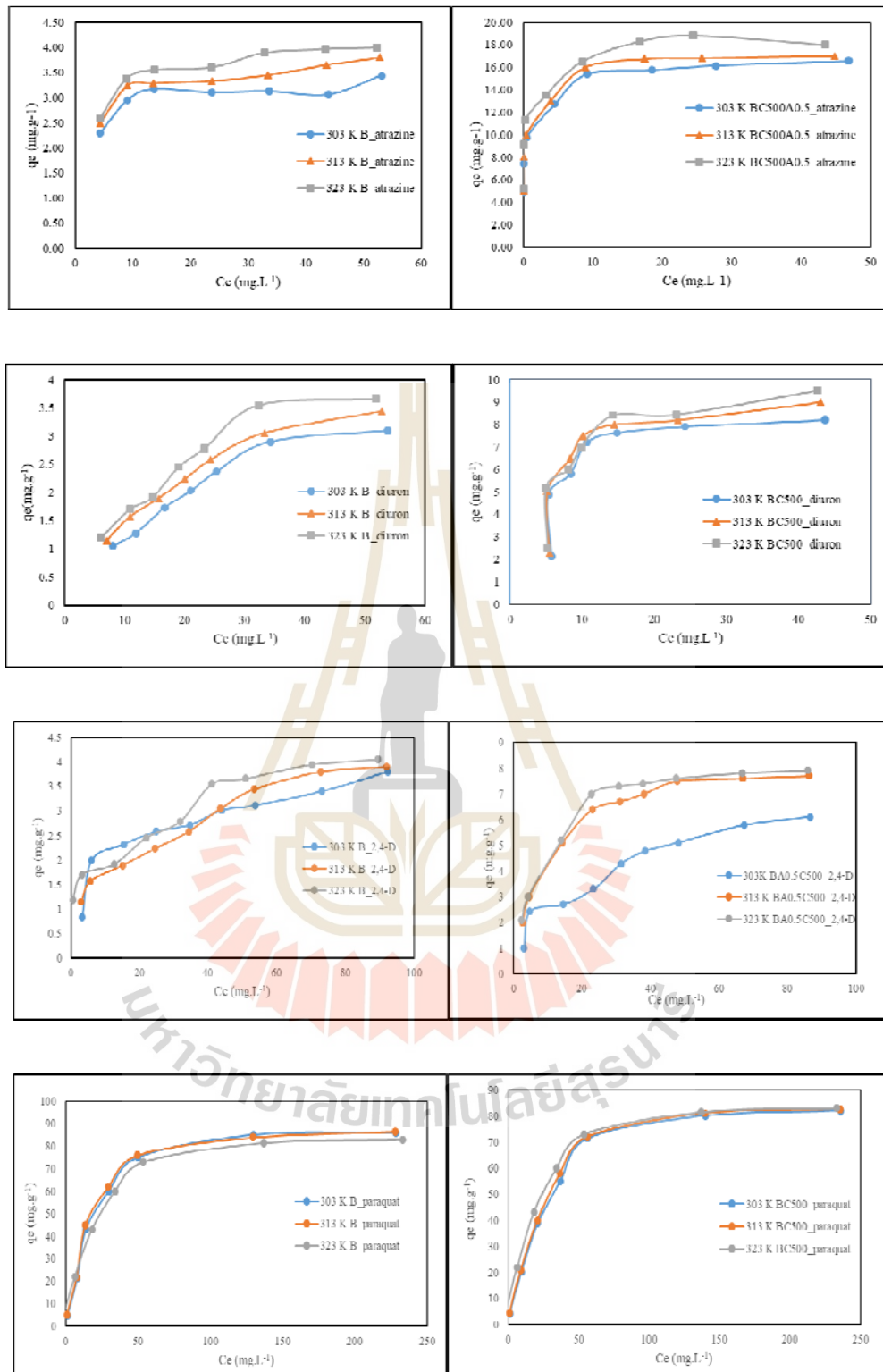


Figure 3.17 Adsorption isotherm of pesticide on bentonite and modified bentonite at 303, 313 and 323 K.

The maximum adsorption monolayer capacity (q_m) and the Langmuir constant (K_L), calculated from the slope and intercept of the linear plot are shown in Table 3.10-3.13.

Table 3.10 Parameters for adsorption of atrazine on bentonite and BC₅₀₀A_{0.5}.

Samples	Temperature (K)	Langmuir isotherm		
		q_m (mg.g ⁻¹)	K_L (M ⁻¹)	R^2
Bentonite	303	3.38	6.15	0.9915
	313	3.89	5.53	0.9964
	323	4.19	6.65	0.9990
BC ₅₀₀ A _{0.5}	303	16.64	452.14	0.9992
	313	17.15	632.94	0.9995
	323	18.35	955.66	0.9986

Table 3.11 Parameters for adsorption of diuron on bentonite and BC₅₀₀.

Samples	Temperature (K)	Langmuir isotherm		
		q_m (mg.g ⁻¹)	K_L (M ⁻¹)	R^2
Bentonite	303	5.12	0.83	0.9580
	313	5.10	1.06	0.9920
	323	5.45	1.30	0.9608
BC ₅₀₀	303	10.34	11.85	0.8725
	313	11.27	13.87	0.8531
	323	11.95	14.86	0.8935



Table 3.12 Parameters for adsorption of 2,4-D on bentonite and BA_{0.5}C₅₀₀.

Samples	Temperature (K)	Langmuir isotherm		
		q_m (mg.g ⁻¹)	K_L (M ⁻¹)	R^2
Bentonite	303	4.07	1.29	0.9829
	313	4.50	1.17	0.9618
	323	4.40	1.85	0.9643
BA _{0.5} C ₅₀₀	303	7.37	2.66	0.9662
	313	8.55	8.64	0.9990
	323	8.66	10.45	0.9981



Table 3.13 Parameters for adsorption of paraquat on bentonite and BC₅₀₀.

Samples	Temperature (K)	Langmuir isotherm		
		q _m (mg.g ⁻¹)	K _L (M ⁻¹)	R ²
Bentonite	303	94.34	480.83	0.9966
	313	92.59	563.90	0.9970
	323	87.72	4023.82	0.9697
BC ₅₀₀	303	92.59	328.58	0.9959
	313	84.03	1446.36	0.9671
	323	84.03	1446.36	0.9671

Enthalpy (ΔH), entropy (ΔS) and free energy (ΔG) changes explained the thermodynamic data for adsorption process which were calculated by:

$$\Delta G^\circ = -RT \ln K_L \quad (3.5)$$

Where R is the gas constant (8.314 J.mol⁻¹.k⁻¹); T is temperature (K) and K_L is adsorption constant in the Langmuir isotherm. The values of ΔH° and ΔS° can be calculated from the slope and intercept of the linear variation of ln K_L with reciprocal of temperature (1/T) as in the following equation.

$$\ln K_L = -\frac{\Delta H^\circ}{RT} + \frac{\Delta S^\circ}{R} \quad (3.6)$$

The thermodynamic parameters of the system: Gibbs free energy change (ΔG°), enthalpy change (ΔH°), and entropy change (ΔS°), are presented in **Table 3.14-3.17**; the free energy values at temperatures 303K, 313K and 323K in adsorption of pesticides are negative in all cases showing the spontaneous nature of the process. ΔH° values are positive for all of the pesticides, showing the endothermic nature of the adsorption process. ΔS° values are also reported; positive values suggest that the organization of the adsorbate in the solid-solution interface becomes more random.

Table 3.14 Thermodynamic parameters for adsorption of atrazine on bentonite and BC_{500A0.5}.

Sample	Temp (K)	ΔG (kJ.mol ⁻¹)	ΔH (kJ.mol ⁻¹)	ΔS (J.mol ⁻¹ .K ⁻¹)	R ²
Bentonite	303	-4.57			0.1668
	313	-4.45	3.08	24.89	
	323	-5.09			
BC _{500A0.5}	303	-15.40			0.9941
	313	-16.78	30.40	151.04	
	323	-18.43			

Table 3.15 Thermodynamic parameters for adsorption of diuron on bentonite and BC₅₀₀.

Sample	Temp (K)	ΔG (kJ.mol ⁻¹)	ΔH (kJ.mol ⁻¹)	ΔS (J.mol ⁻¹ .K ⁻¹)	R ²
Bentonite	303	0.475			
	313	-0.154	18.35	59.05	0.9988
	323	-0.70			
303	-15.40				
BC ₅₀₀	313	-16.78	9.24	51.18	0.9591
	323	-18.43			

Table 3.16 Thermodynamic parameters for adsorption of 2,4-D on bentonite and BA_{0.5}C₅₀₀.

Sample	Temp (K)	ΔG (kJ.mol ⁻¹)	ΔH (kJ.mol ⁻¹)	ΔS (J.mol ⁻¹ .K ⁻¹)	R ²
	303	-0.64			
Bentonite	313	-0.42	14.30	48.59	0.5432
	323	-1.65			
	303	-2.46			
BA _{0.5} C ₅₀₀	313	-5.61	56.16	194.74	0.8648
	323	-6.30			



Table 3.17 Thermodynamic parameters for adsorption of paraquat on bentonite and BC₅₀₀.

Sample	Temp (K)	ΔG (kJ.mol ⁻¹)	ΔH (kJ.mol ⁻¹)	ΔS (J.mol ⁻¹ .K ⁻¹)	R ²
Bentonite	303	-15.56			
	313	-16.48	85.62	331.40	0.7911
	323	-22.28			
BC ₅₀₀	303	-14.6			
	313	-18.96	60.92	251.15	0.7658
	323	-19.54			

3.4.5 Kinetic Experiments

Kinetics studies on the adsorption of pesticide onto bentonite and modified bentonites were performed and the results are shown in **Figure 3.18**. Measurements were made using 20 mg adsorbent at 30°C, with atrazine concentrations of 50 ppm. All adsorbents exhibit high affinity for atrazine during the first 50 minutes, and equilibrium was reached within 200 min.

Pseudo-first and pseudo-second order models were employed to correlate the kinetics data. A pseudo-first order kinetics adsorption model was suggested for the sorption of solid/ liquid systems and is expressed in integrated and linear form **Equation (3.7)** (Yuh-Shan, 2004).

$$\log(q_e - q_t) = \log q_e - \frac{k_1}{2.303} t \quad (3.7)$$

Where, k_1 is the adsorption rate constant (min^{-1}), q_e and q_t are the atrazine adsorption loadings (mg.g^{-1}) at equilibrium and at time, t (min), respectively. If the pseudo-first-order kinetics is applicable, a plot of $\log(q_e - q_t)$ versus t should provide a straight line, from which k_1 and a predicted value for q_e can be determined from the slope and intercept of the plot.

The pseudo-second order kinetics model is expressed by **Equation (3.8)** (Ho and McKay, 1999).

$$\frac{t}{q_t} = \frac{1}{q_e} t + \frac{1}{k_2 q_e^2} \quad (3.8)$$

Where k_2 ($\text{g.mg}^{-1}.\text{min}^{-1}$) is the pseudo-second-order adsorption rate constant. A plot of t/q_t against t (**Figure 3.18**) yields a straight line, from which the rate constant K_2 and q_e can be calculated. The pseudo-second order model is based on the assumption that the rate-limiting step may be chemisorption, which involves valence forces by electron sharing or electron exchange between the adsorbent and the adsorbate. **Table 3.18-3.21** shows maximum adsorption capacities q_e , k_1 , k_2 and the correlation coefficient R^2 , calculated from the pseudo-first and pseudo-second order models. The maximum adsorption capacity, q_e , calculated from the pseudo-second order equation are in accordance with the experimentally determined values. The R^2 values for the pseudo-second order are greater than they are in the pseudo-first order

model. These results suggest that adsorption obeys a pseudo-second order model. It indicated that the adsorption of pesticide occurs by a chemisorption mechanism between pesticide and adsorbent by innersphere complexes through Si-O- and Al-O-groups at clay particle edges.

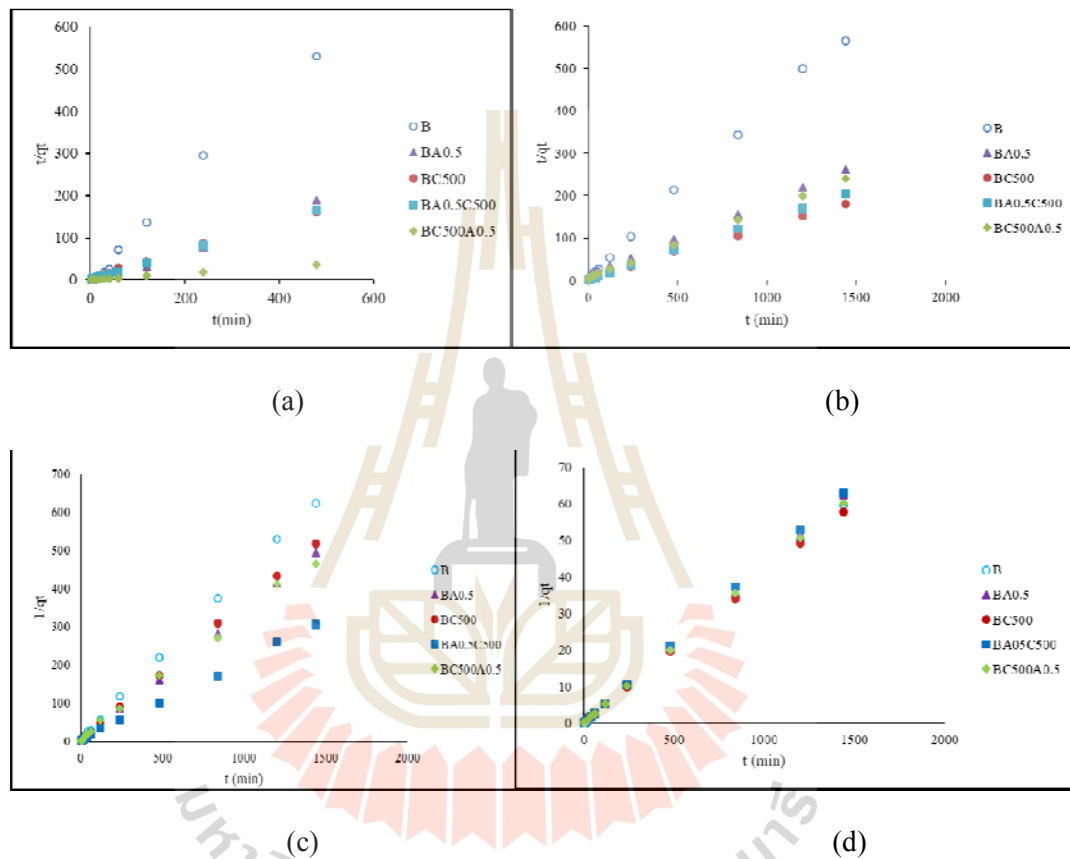


Figure 3.18 pseudo-second order plots of atrazine (a) diuron (b) 2,4-D (c) and paraquat (d) adsorption onto bentonite and modified bentonites.

Table 3.18 Kinetic model parameters obtained for the adsorption of atrazine onto bentonite and modified bentonite adsorbents.

Samples	$q_{e,exp}$	pseudo-first order			pseudo-second order		
		q_e	k_1	R^2	q_e	k_2	R^2
B	2.89	0.692	5.0×10^{-4}	0.0515	1.24	4.22×10^{-2}	0.9707
BA _{0.5}	4.20	1.90	4.8×10^{-3}	0.6589	2.59	-4.10×10^{-2}	0.9887
BC ₅₀₀	3.16	0.989	2.9×10^{-3}	0.6375	2.98	4.66×10^{-2}	0.9974
BA _{0.5} C ₅₀₀	4.12	0.0657	3.2×10^{-3}	0.7759	2.94	2.50×10^{-1}	0.9993
BC ₅₀₀ A _{0.5}	14.65	2.02	1.7×10^{-1}	0.8638	13.50	3.86×10^{-2}	0.9995

Table 3.19 Kinetic model parameters obtained for the adsorption of diuron onto bentonite and modified bentonite adsorbents.

Samples	$q_{e,exp}$	pseudo-first order			pseudo-second order		
		q_e	k_1	R^2	q_e	k_2	R^2
B	2.90	0.811	1.84×10^{-3}	0.6086	2.49	3.46×10^{-2}	0.9983
BA _{0.5}	5.44	3.79	3.92×10^{-3}	0.9756	5.61	4.76×10^{-3}	0.9983
BC ₅₀₀	7.90	4.80	3.68×10^{-3}	0.9084	8.10	4.24×10^{-3}	0.9991
BA _{0.5} C ₅₀₀	7.18	2.50	4.84×10^{-3}	0.7121	7.07	1.45×10^{-2}	0.9999
BC ₅₀₀ A _{0.5}	6.07	3.87	4.84×10^{-3}	0.9116	6.15	4.77×10^{-3}	0.9993

Table 3.20 Kinetic model parameters obtained for the adsorption of 2,4-D onto bentonite and modified bentonite adsorbents.

Samples	$q_{e,exp}$	pseudo-first order			pseudo-second order		
		q_e	k_1	R^2	q_e	k_2	R^2
B	2.16	0.704	2.76×10^{-3}	0.6545	2.30	4.29×10^{-2}	0.9996
BA _{0.5}	2.36	0.649	3.92×10^{-3}	0.5823	2.93	8.91×10^{-2}	0.9997
BC ₅₀₀	2.97	0.725	6.45×10^{-3}	0.6964	2.77	8.41×10^{-2}	0.9999
BA _{0.5} C ₅₀₀	6.25	2.05	2.76×10^{-3}	0.8608	4.74	1.50×10^{-2}	0.9985
BC ₅₀₀ A _{0.5}	2.75	0.950	1.61×10^{-3}	0.4462	3.05	2.22×10^{-2}	0.9978

Table 3.21 Kinetic model parameters obtained for the adsorption of paraquat onto bentonite and modified bentonite adsorbents.

Samples	$q_{e,exp}$	pseudo-first order			pseudo-second order		
		q_e	k_1	R^2	q_e	k_2	R^2
B	24.76	2.53	3.22×10^{-3}	0.728	24.10	1.36×10^{-2}	0.9999
BA _{0.5}	24.60	1.54	1.22×10^{-3}	0.6667	23.20	8.64×10^{-2}	0.9999
BC ₅₀₀	24.90	2.90	2.07×10^{-3}	0.509	24.75	1.31×10^{-2}	0.9999
BA _{0.5} C ₅₀₀	22.73	1.58	2.76×10^{-3}	0.3203	22.78	3.34×10^{-2}	0.9999
BC ₅₀₀ A _{0.5}	24.26	2.48	2.99×10^{-3}	0.4878	23.87	1.82×10^{-2}	0.9999

3.5 Conclusion

Bentonite was modified by either acid or heat, or both, by single and combined treatments for removal of pesticides from aqueous solution. It was found that the sequence of treatments has a strong effect on atrazine adsorption. Modified bentonite exhibits atrazine removal efficiency greater than bentonite; the BC₅₀₀A_{0.5} sample provides the maximal adsorption capacity at pH 6.0±0.5 as a result of it containing high active Al Lewis-acid sites, and Si-OH and Si-OH₂⁺ groups present on edges and faces. While, diuron and 2,4-D adsorption depend on hydrophobic site of BC₅₀₀ and BA_{0.5}C₅₀₀, respectively. Additionally, the high adsorption of paraquat pesticides favour on all adsorbents, except BA_{0.5}C₅₀₀ because of BA_{0.5}C₅₀₀ with low CEC, low swelling and low zeta potential. An increase in the solution pH results in a decrease in the adsorption of atrazine, diuron and 2,4-D, but the paraquat adsorption capacity increases. The optimum pH for each pesticide was found to be pH 2-3 for atrazine and 2,4-D, pH 2-4 for diuron and pH 11 for paraquat. Moreover, BC₅₀₀A_{0.5} was found to be an effective as multifunctional adsorbent for the simultaneous pesticides removal from aqueous solution. The adsorption of the pesticides is best fitted with the Langmuir adsorption model compared to Freundlich model and the adsorption kinetics follows a pseudo-second order. The thermodynamic parameters of the system: Gibbs free energy change (ΔG°), the free energy values at temperatures 303K, 313K and 323K in adsorption of pesticides are negative in all cases showing the spontaneous nature of the process. ΔH° values are positive for all of the pesticides, showing the endothermic nature of the adsorption process. ΔS° values are also reported; positive values suggest that the organization of the adsorbate in the solid-solution interface becomes more random. Thermal and acid treatments to enhance the adsorption

performance of the adsorbent offer a number of benefits as low costs, easy implementation and low chemical consumption, including for using as multifunctional adsorbent

3.6 References

- Amaral, B. d., de Araujo, J. A., Peralta-Zamora, P. G., and Nagata, N. (2014). Simultaneous determination of atrazine and metabolites (DIA and DEA) in natural water by multivariate electronic spectroscopy. **Microchemical Journal**. 117:262-267.
- Bojemueller, E., Nennemann, A., and Lagaly, G. (2001). Enhanced pesticide adsorption by thermally modified bentonites. **Applied Clay Science**. 18: 277-284.
- Bouras, O., Bollinger, J.-C., Baudu, M., and Khalaf, H. (2007). Adsorption of diuron and its degradation products from aqueous solution by surfactant-modified pillared clays. **Applied Clay Science**. 37: 240-250.
- Brus, J., Kobera, L., Schoefberger, W., Urbanová, M., Klein, P., Sazama, P., Tabor, E., Sklenak, S., Fishchuk, A. V., and Dědeček, J. (2015). Structure of framework aluminum Lewis sites and perturbed aluminum atoms in zeolites as determined by $^{27}\text{Al}\{1\text{H}\}$ REDOR (3Q) MAS NMR spectroscopy and DFT/molecular mechanics. **Angewandte Chemie**. 54:541-545.
- Calvet, R., and Prost, R.(1971). Cation migration into empty octahedral sites and surface properties of clays. **Clays and Clay Minerals**. 19:175-186.

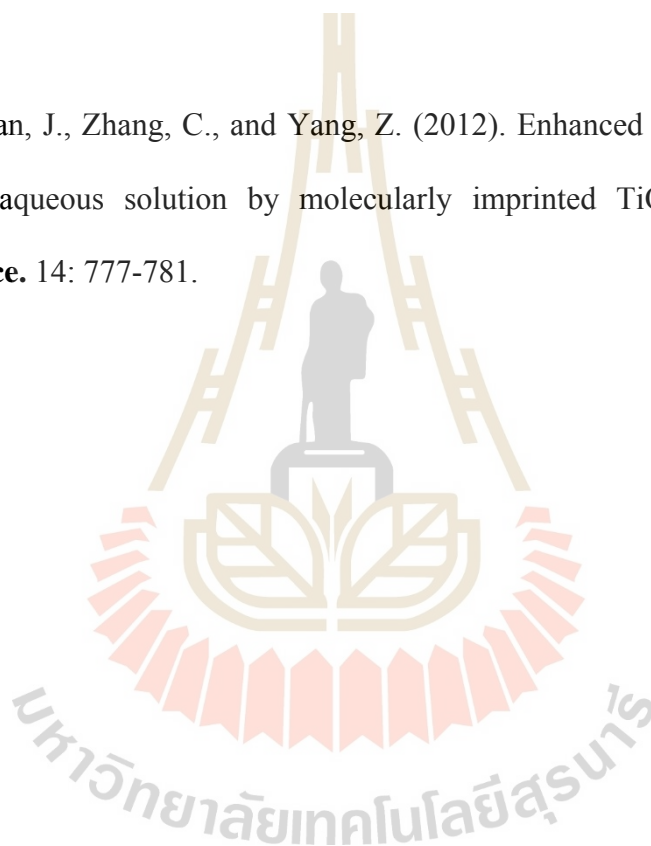
- Castro, C. S., Guerreiro, M. C., Goncalves, M., Oliveira, L. C. A., and Anastacio, A. S. (2009). Activated carbon/iron oxide composites for the removal of atrazine from aqueous medium. **Journal of Hazardous Materials**.164: 609-614.
- Chen, G. C., Shan, X. Q., Zhou, Y. Q., Shen, X. E., Huang, H. L., and Khan, S. U. (2009). Adsorption kinetics, isotherms and thermodynamics of atrazine on surface oxidized multiwalled carbon nanotube **Journal of Hazardous Materials**. 169: 912-918.
- Choo, K. Y., and Bai, K. (2016). The effect of the mineralogical composition of various bentonites on CEC values determined by three different analytical methods. **Applied Clay Science**.126: 153-159.
- Chorom, M., and Rengasamy, P. (1996). Effect of heating on swelling and dispersion of different cationin forms of a smectite. **Clays and Clay Minerals**. 44: 783-790.
- Deutsch, W. J. (1997) Groundwater geochemistry. **Fundamentals and Applications to Contamination**. Lewis Publishers, New York.
- Ding, L., Lu, X., Deng, H., and Zhang, X. (2012). Adsorptive Removal of 2,4-Dichlorophenoxyacetic Acid (2,4-D) from Aqueous Solutions Using MIEX Resin. **Industrial and Engineering Chemistry Research**. 51(34): 11226-11235.
- Ghimire, N., and Woodward, R. T. (2013). Under- and over-use of pesticides: An international analysis. **Ecologicon Economics**. 89: 73-81.
- Grovermann, C., Schreinemachers, P., and Berger, T. (2013). Quantifying pesticide overuse from farmer and societal points of view: An application to Thailand. **Crop Protection**. 53: 161-168.

- Gupta, V. K., Sharma, M., and Vyas, R. K. (2015). Hydrothermal modification and characterization of bentonite for reactive adsorption of methylene blue: An ESI-MS study. **Journal of Environmental Chemical Engineering**. 3: 2172-2179.
- Heller-Kallai, L. (2006). Chapter 7.2 Thermally Modified Clay Minerals, in: Faïza Bergaya B. K. G. T., Gerhard L (Eds.), **Developments in Clay Science**. Elsevier, pp. 289-308.
- Jamil, T. S., Gad-Allah, T. A., Ibrahim, H. S., and Saleh, T. S. (2011). Adsorption and isothermal models of atrazine by zeolite prepared from Egyptian kaolin. **Solid State Science**. 13: 198-203.
- Komadel, P. (2016). Acid activated clays: Materials in continuous demand. **Applied Clay Science**. 131: 84-99.
- Komadel, P., and Madejová, J. (2006). Chapter 7.1 Acid Activation of Clay Minerals, in: Faïza Bergaya B. K. G. T., Gerhard L (Eds.), **Developments in Clay Science**. Elsevier, pp. 263-287.
- Komadel, P., and Madejová, J. (2013). Acid Activation of Clay Minerals. in: B.K.G.T. Faïza Bergaya, L. Gerhard (Eds.) **Developments in Clay Science**, Elsevier, pp. 385-409.
- Kovaios, I. D., Paraskeva, C. A., and Koutsoukos, P. G. (2011). Adsorption of atrazine from aqueous electrolyte solutions on humic acid and silica. **Journal of Colloid Interface Science**. 356: 277-285.
- Lee, S. Y., and Kim, S. J. (2002). Expansion characteristics of organoclay as a precursor to nanocomposites. **Colloid Surface**. A. 211: 19-26.

- Leite, M. P., dos Reis, L. G. T., Robaina, N. F., Pacheco, W. F., and Cassella, R. J. (2013). Adsorption of paraquat from aqueous medium by Amberlite XAD-2 and XAD-4 resins using dodecylsulfate as counter ion. **Chemical Engineering Journal**. 215–216(0): 691-698.
- Li, K., Wu, J. Q., Jiang, L. L., Shen, L. Z., Li, J. Y., He, Z. H., Wei, P., Lv, Z., and He, M. F. (2017). Developmental toxicity of 2,4-dichlorophenoxyacetic acid in zebrafish embryos. **Chemosphere**. 171: 40-48.
- Murray, H. H. (2006). Chapter 2 Structure and Composition of the Clay Minerals and their Physical and Chemical Properties, in: Haydn H M (Ed.), **Developments in Clay Science**. Elsevier, pp. 7-31.
- Nithaya, K. M., Arnepalli, D. N., and Gandhi, S. R. (2010). 6th International Congress on Environmental Geotechnics, New Delhi, India.
- Nones, J., Nones, J., Riella, H. G., Poli, A., Trentin, A. G., and Kuhnen, N. C. (2015). Thermal treatment of bentonite reduces aflatoxin b1 adsorption and affects stem cell death. **Materials Science and Engineering: C**. 55: 530-537.
- Rao, Y. F., and Chu, W. (2010). Degradation of linuron by UV, ozonation, and UV/O₃ processes—Effect of anions and reaction mechanism. **Journal of Hazardous Materials**. 180(1–3): 514-523.
- Salawudeen T. Olalekan, Suleyman A. Muyibi, Qasim H. Shah, Ma'an, F. Alkhatib, Faridah Yusof, and Isam Y. Qudsieh. (2010). Improving the Polypropylene-Clay Composite Using Carbon Nanotubes as Secondary Filler. **Energy Research Journal**. 1: 68-72.

- Salvestrini, S., Sagliano, P., Iovino, P., Capasso, S., and Colella, C. (2010). Atrazine adsorption by acid-activated zeolite-rich tuffs. **Applied Clay Science**. 49: 330-335.
- Salman, J. M., Njoku, V. O., and Hameed, B. H. (2011). Adsorption of pesticides from aqueous solution onto banana stalk activated carbon. **Chemical Engineering Journal**. 174(1): 41-48.
- Takahashi, T., Ohkubo, T., Suzuki, K., and Ikeda, Y. (2007). High resolution solid-state NMR studies on dissolution and alteration of Na-montmorillonite under highly alkaline conditions. **Microporous Mesoporous Materials**. 106: 284-297.
- Tomkins, B. A., and Ilgner, R. H. (2002). Determination of atrazine and four organophosphorus pesticides in ground water using solid phase microextraction (SPME) followed by gas chromatography with selected-ion monitoring. **Journal of Chromatography A**. 972: 183-194.
- Tong, D. S., Zheng, Y. M., Yu, W. H., Wu, L. M., and Zhou, C. H. (2014). Catalytic cracking of rosin over acid-activated montmorillonite catalysts. **Applied Clay Science**. 100: 123-128.
- Velki, M., Di Paolo, C., Nelles, J., Seiler, T. B., and Hollert, H. (2017). Diuron and diazinon alter the behavior of zebrafish embryos and larvae in the absence of acute toxicity. **Chemosphere**. 180: 65-76.
- Wu, P., Wu, H., and Li, R. (2005). The microstructural study of thermal treatment montmorillonite from Heping, China. **Spectrochim Acta A**. 61: 3020-3025.

- Zadaka, D., Nir, S., Radian, A., and Mishael, Y. G. (2009). Atrazine removal from water by polycation-clay composites: effect of dissolved organic matter and comparison to activated carbon. **Water Research**. 43: 677-683.
- Zaghouane-Boudiaf, H., Boutahala, M., Sahnoun, S., Tiar, C., and Gomri, F. (2014). Adsorption characteristics, isotherm, kinetics, and diffusion of modified natural bentonite for removing the 2,4,5-trichlorophenol. **Applied Clay Science**. 90: 81-87.
- Zhang, C., Yan, J., Zhang, C., and Yang, Z. (2012). Enhanced adsorption of atrazine from aqueous solution by molecularly imprinted TiO₂ film. **Solid State Science**. 14: 777-781.



CHAPTER IV

EFFECT OF SURFACTANT MODIFIED BENTONITE ON PESTICIDE ADSORPTION

4.1 Abstract

Adsorption of the pesticides (atrazine, diuron, 2,4-D and paraquat) from aqueous solution onto organo-bentonite was investigated. Bentonite was modified with cationic-surfactant (HDTMA) and anionic-surfactant (SDS) with different concentrations of the surfactants for evaluation of the effect of concentration on the pesticides adsorption. The prepared organo-bentonite was investigated with FT-IR, XRD, TG/DTG and particle size analysis. It was found that the basal spacing of the bentonite increases from 14.02 Å to 19.26 Å by intercalation of HDTMA with the concentration of 60 mM in the interlayer space of the bentonite. The adsorption results show that the adsorption capacity is increased with increasing HDTMA concentration. In the case of SDS modification, the arrangement of SDS on the surface of bentonite does not affect the reduction or increment of the adsorption capacity, except in the adsorption of PQ^{2+} . Conversely, with high HDTMA density results in a decrease in the adsorption capacity. For simultaneous adsorption of various pesticides, it was found that bentonite modified with 60 mM HDTM is the most suitable adsorbent, consequently, it could be used as multifunctional adsorbent.

4.2 Introduction

The pesticides are widely used in agriculture, and its presence in surface and ground water has consequently increased pesticides (Castro et al., 2009; Chen et al., 2009; Kovaivos et al., 2011; Zadaka et al., 2009; Zhang et al., 2012). Adsorption on solid surfaces is an important strategy for controlling the presence of organic contaminants in water. Clay minerals are natural, abundant and inexpensive materials; they are widely applied in many fields as adsorbents for water pollution (Aydin et al., 2009; González-Pradas et al., 2003; Liu and Zhang, 2007). Clays contain a net negative charge due to isomorphous substitution in layers of clay neutralized by inorganic cations, which are strongly hydrated and confer the clay surface a hydrophilic character. The negative charge on the surface of bentonite, facilitates to change surface properties. One of the modification method widely employed is to use organic surfactants. Surfactants are long-chain molecules that contain both hydrophilic and hydrophobic moieties. Depending on their origin, surfactants are either biosurfactants or synthetic, and they can be classified as ionic and nonionic, according to their hydrophilic moiety. A general model of adsorption of ionic surfactants on a solid surface is the formation of a monolayer or “hemomicelle” at the solid-aqueous interface via strong coulombic or ionic interaction at surfactant concentration is equal or less than below its critical micelle concentration (CMC). If the surfactant concentration in solution exceeds the CMC, the hydrophobic tails of the surfactant molecules associate to form a bilayer or “admicelle” (Gangula et al., 2010). In this study bentonite has been used for modification with hexadecyltrimethylammonium chloride (HDTMA) and sodium dodecyl sulfate (SDS) with the molecular formula $C_{19}H_{42}ClN$ and $C_{12}H_{25}SO_4Na$, respectively, as well as the

applications of modified clay (organoclays) for adsorption of atrazine, diuron, 2,4-D and paraquat have been investigated.

4.3 Experiment

4.3.1 Materials

Bentonite (B) was purchased from Thai Nippon Chemical Industry Co., Ltd. Reagent grade of atrazine (2-chlo-4-ethylamino-6-isopropylamine-5-triaine) , diuron (1,2-dimethyl-3,5-diphenylpyrazolium methyl sulfate) , 2,4-D (2,4-dichlorophenoxy acetic acid), paraquat (1,1'-dimethyl-4,4-bipyridinium dichloride), SDS and HDTMA were obtained from Sigma.

4.3.2 Modification of bentonite

4.3.2.1 Preparation of organo-bentonite

Organo-bentonite was prepared as follows. Bentonite was dispersed in deionized-water (ratio of 1 g bentonite/ 10 mL DI water) around 30 min, then a HDTMA solution was added dropwise into the bentonite suspension (ratio of 1 g bentonite/ 50 mL HDTMA) and stirred for 24 h at ambient temperature. The mixture was filtered by vacuum filtration. Then the solid was washed with DI water and dried at 70°C for 12 h. Organo-bentonites were prepared with different concentrations of HDTMA from 0.5 to 120 mM. For organo-bentonite by using SDS surfactant was prepared as the same as mentioned above. The HDTMA-bentonite and SDS-bentonite were denoted in this work as HDTMA-modified (BH_z) and SDS-modified bentonite samples (BS_z), respectively; (z = concentration of surfactant solution)

4.3.2.2 Characterization

The interlayer spacing of the samples is determined by X-ray diffraction patterns obtained from back-pressed powder samples recorded on Bruker, D5005 Cu K α radiations scanning from 3.5-50° at a rate of 0.05°/s with current 35 mV and 35 mA. The framework and OH groups are confirmed by FT-IR (Spectrum GX, perkin-Elmer) with KBr pellet technique in the range of mid-IR and near-IR between 4000-400 cm⁻¹ and 8000-4000 cm⁻¹, respectively. The particle size distributions (PDS) of all samples are analyzed by Horiba laser scattering particle size distribution analyzer (LA-950). The residual atrazine, diuron, paraquat and 2,4-D concentrations are finally determined using a UV-Vis spectrophotometer (Agilent 8453 UV-Vis spectrophotometer) at the maximum wavelength 223 nm, 247, 257 nm and 283 nm, respectively. The measurements are made in duplicates for each experiment.

4.3.3 Batch adsorption

4.3.3.1 Kinetic adsorption

Kinetic adsorption experiment was conducted at 30°C by contacting the adsorbents with pesticide solutions at solid/liquid ratio = 20 mg/10 mL. The mixtures were shaken and the supernatants were withdrawn, at the first phase as following 2, 4, 6, 8, 10, 30, 60, 90, 120, 180 and 240 min, afterwards they were collected in the range of 6, 12, 18 and 24 h.

4.3.3.2 Effect of surfactant loading

The adsorption efficiency of the pesticides depends on the formation surfactant on the surface of the adsorbents. The experiment was performed with keeping the concentration of pesticides constant (depending on the type of pesticide at desired concentration) and using the modified bentonite treated with

surfactant concentrations of 0.5-120 mM. For this purpose, 20 mg of the adsorbents were added into 125 mL conical flasks with 10 mL of the pesticides aqueous solution. The experiments were carried out at ambient temperature for 24 h in a water bath shaker. After that, the suspensions were centrifuged at 3000 rpm, for 10 min and filtered before using (using nylon syringe filter). All the adsorption experiments were carried out at the natural pH of the solutions. The residual atrazine, diuron, paraquat and 2,4-D concentration were finally determined using a UV-Vis spectrophotometer at the maximum wavelength 223 nm, 247, 257 nm and 283 nm, respectively. The pesticides adsorption capacity for each adsorbent at present time t (q_t , mg.g⁻¹) was calculated using the following equation:

$$q_t = \frac{(C_0 - C_t)V}{m} \quad (4.1)$$

Where C_0 and C_t are the concentrations of adsorbates in aqueous solution at initial time and at time t , respectively (mg.L⁻¹); V is the volume of adsorbate solution (L); m is the mass of adsorbent (g). The adsorbate removal efficiency is calculated using the following equation:

$$\text{Removal efficiency (R) (\%)} = \frac{(C_0 - C_t)}{C_0} \times 100 \quad (4.2)$$

Where R is the efficiency of extraction (expressed as retention percentage), C_0 is the initial concentration of pesticides in the solution and C_t represents the concentration of pesticides at time t .

4.3.3.3 Optimum contact time and equilibrium time

Batch adsorption experiment was conducted for removal of the pesticides at ambient temperature at natural pH of each pesticide by contacting the adsorbent with the pesticide solutions at solid/liquid ratio = 300 mg/150 mL. The mixtures were shaken for 24 h, 1 mL of the supernatant were collected, at the first phase as following times of 2, 4, 6, 8, 10, 30, 60, 90, 120, 180 and 240 min, afterwards the supernatants were collected at 6, 12, 18 and 24 h.

4.3.3.4 Effect of pH

The effect of pH on the adsorption of the pesticides by bentonite and the modified bentonite was investigated over the pH range of 2.0 to 12.0. The pesticide solutions were prepared by dissolving in distilled water. The adsorbents were contacted with 50 ppm of the pesticide solution at solid/liquid ratio = 20 mg/10 mL. A pH of the solution was adjusted by adding with 0.1 or 0.01 mol.L⁻¹ of HCl or NaOH solutions. The mixture was placed on a water bath shaker at 30°C until it reached to equilibrium time, then centrifuged for separation of filtrate from solid phase. The filtrate was analyzed for residual pesticide concentration. Duplicate test was performed in all cases.

4.3.4 Adsorption isotherm

The bentonite and modified bentonite samples were dispersed in the 50 ppm pesticide solution for 24 h at 30°C. The pesticide adsorptions were performed by shaking 20 mg of the bentonite and modified bentonite in 10 ml of the pesticide aqueous solution at various concentrations of 10-50 ppm. After equilibrium, the solid phases were separated from the liquid phases by centrifugation. The concentration of atrazine, diuron, paraquat and 2,4-D concentration was finally determined using a UV-

Vis spectrophotometer at the maximum wavelength 223 nm, 247, 257 nm and 283 nm, respectively. The data obtained from the adsorption tests were calculate the adsorption capacity, q_e (mol. g⁻¹). The adsorption isotherms were evaluated by the model of Langmuir and Freundlich.

The amount of the pesticide would be determined by UV-vis spectroscopy at maximum wavelength of each pesticide. The amount of adsorbed pesticide was calculated from following equation

$$q_e = \frac{(C_0 - C_e)V}{W} \quad (4.3)$$

Where q_e is an amount of adsorbed pesticide on to bentonite (mol.g⁻¹); C_0 and C_e are initial and equilibrium concentration (M), respectively; V is volume of solution (L) and W is weight of bentonite and modified bentonite (g).

4.3.5 Simultaneous adsorption of various pesticides in solution.

Pesticides in commercial grade were prepared as stock solution in absolute ethanol at concentration 1000 ppm, except paraquat dissolved in water. The initial concentration of each adsorbate in all solution was 50 ppm. The initial pH value was unadjusted (6.0±0.5). The suspensions were shaken at ambient temperature, for 24 h at 130 rpm, and then filtered using a 0.45 μm membrane. The mixture solution of atrazine, diuron, 2,4-D and paraquat concentration were determined using HPLC (Hewlett Packard series 1100) with diode array detector and UV detector. The ZORBAX Eclipse ODS C18 column (250 mm×4.6 mm, particle size 5μm) was equipped with HPLC system and the UV detector wavelength was set at 201, 223, 254 and 283 nm. Acetonitrile (A) and water pesticide (2% phosphoric acid) (B) used as

mobile phases. The gradient program of HPLC was as follows: 0–13 min 100% B, 3–15 min 60% A and 40% B, 15–18 min 100%(A) and 20–30 min 100%A. The flow rate was set as 0.9 mL min⁻¹. The bentonite and modified bentonite samples were dispersed in the 50 ppm pesticide solution for 24 h at 30°C. The pesticide adsorptions were performed by shaking 20 mg of the bentonite and modified bentonite in 10 ml of the mixing pesticide aqueous solution at each pesticide concentration of 50 ppm.

4.4 Results and discussion

The bentonite-HDTMA (BH) and bentonite-SDS (BS) were selected for the dual-adsorption study.

4.4.1 Characterization of bentonite and modified bentonite

4.4.1.1 XRD analysis

The XRD patterns of bentonite and modified bentonite show a main reflection at approximately of $2\theta = 6.30, 19.77$ and 34.98 . Quartz (Q) and critobalite (C) impurities are observed in the patterns. Diffraction characteristics of the bentonite show a reflection peak at about $2\theta = 6.30$ which corresponds to a basal spacing of $d_{001} 14.02 \text{ \AA}$. For modified bentonite with various concentrations (0.5-120 mM) of HDTMA (BH) and SDS (BS) as shown in **Figure 4.4 and 4.5**, respectively. The basal spacing of d_{001} is almost changed. It indicates that the modified bentonited with surfactant has an influence on the layered structure of bentonite. In the case of modified bentonite with HDTMA, the d_{001} peak of bentonite shifts to lower than that of $2\theta = 6.30$ of all samples. This indicates that HDTMA enters into the interlayer space of bentonite by ion exchange. The effect of concentration loading on the basal spacing of organo-bentonite and arrangement of intercalated surfactants was investigated by other

authors (Heinz et al., 2007). It was found that the basal spacing of the organo-bentonite increases with increasing concentration of HDTMA-surfactant. The basal spacing of d_{001} of BH0.5 and BH1 is slightly increased to 14.46 and 14.38 Å with the concentration of 0.5 and 1 mM HDTMA, respectively, whereas it dramatically increases to 16.31, 19.21 and 18.79 Å with the concentration of 10, 60 and 120 mM HDTMA, respectively, as shown in **Table 4.1**. In addition, the XRD patterns of the modified bentonite with SDS show the reflection peaks at $2\theta = 6.13, 6.61, 7.31$ and 7.29° which correspond to a basal spacing of 14.40, 13.36, 12.09 and 12.12 Å with concentration of 5, 10, 80 and 100 mM SDS, respectively. It indicates that almost SDS-bentonite with the basal spacing of d_{001} is slightly decreased except BS5. With 100 mM SDS it shows less increased of basal spacing of d_{001} . For HDTMA it is mostly adsorbed on the interlayer spacing in bentonite whereas SDS it is mostly adsorbed on external surface.

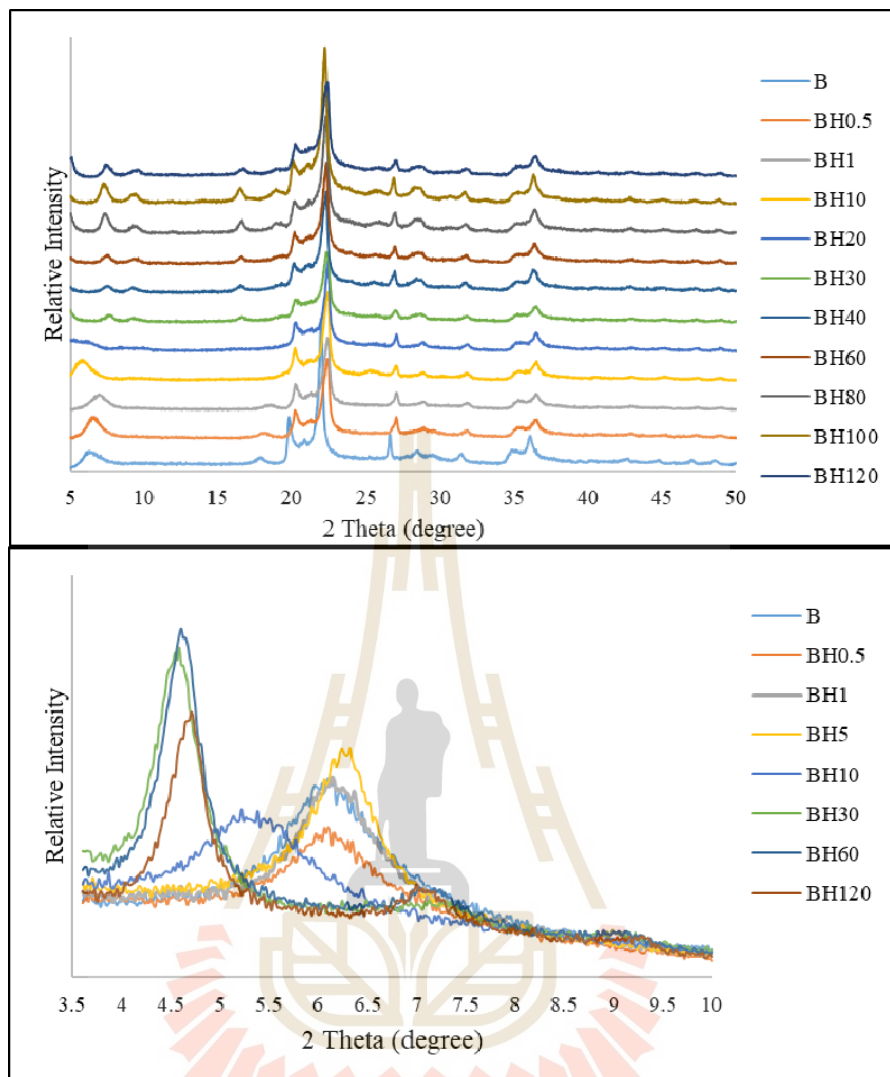


Figure 4.4 The XRD patterns of the HDTMA-bentonite with various concentrations of HDTMA (0.5-120 mM).

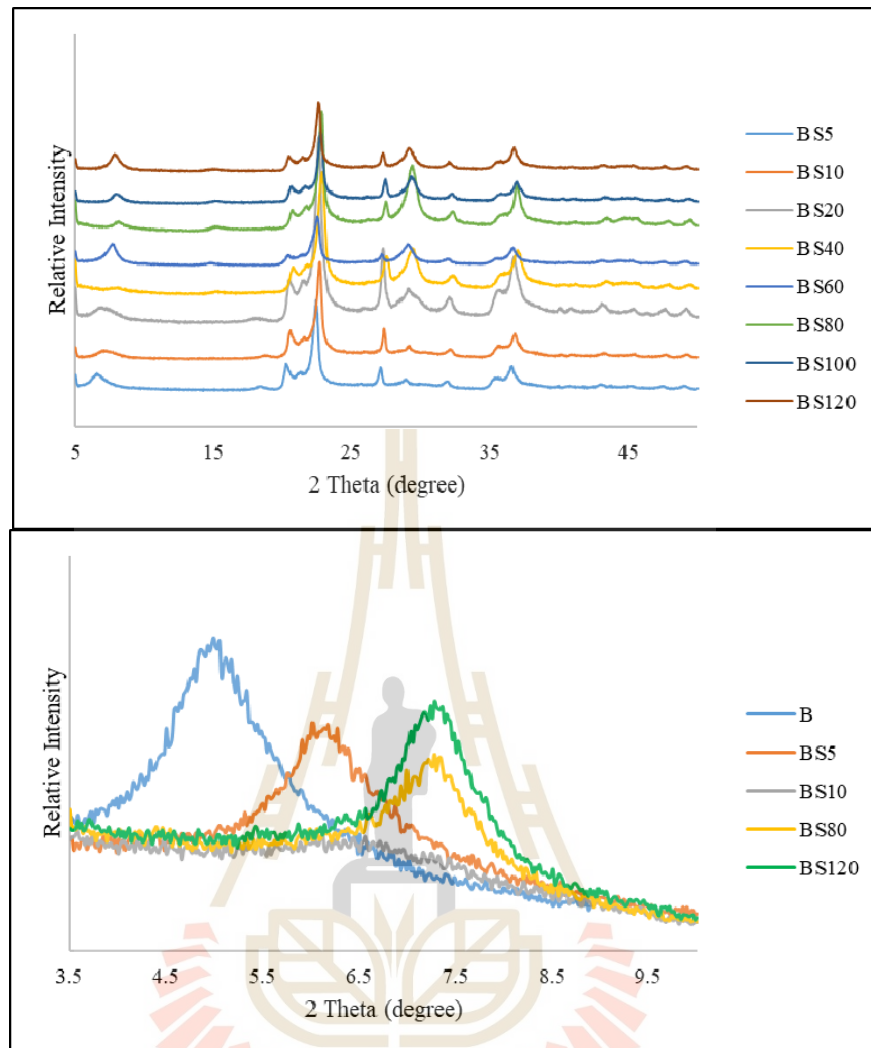


Figure 4.5 The XRD patterns of the SDS-bentonite with various concentrations of SDS (5-120 mM).

Table 4.1 The d-spacing (Å) of bentonite and modified bentonite changes upon type and concentration of surfactant.

Samples	2θ (degree)	d-spacing (Å)
Bentonite	6.30	14.02
BH0.5	6.10	14.46
BH1	6.14	14.38
BH10	5.42	16.31
BH30	4.58	19.26
BH60	4.58	19.26
BH120	4.69	18.79
BS5	6.13	14.40
BS10	6.61	13.36
BS80	7.31	12.09
BS120	7.29	12.12

4.4.1.2 FTIR analysis

FTIR spectroscopy is very sensitive to modification of the clay structure upon intercalated surfactants. In order to obtain complementary evidence for the intercalation of surfactant ions into the silicate lattice, FTIR spectra were recorded in the region of 4000 – 400 cm⁻¹ as shown in **Figure 4.6 and 4.7**. When the surfactants intercalated into the gallery of bentonite, the water bound directly to the hydrated cations was removed with the replacement of the hydrated cations by surfactant cations. Simultaneously, the surface property of bentonite is modified from

hydrophilic to hydrophobic surface. H₂O is not easily adsorbed on the organo-bentonite. In all FT-IR spectra of **Figure 4.6 and 4.7** show also intense band at 2921 and 2853 cm⁻¹. These bands are attributed to the asymmetric (ν_{as} (CH₂)) and symmetric -CH₂ stretching (ν_s (CH₂)) modes. The bands in the range 1400–1500 cm⁻¹ result from C–H bending vibrations. These absorption bands indicate successful loading of surfactant on the bentonite surface. These bands were detected only in bentonite modified with HDTMA and SDS. In the vibration range of 3000-2800 cm⁻¹, their intensities increase with increasing HDTMA concentration. It indicates that its packing form is more dense in the solid phase. These bands shift to lower wave number probably the on sequence of change in the arrangement of surfactant in the clay interlayer from disorder to ordered form (Majdan et al., 2005). It causes the increased Van der Waals interaction and consequently in the increased number of ordered conformers. In the case of modification by SDS it found that the intensity of the band at 3000 and 2800 and 1450 cm⁻¹ is slightly increased. It indicates that SDS attaches weakly on the surface of bentonite because negatively charged surface of bentonite repulses negative ionic head groups of SDS. The other bands appear the spectra of the organo-bentonite at 1475 and 722 cm⁻¹. These two bands are attributed to scissoring and rocking vibration of methylene group (CH₂), respectively. The positions of these two bands remain constant with an increase in the concentration of surfactant.

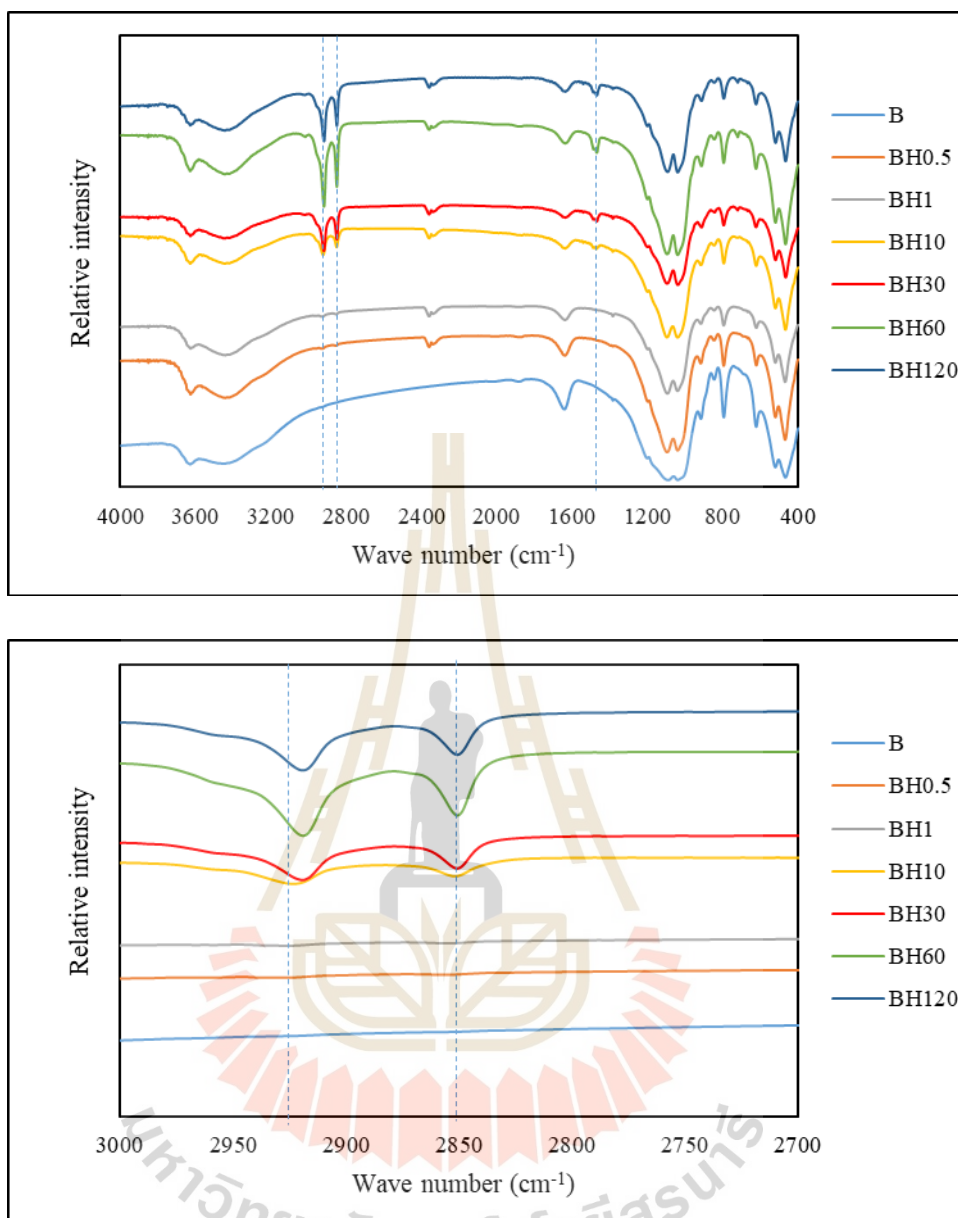


Figure 4.6 IR spectra of bentonite modified with 0.5-120 mM HDTMA.

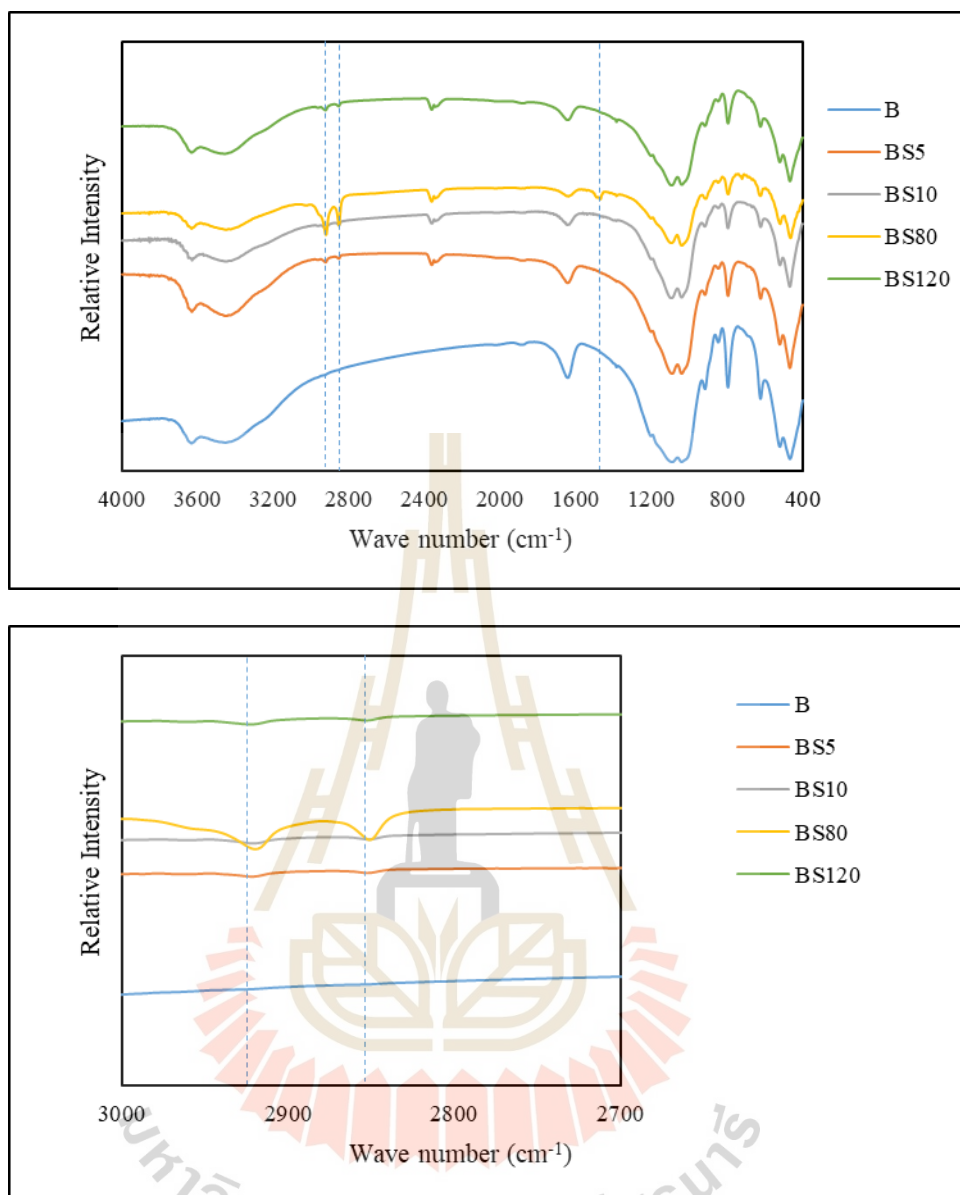


Figure 4.7 IR spectra of bentonite modified with 5-120 mM SDS.

4.4.1.3 Thermal analysis of bentonite and modified bentonite

The TGA and derivative thermogravimetric (DTG) curves of bentonite, HDTMA-bentonite and SDS-bentonite are illustrated in **Figure 4.8 and 4.9**. The TGA/DTG curves of the bentonite show a three peaks of mass loss at the temperature of 67.17, 157.17 and 673.17°C, respectively. The first peak can be attributed to the loss of weakly bound water and the second peak corresponds to the loss of hydrating water strongly bound to the bentonite. Above 500°C, the weight loss is traceable to dehydration of some trapped water molecules in the interstices of the clay layers and that due to dehydroxylation of the mineral, which is accompanied by a change in the crystal structure (Nones, J. et al., 2015). On the other hand, no mass loss of bentonite is observed in the temperature range of 200-500°C, which means that the bentonite is relatively stable in this range of temperature (Bousbaa, S.N., 2018). The TGA/DTG curves of HDTMA-bentonite and SDS-bentonite are given in **Figure 4.8, 4.9** and **Table 4.2**. For HDTMA-bentonite the TGA/DTG curve shows three stages of the mass loss. In the first stage about 35-200°C for BH0.5 with two peaks at the mean temperature of 70.17°C (2.87% of mass loss) and 152.85°C (0.15% of mass loss). While, BH10, BH60 and BH120 shows a single peak at this temperature range and the mass loss decreases with increasing HDTMA concentration. According to the lower mass loss of water for HDTMA-bentonite compared to that for bentonite confirms the hydrophobic nature of the modified bentonite (Houhoune, F., et al., 2016.). The second stage occurs in the temperature range about 200-500°C responsible to the decomposition of the surfactant. DTG curve shows two peaks for BH10 and three peaks for BH60 and BH120 as shown in **Figure 4.8**. This peak corresponds to the decomposition of the surfactant on the surface of bentonite and the temperature

range of 325-450 indicates the surfactant decomposition in the interlayer spaces of the bentonite (Erdem, B. et al., 2010, Houhoune, F. et al., 2016.). The decomposition of HB10 (Figure 4.8) shows two peaks of 325.00°C (5.91% of mass loss) and 414.23°C (4.69%) which correspond to the surfactant decomposition in the interlayer spaces. While, BH60 and BH120 show three peaks. The mass loss from the removal of the interlayer is at 307.96 and 416.74°C for BH60 and 309.00 and 425.33°C for BH120. Moreover, BH60 and BH120 show a new band apparent at 250.05 and 244.33°C, respectively, which is attributed to the decomposition of the surfactant adsorbed on the external surface of bentonite. The results of DTA agree with that of XRD. The XRD shows the interlayer spacing of bentonite increases with HDTMA from 14.01 Å to 16.31 Å with 10 mM HDTMA. When the concentration increases to 60 and 120mM HDTMA, the interlayer spacing changes extremely to 19.26 and 18.79 Å, respectively. It indicates that in the concentration range of 10-120 mM HDTMA, most of HDTMA adsorb in the interlayer. While all of SDS modified samples cannot adsorb in the interlayer of bentonite because the mass loss does not occur at the temperature range of 325-450°C. This corresponds with XRD results that the interlayer spacing decreases. Therefore, BS5, BS10, BS80 and BS120 contain SDS mainly adsorbed on external surface of bentonite. The final stage occurs in the temperature range above 500°C is ascribed to the dehydroxylation of the layer of bentonite.

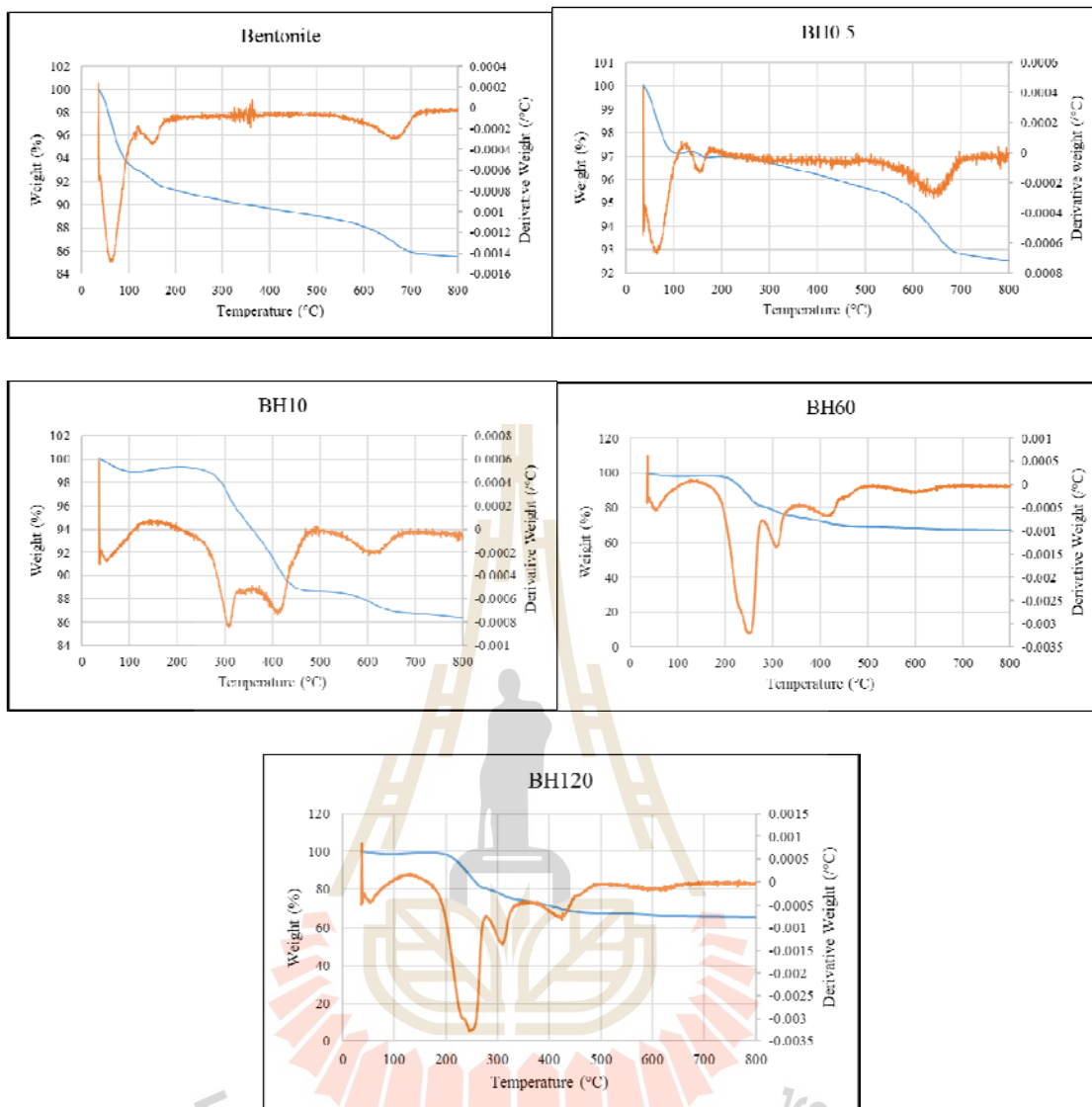


Figure 4.8 Thermogravimetric (TG) and differential thermogravimetric (DTG) analyses of Bentonite, BH0.5, BH10, BH60 and BH120

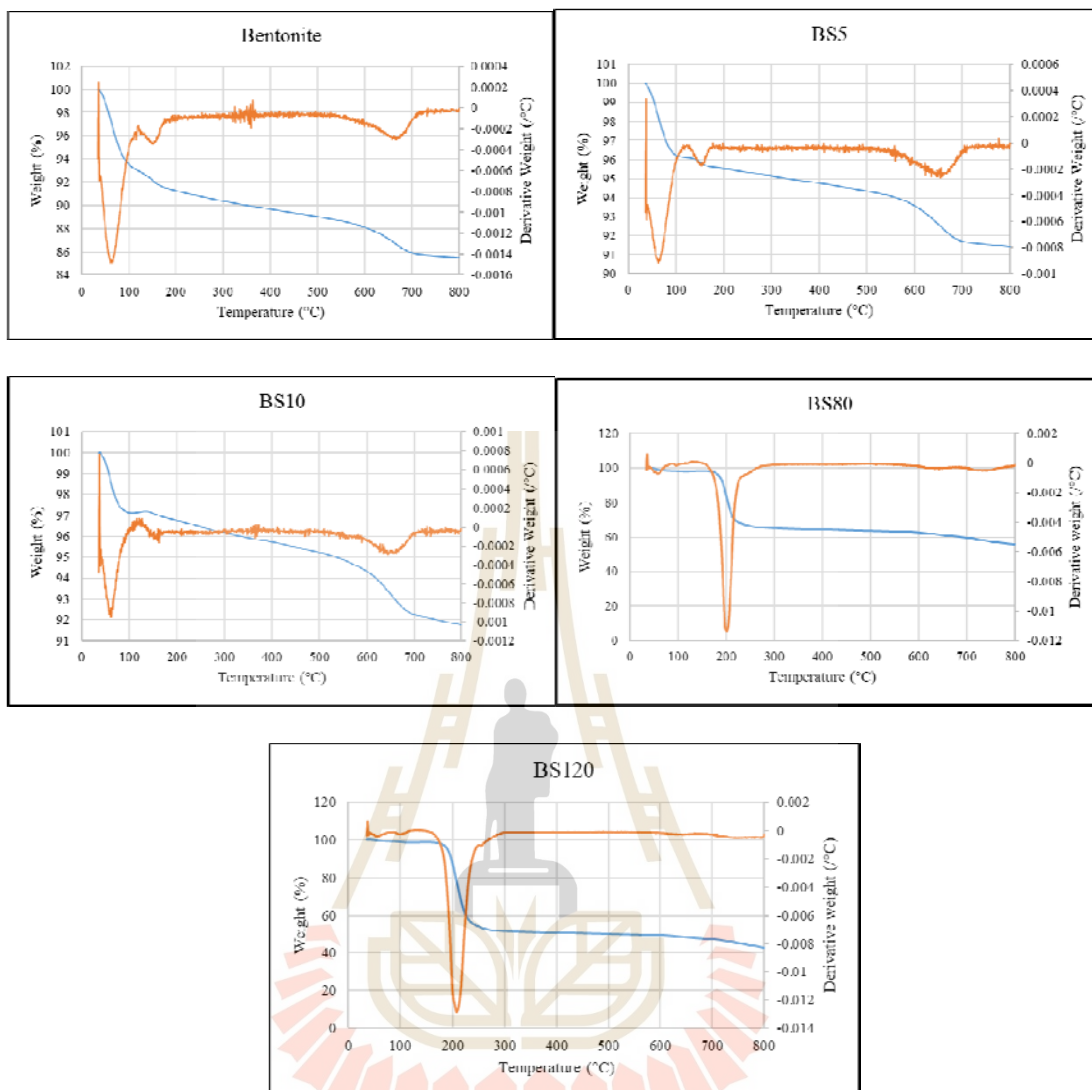


Figure 4.9 Thermogravimetric (TG) and differential thermogravimetric (DTG) analyses of Bentonite, BS5, BS10, BS80 and BS120

Table 4.2 The percent composition of water and surfactants of bentonite.

Adsorbents	Weight loss (%)			
	35–100°C	100–200°C	200–500°C	500–800°C
Bentonite	6.46	2.29	-	3.51
BH0.5	2.87	0.15	-	3.11
BH10	1.08	-	10.65	2.26
BH60	1.84	-	28.6	1.89
BH120	1.26	-	30.51	2.12
BS5	3.75	0.70	-	2.92
BS10	2.87	0.37	-	3.47
BS80	1.98	-	20.75	-
BS120	1.17	-	37.34	-

4.4.1.4 Particle size analysis

The particle size distributions and mean particle sizes are shown in **Figure 4.10** and **Table 4.3** and **4.4**, respectively. The samples modified with 10-120 mM HDTMA show a bimodal particle-size-distribution. The mean particle size of BH10, BH60 and BH120 samples have the maxima at approximately 10.10 μm (29.02%) and 200 μm (70.98%), 13.25 μm (43.14%) and 77.43 μm (56.86%) and 13.25 μm (45.85%) and 101.46 μm (54.15%), respectively. The large particle size seen for high concentration of HDTMA arises from the formation of admicelles at the interlayer spacing and the surface of the bentonite. While BH0.5 exhibits the monomodal particle-size-distribution. On the other hand, the particle size distributions for SDS-bentonite show only monomodal distributions. The mean particle size decreases with increasing SDS concentration (**Table 4.4**). It may be due to formation of admicelles not occurring.

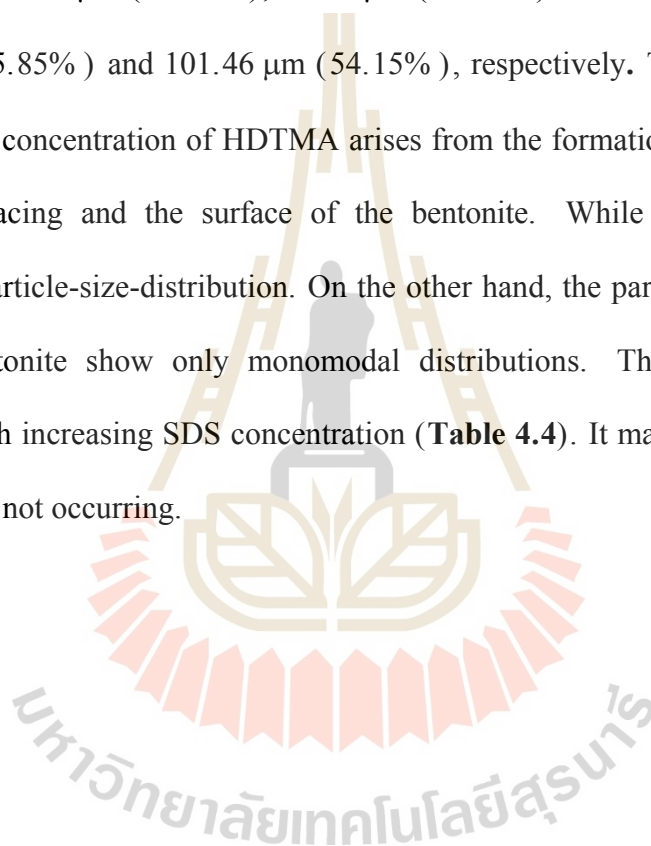
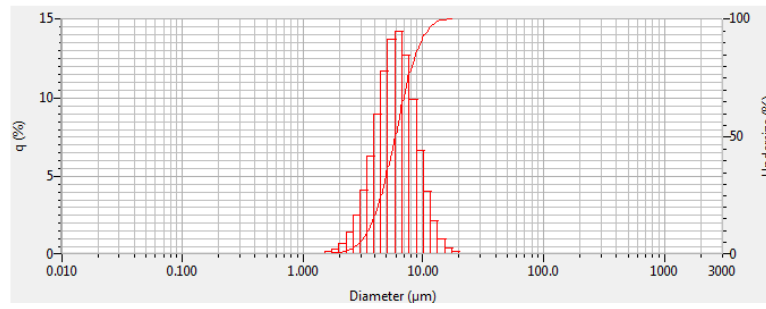


Table 4.3 Measurement of particle size distribution of modified bentonite by HDTMA.

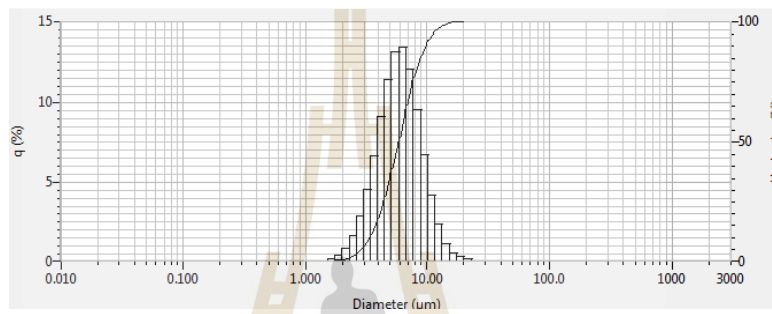
	Monomodal		Bimodal					
	B	BH0.5	BH10	BH60	BH120			
Diameter (μm)			Node1	Node2	Node1	Node2	Node1	Node2
			10.10	200	13.25	77.43	13.25	101.46
Undersize (%)			29.02	70.98	43.14	56.86	45.85	54.15
Mean particle size (μm)	6.28	6.30	109.18		52.46		69.80	

Table 4.4 Measurement of particle size distribution of modified bentonite by SDS.

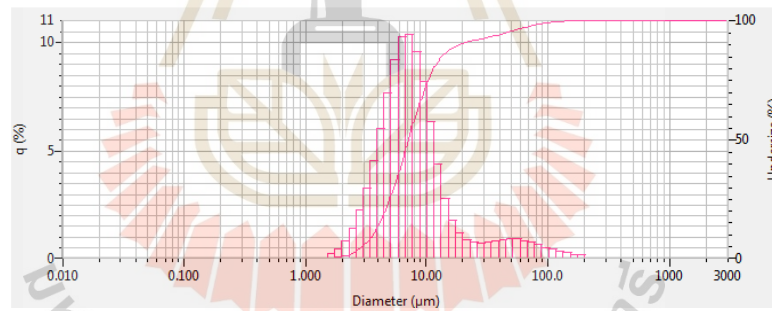
	Monomodal				Bimodal	
	B	BS5	BS10	BS80	BS120	
Diameter (μm)					Node1	Node2
					0.259	4.47
Undersize (%)					10.91	89.09
Mean particle size (μm)	6.28	5.89	6.42	4.40	3.78	



(a)

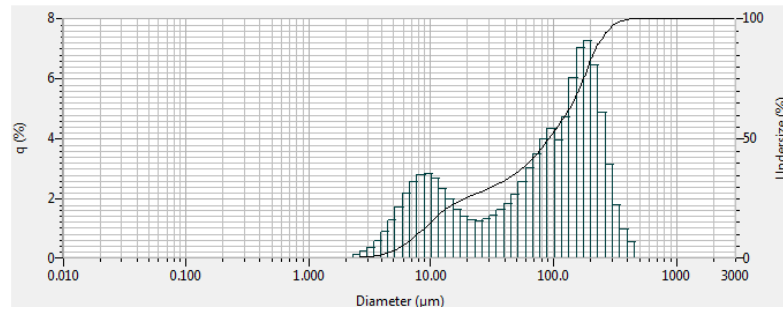


(b)

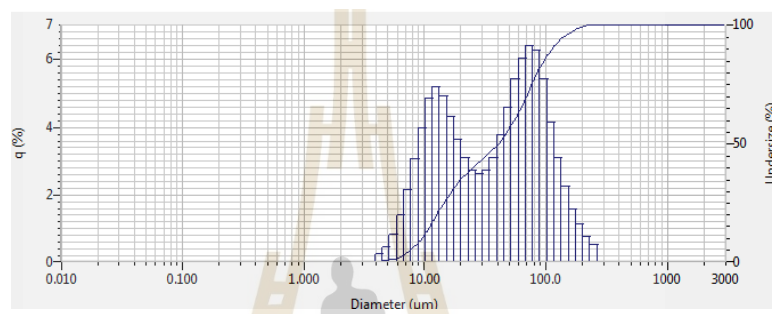


(c)

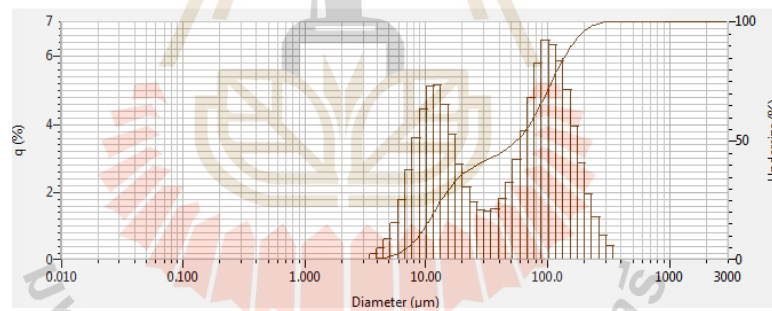
Figure 4.10 Particle size distribution of Bentonite (a), BH0.5 (b), BH1 (c), BH10 (d), BH60 (e), BH120 (f), BS5 (g), BS10 (h), BS80 (i) and BS120 (j).



(d)

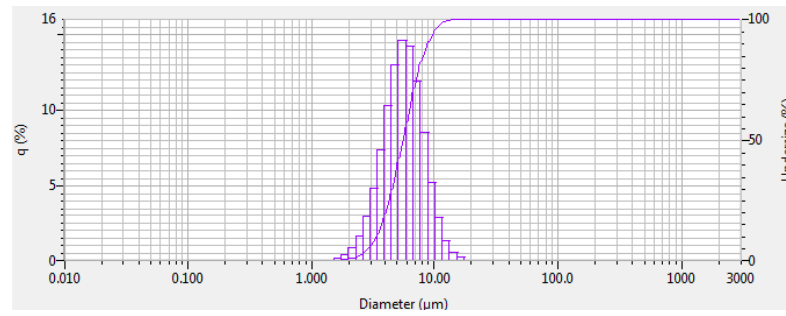


(e)

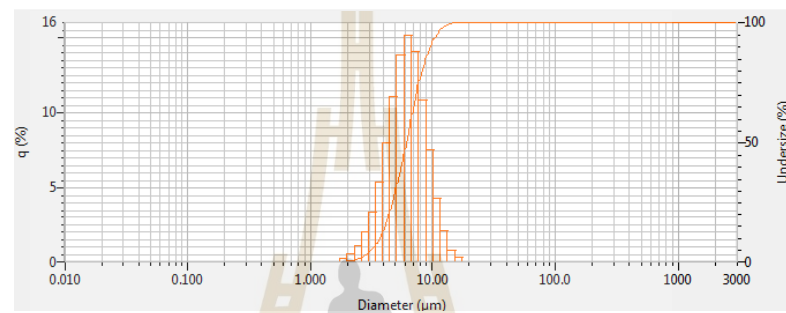


(f)

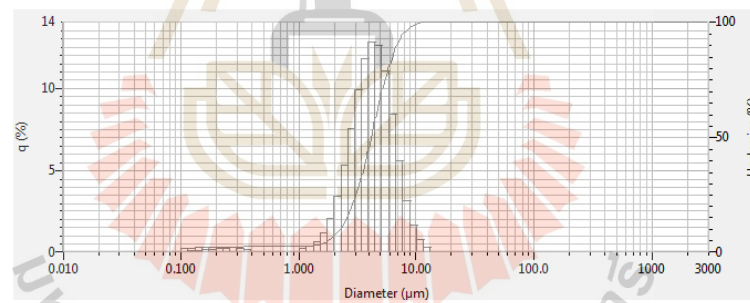
Figure 4.10 (Continued) Particle size distribution of Bentonite (a), BH0.5 (b), BH1 (c), BH10 (d), BH60 (e), BH120 (f), BS5 (g), BS10 (h), BS80 (i) and BS120 (j).



(g)

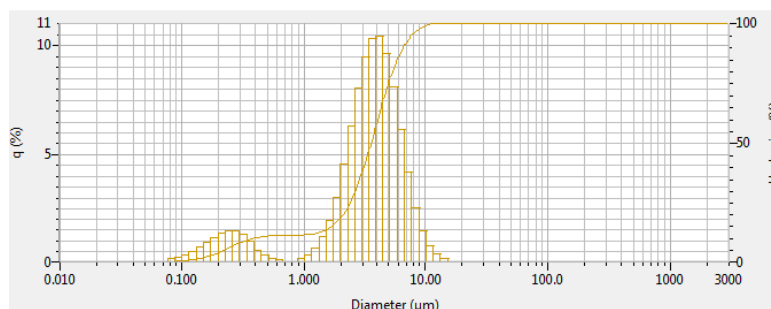


(h)



(i)

Figure 4.10 (Continued) Particle size distribution of Bentonite (a), BH0.5 (b), BH1 (c), BH10 (d), BH60 (e), BH120 (f), BS5 (g), BS10 (h), BS80 (i) and BS120 (j).

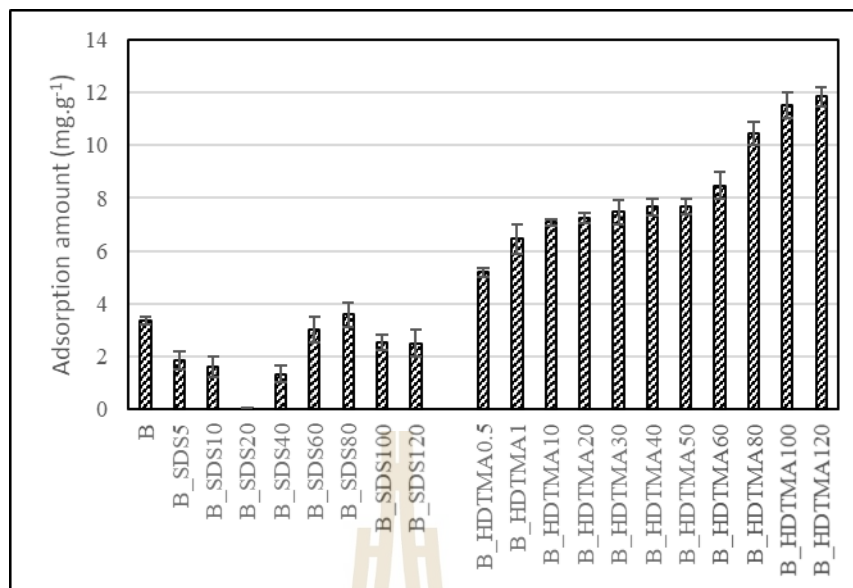


(j)

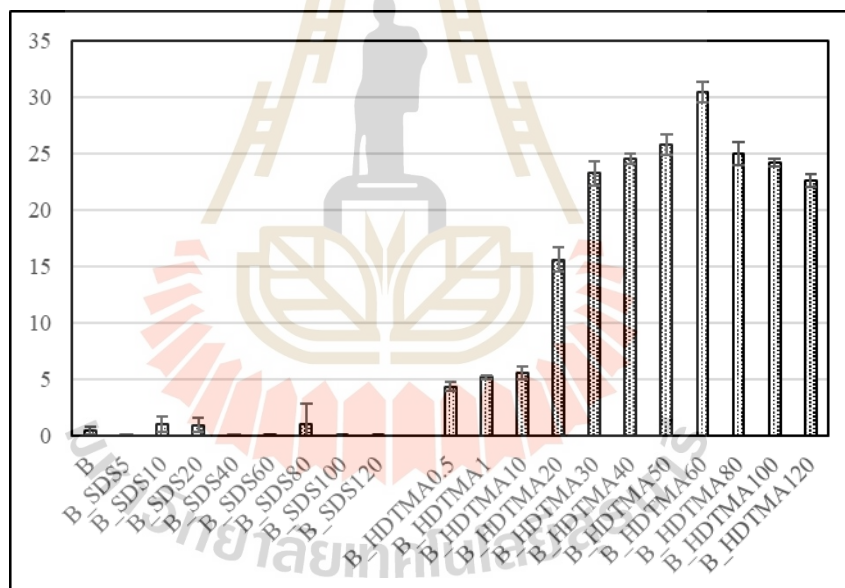
Figure 4.10 (Continued) Particle size distribution of Bentonite (a), BH0.5 (b), BH1 (c), BH10 (d), BH60 (e), BH120 (f), BS5 (g), BS10 (h), BS80 (i) and BS120 (j).

4.4.2 Effect of surfactant loading level on adsorption of pesticides

Atrazine and diuron are the pesticides that occur in neutral form at ambient condition. The nature of these pesticides trends to favor to adsorb on hydrophobic surface more than hydrophilic surface of adsorbent. The adsorption data in **Figure 4.11(a) and (b)** show that the atrazine and diuron are more removed by HDTMA-bentonite and with an increase in the concentration of HDTMA can improve the adsorption capacity. However, with the concentration of HDTMA over 60 mM, the result is a decrease in the adsorption capacity of diuron. The adsorption results of SDS-bentonite shown in **Figure 4.11(a) and (b)** indicate that the concentration of SDS has no effect on the removal of the atrazine and diuron.



(a)

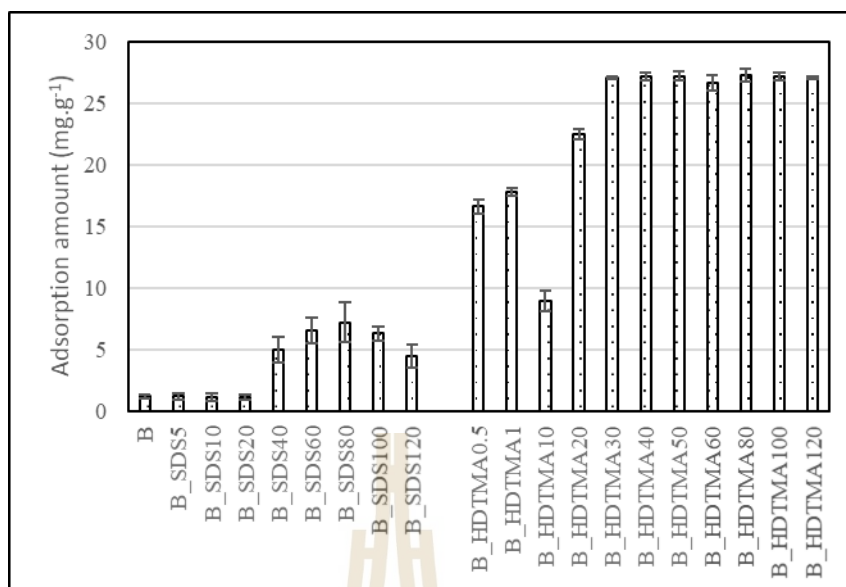


(b)

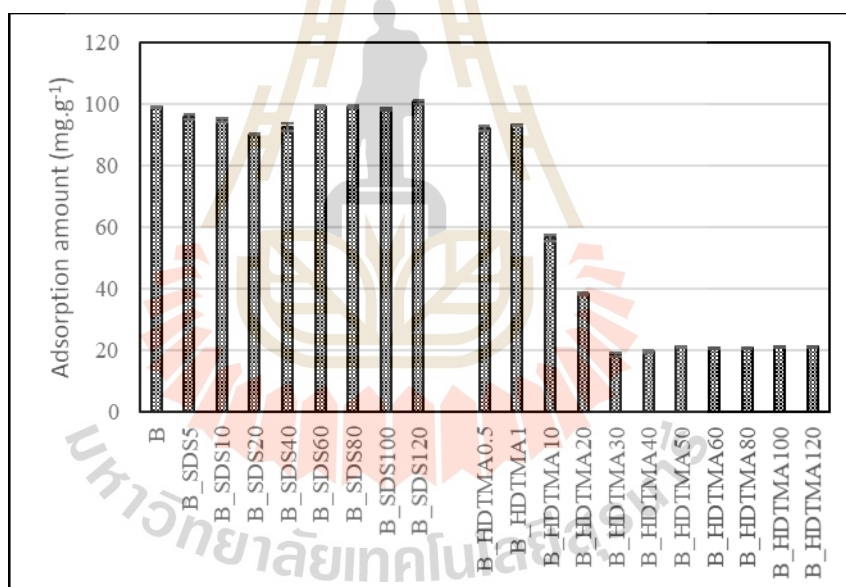
Figure 4.11 Effect of surfactant concentration loading on adsorption capacity of atrazine (a) and diuron (b) on various adsorbent at initial concentration 50 ppm.

2,4-D and Paraquat are classified as ionic pesticides which are anionic and cationic pesticides at the study condition, respectively. The **Figure 4.12** shows the quantities of the pesticides adsorbed on the HDTMA-bentonite and SDS-bentonite at various surfactant concentrations. The result shows that the extent of the adsorption ability is dependent on the surfactant loading level and the method used to modify the adsorbents. The adsorption capacities of the modified bentonite for removal of 2,4-D (**Figure 4.12(a)**) show the values in contrast to PQ^{2+} (**Figure 4.12(b)**).

The increase in concentration of HDTMA can improve the adsorption capacity due to the positive head group of HDTMA bilayer able to interact with the negative charge of 2,4-D. This result reveals that the HDTMA-modified at the concentration more than 30 mM (BH30) can adsorb 2,4-D better than unmodified bentonite and bentonite modified with SDS. In the case of SDS modification (**Figure 4.12(b)**), the result was found that the surface of bentonite can adsorb 2,4-D in a larger amount than that of bentonite. This is a result of an increase in an active site of SDS-bentonite due to a hydrophobic part of SDS on the bentonite surface can attach to 2,4-D more.



(a)



(b)

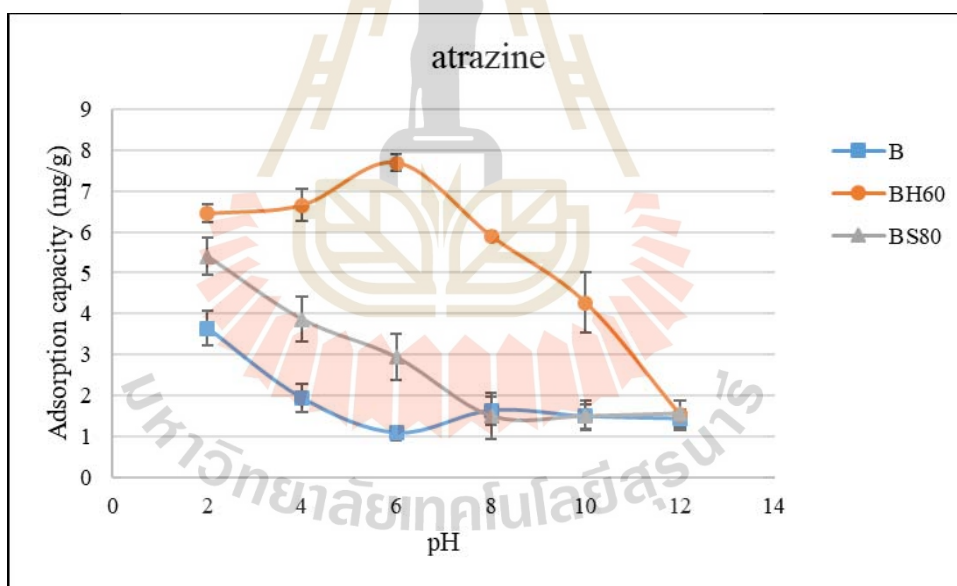
Figure 4.12 Effect of surfactant concentration loading on adsorption capacity of 2,4-D (a) and paraquat (b) on various adsorbent at initial concentration 50 and 200 ppm, respectively.

In the case of paraquat adsorption result (**Figure 4.12(b)**), it was found that HDTMA modification with high concentration until it forms a bilayer (more than 30 mM) that affects significantly the reduction of the adsorption capacity, because the positive head group of HDTMA bilayer repels the positive charge of paraquat (PQ^{2+}). An increase in SDS concentration loading does not affect the PQ^{2+} adsorption, because SDS on the surface of bentonite keeps still a space for PQ^{2+} to penetrate to interlayer space for an occurrence of cationic exchange to bentonite. Based on the maximal adsorption capacity of BH60 and BS80 for those pesticides, so they were chosen for further study of the effect of pH on the pesticide adsorption.

4.4.3 The Effect of pH on adsorption of pesticides

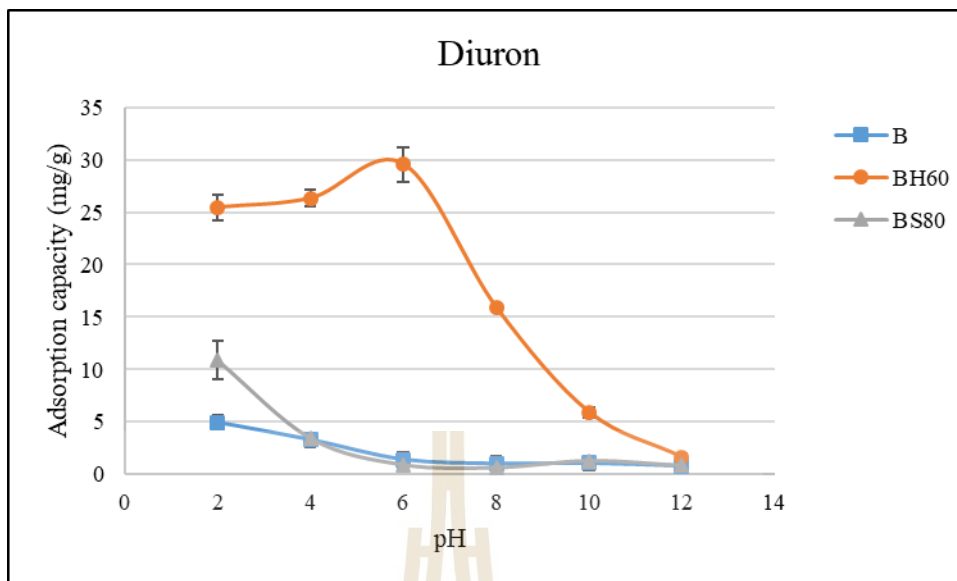
As pH is an important factor affecting the uptake speciation of adsorbent species, the adsorbent surface charge, and the degree of pesticide ionization (Moradi, 2014; Nejati, Davary and Saati, 2013). The pesticides adsorption depending on the solution pH was investigated. The results are shown in **Figure 4.13** demonstrates the atrazine and diuron removal was evidently dependent on the pH. The great difference in the adsorption of these pesticides between the modified bentonite and bentonite is found to be in the wide pH range of 4-8. For atrazine and diuron, it is significant differences in the adsorption capacity between BH60 and bentonite at this pH range, because they are in neutral form at this pH and the neutral pesticides preferentially adsorb to the hydrophobic tail of HDTMA of BH60. At pH values greater than pka of 2,4-D, 2,4-D exists predominantly in anionic form in solution. The anions preferentially adsorb to the positively charged head group on HDTMA (BH60). Therefore, anions 2,4-D adsorb to (BH60) more than negatively charged surface of

bentonite and negatively charged head group of SDS (BS80). The lower adsorption capacity at high pH with an increase in pH is probably due to repulsion of more negative charge of the adsorbents and anion 2,4-D. All adsorbents exhibit an increase in the adsorption capacity with increasing pH for PQ^{2+} , with the greatest capacity at pH 12 (**Figure 14.3(d)**). At pH values less than 6.0, the adsorption capacity of BS80 is greater than that of bentonite and BH60, that is a result of a stronger interaction between PQ^{2+} and negatively charged head groups on SDS. At pH values greater than 6.0, the adsorption capacity of BS80 and bentonite is similar and they are higher than BH60.

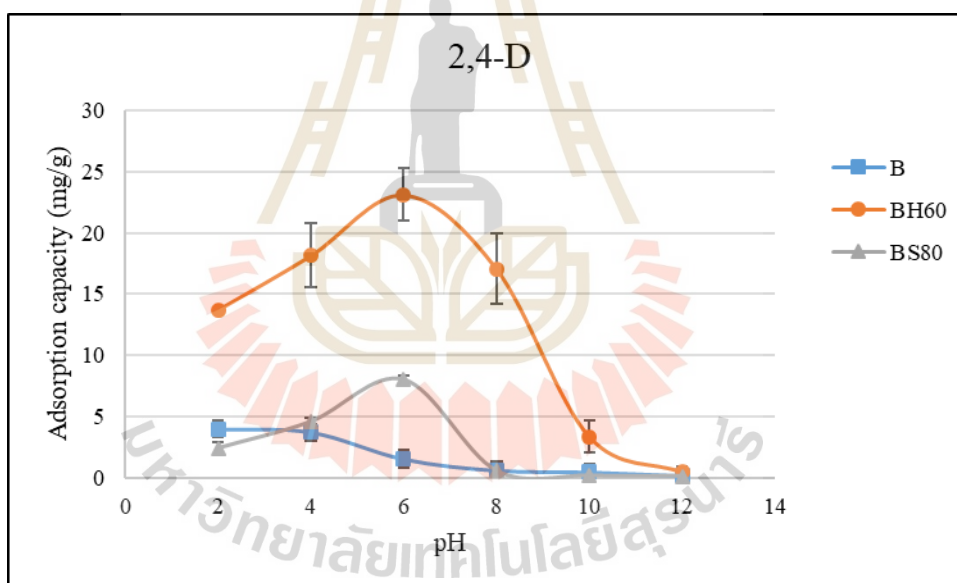


(a)

Figure 4.13 Effect of pH on adsorption capacity for removal of (a) atrazine (b) diuron (c) 2,4-D and (d) paraquat.

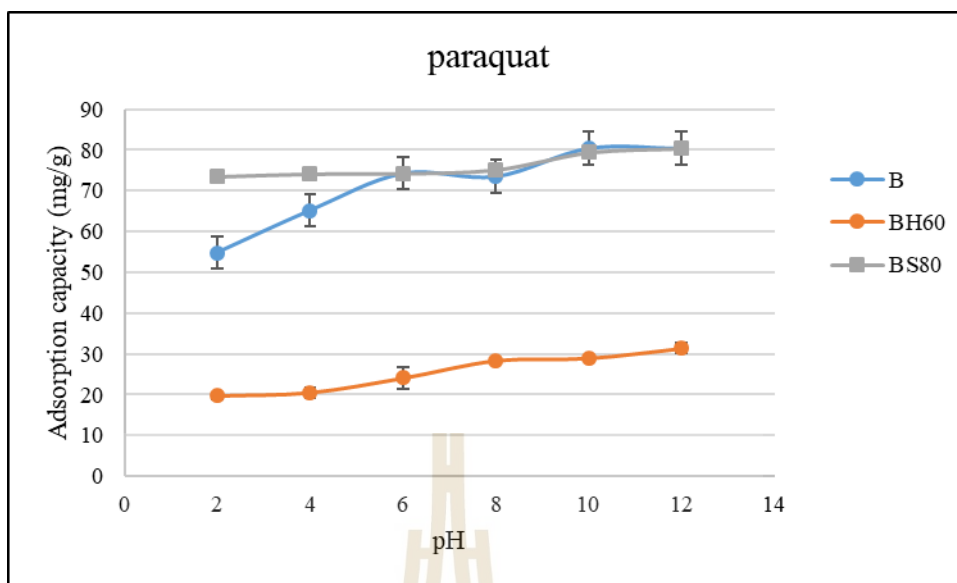


(b)



(c)

Figure 4.13 (Continued) Effect of pH on adsorption capacity for removal of (a) atrazine (b) diuron (c) 2,4-D and (d) paraquat.



(d)

Figure 4.13 (Continued) Effect of pH on adsorption capacity for removal of (a) atrazine (b) diuron (c) 2,4-D and (d) paraquat.

4.4.4 Simultaneous adsorption of various pesticides in solution

Simultaneous adsorptions of the pesticides (atrazine, diuron, 2,4-D and paraquat) from aqueous solution onto all adsorbents at ambient temperature and at initial pH of solution (6.5 ± 0.5) without pH adjustment are shown in **Figure 4.14**. BH60 provides the greatest removal efficiency of atrazine, diuron and 2,4-D with 7.54, 18.36 and 26.48 $\text{mg} \cdot \text{g}^{-1}$, respectively, and small adsorbed paraquat with 1.54 $\text{mg} \cdot \text{g}^{-1}$. For BH120 the removal of pesticides is the same order as BH60. On the other hand, SDS-bentonite of BS5, BS80 and BS100 preferentially adsorb paraquat with 23.98, 25.77 and 26.24, respectively. The maximum total values of pesticides removed from aqueous belong to bentonite modified with HDTMA. This value confirms that BH60 and BH120 is the most suitable for removal various pesticides simultaneously,

consequently, it could be regarded as an efficient multifunctional adsorbent for the investigated types of the pesticides.

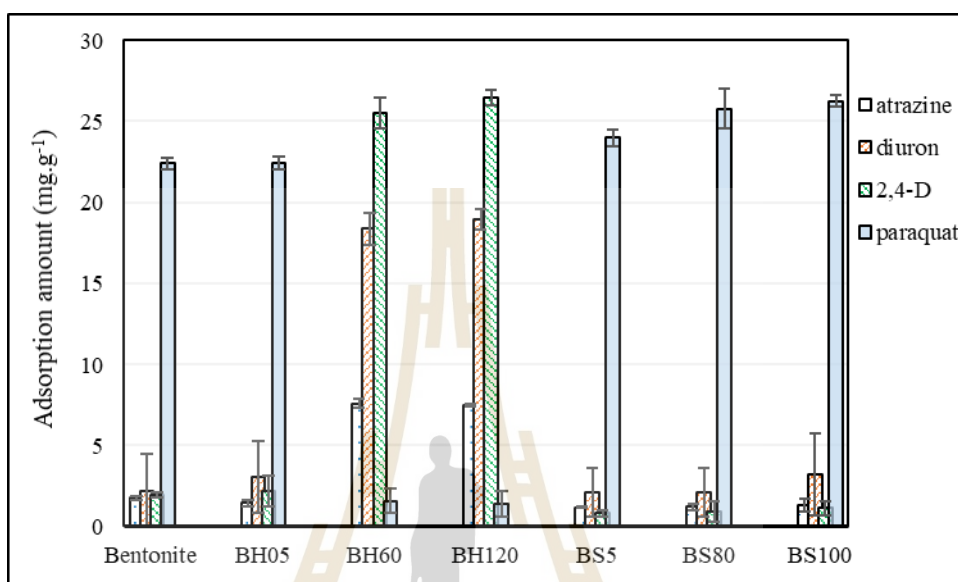


Figure 4.14 Adsorption of quaternary-component pesticides (50 ppm) at pH 6.5 ± 0.5 onto bentonite and modified bentonite.

4.4.5 Kinetic Experiments

The uptake of pesticide by bentonite and surfactant-bentonite (HDTMA and SDS) is examined at different time intervals and the results are shown in **Figure 4.15**.

As can be seen from the **Figure 4.15(a)** during the first 200 min of the experiment, the concentration of pesticides adsorbed on the bentonite and modified bentonite increases with the prolonged time. From 200 to 1400 min, no significant change of pesticides concentration is observed. The results indicate that the adsorption equilibrium is reached after only 200 min. Similarly, the adsorption of

pesticides on the bentonite and modified bentonite also occurs quickly and 4 h are enough to achieve the adsorption equilibrium.

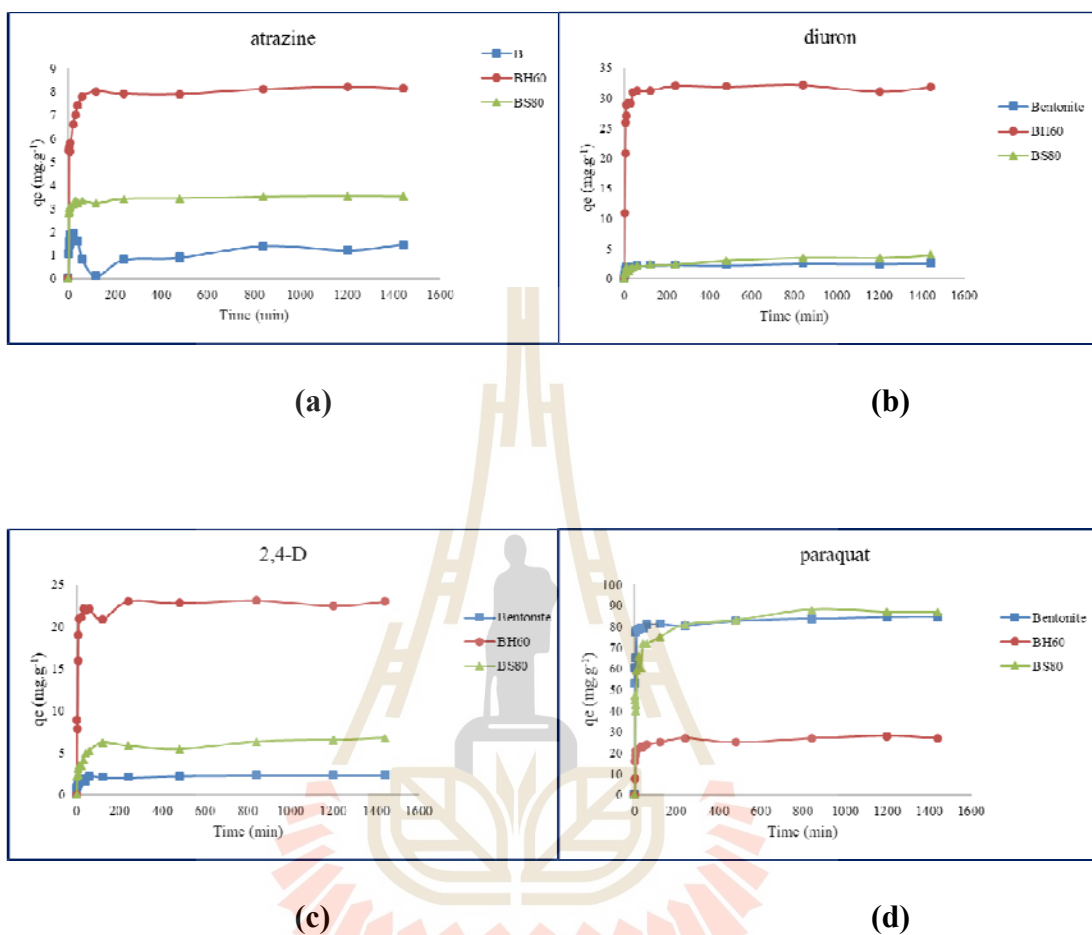


Figure 4.15 Effect of the contact time on the adsorption of atrazine (a), diuron (b), 2,4-D (c) and paraquat (d) on bentonite, BH60 and BS80.

Pseudo-first and pseudo-second order models were employed to correlate the kinetics data. A pseudo-first order kinetics adsorption model was suggested for the sorption of solid/liquid systems and is expressed in integrated and linear form **Equation (4.4)**

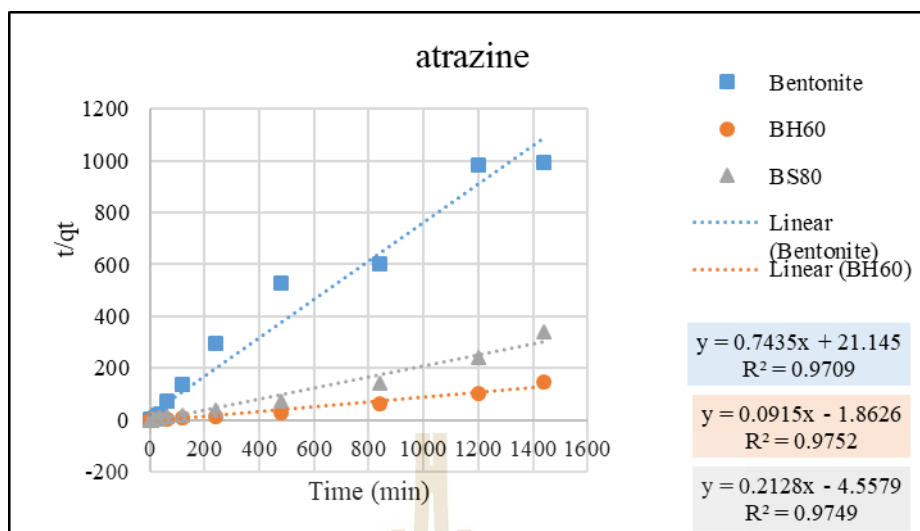
$$\log(q_e - q_t) = \log q_e - \frac{k_1}{2.303} t \quad (4.4)$$

Where, k_1 is the adsorption rate constant (min^{-1}); q_e and q_t are the atrazine adsorption loadings (mg.g^{-1}) at equilibrium and at time, t (min), respectively. If the pseudo-first-order kinetics is applicable, a plot of $\log(q_e - q_t)$ versus t should provide a straight line, from which k_1 and a predicted value for q_e can be determined from the slope and intercept of the plot.

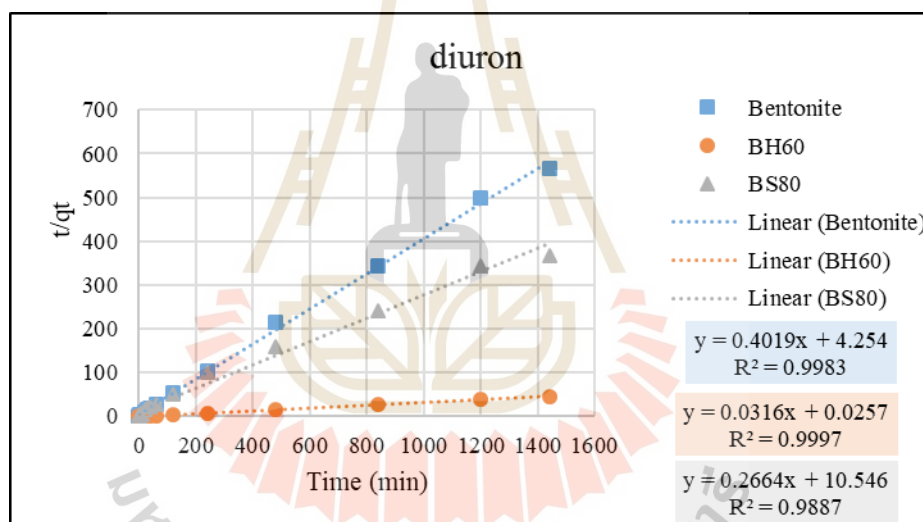
The pseudo-second-order equation is often successfully used to describe the kinetics of the adsorption process. Its expression is as follows;

$$\frac{t}{q_t} = \frac{1}{q_e} t + \frac{1}{k_2 q_e^2} \quad (4.5)$$

Where k_2 ($\text{g.mg}^{-1}.\text{min}^{-1}$) is the pseudo-second-order adsorption rate constant. A plot of t/q_t against t (**Figure 4.16**) yields a straight line, from which the rate constant K_2 and q_e can be calculated. The R^2 values for the pseudo-second order are greater than they are in the pseudo-first order model. These results suggest that adsorption obeys a pseudo-second order model indicating that the adsorption of pesticide occurs by a chemisorption mechanism, driven by electrostatic attraction between pesticide and adsorbent (Moradi, 2014; Shariati, Faraji, Yamini, and Rajabi, 2011).

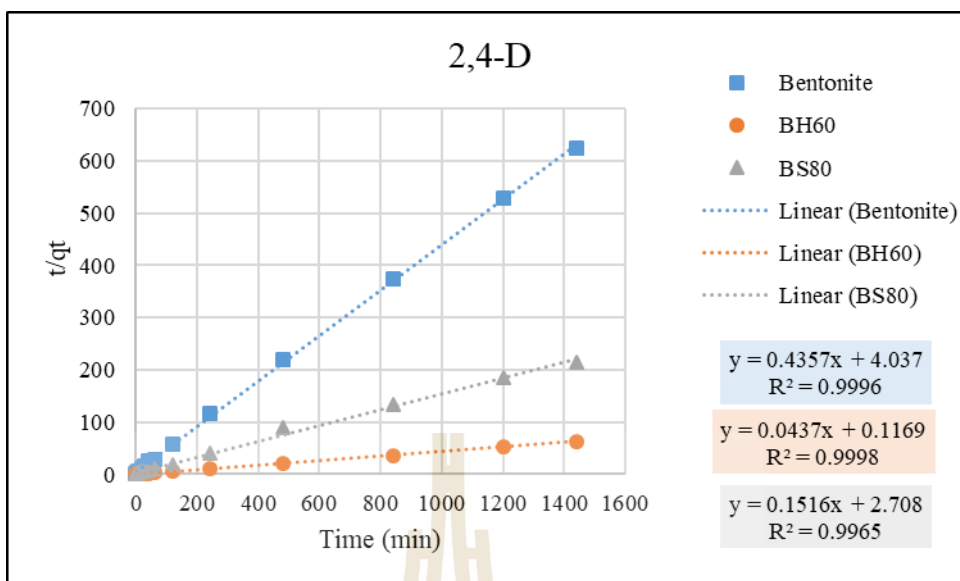


(a)

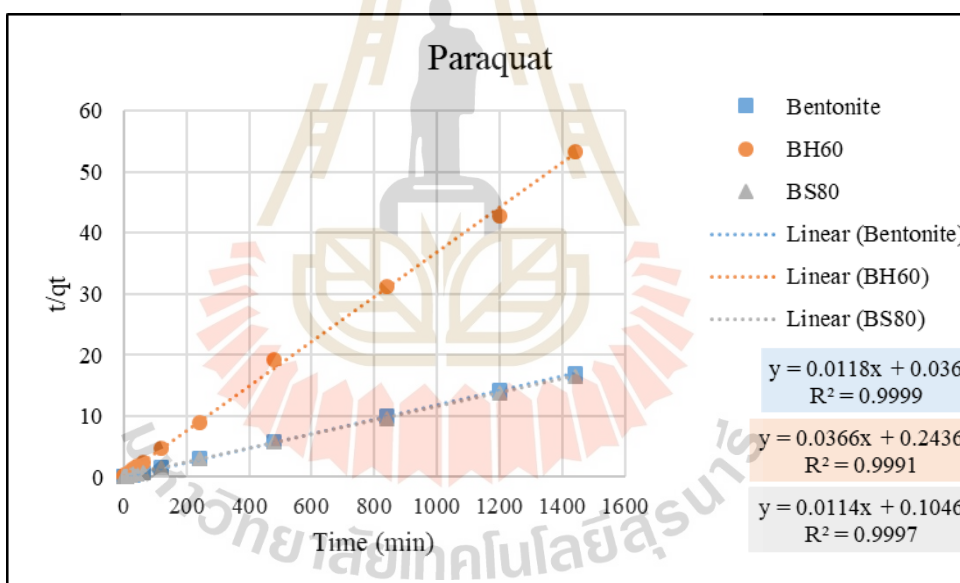


(b)

Figure 4.16 Pseudo-second order plots of atrazine (a) diuron (b) 2,4-D (c) and paraquat (d) adsorption onto bentonite and modified bentonites.



(c)



(d)

Figure 4.16 (Continued) Pseudo-second order plots of atrazine (a) diuron (b) 2,4-D (c) and paraquat (d) adsorption onto bentonite and modified bentonites.

Table 4.5 Kinetic model parameters obtained for the adsorption of atrazine (50 ppm) onto bentonite and modified bentonite adsorbents.

Samples	$q_{e,exp}$	pseudo-first order			pseudo-second order		
		q_e	k_1	R^2	q_e	k_2	R^2
B	2.89	0.692	5.0×10^{-4}	0.0515	1.34	2.6×10^{-2}	0.9709
BH60	8.12	1.417	1.8×10^{-3}	0.3648	10.93	-4.5×10^{-3}	0.9752
BS80	3.51	0.454	1.4×10^{-3}	0.2094	4.70	-9.9×10^{-3}	0.9749

Table 4.6 Kinetic model parameters obtained for the adsorption of diuron (50 ppm) onto bentonite and modified bentonite adsorbents.

Samples	$q_{e,exp}$	pseudo-first order			pseudo-second order		
		q_e	k_1	R^2	q_e	k_2	R^2
B	2.90	0.811	1.84×10^{-3}	0.6086	2.49	3.8×10^{-2}	0.9983
BH60	31.8	3.45	1.4×10^{-3}	0.2273	31.64	3.9×10^{-2}	0.9997
BS80	3.93	2.33	1.2×10^{-3}	0.6903	0.27	6.7×10^{-3}	0.9887

Table 4.7 Kinetic model parameters obtained for the adsorption of 2,4-D (50 ppm) onto bentonite and modified bentonite adsorbents.

Samples	$q_{e,exp}$	pseudo-first order			pseudo-second order		
		q_e	k_1	R^2	q_e	k_2	R^2
B	2.16	0.704	2.76×10^{-3}	0.6545	2.29	4.7×10^{-2}	0.9996
BH60	23	3.09	1.4×10^{-3}	0.2591	22.88	1.6×10^{-2}	0.9998
BS80	6.72	2.72	1.6×10^{-3}	0.5165	6.59	8.4×10^{-3}	0.9965

Table 4.8 Kinetic model parameters obtained for the adsorption of paraquat (200 ppm) onto bentonite and modified bentonite adsorbents.

Samples	$q_{e,exp}$	pseudo-first order			pseudo-second order		
		q_e	k_1	R^2	q_e	k_2	R^2
B	84.54	16.13	6.9×10^{-3}	0.7226	84.74	3.9×10^{-3}	0.9999
BH60	27.00	5.73	2.1×10^{-3}	0.4777	27.32	5.5×10^{-3}	0.9991
BS80	87.00	28.95	3.4×10^{-3}	0.8281	87.72	1.2×10^{-3}	0.9967

4.5 Conclusions

The effect of surfactant modification on the bentonite can change the surface properties of bentonite. HDTMA can change the hydrophilic to hydrophobic properties of bentonite with increase the adsorption capacity of natural atrazine and diuron. The increase in concentration of HDTMA can improve the 2,4-D adsorption capacity due to the positive head group of HDTMA bilayer able to interact with the negative charge of 2,4-D. For the SDS concentration loading does not affect the PQ^{2+} adsorption, because SDS on the surface of bentonite keeps a space for PQ^{2+} to penetrate to interlayer space for an occurrence of cationic exchange to bentonite. Moreover, the changing pH in solution that affect the pesticides adsorption.

4.6 Reference

- Aydin, M. E., Ozcan, S., and Beluk, F. (2009). Removal of lindane and dieldrin from aqueous solutions by montmorillonite and bentonite and optimization of parameters. **Fresenius' Environmental Bulletin** 18: 911-916.
- Bousbaa, S. N., Bougdahb, Messikhb N., and MagriAdsorption, P. (2018). Adsorption Removal of Humic Acid from Water Using a Modified Algerian Bentonite. **Physical. Chemistry. Research.** 6: 613-625.
- Castro, C. S., Guerreiro, M. C., Goncalves, M., Oliveira, L. C. A., and Anastacio, A. S. (2009). Activated carbon/iron oxide composites for the removal of atrazine from aqueous medium. **Journal of Hazardous Materials.** 164: 609-614.
- Chen, G. C., Shan, X. Q., Zhou, Y. Q., Shen, X. E., Huang, H. L., and Khan, S. U. (2009). Adsorption kinetics, isotherms and thermodynamics of atrazine on surface oxidized multiwalled carbon nanotube **Journal of Hazardous Materials.** 169: 912-918.
- Erdem, B., Özcan, A. S., and Özcan, A. (2010). Preparation of HDTMA-bentonite: Characterization studies and its adsorption behavior toward dibenzofuran. **Surface and Interface Analysis.** 42: 1351-1356.
- Gangula, S., Suen, S. -Y., and Conte, E. D. (2010). Analytical applications of admicelle and hemimicelle solid phase extraction of organic analytes. **Microchemical Journal.** 95: 2-4.
- González-Pradas, E., Socias-Viciano, M., Saifi, M., Ureña-Amate, M. D., Flores-Céspedes, F., Fernandez-Perez, M., and Villafranca-Sanchez, M. (2003). Adsorption of atrazine from aqueous solution in heat treated kerolites. **Chemosphere.** 51: 85-93.

- Houhoune, F., Nibou, D., Chegrouche, S., and Menacer, S. (2016). Behaviour of modified hexadecyltrimethylammonium bromide bentonite toward uranium species. **Journal of Environmental. Chemical. Engineering.** 4: 3459-3467.
- Kovaios, I. D., Paraskeva, C. A., and Koutsoukos, P. G. (2011). Adsorption of atrazine from aqueous electrolyte solutions on humic acid and silica. **Journal of Colloid and Interface Science.** 356: 277-285.
- Liu, P., and Zhang, LX. (2007). Adsorption of dyes from aqueous solutions of suspension with clay nano-adsorbents. **Separation and Purification Technology** 58: 32-39.
- Moradi, S. E. (2014). Microwave assisted preparation of sodium dodecyl sulphate (SDS) modified ordered nanoporous carbon and its adsorption for MB dye. **Journal of Industrial and Engineering Chemistry.** 20(1): 208-215.
- Nejati, K., Davary, S., and Saati, M. (2013). Study of 2,4-dichlorophenoxyacetic acid (2,4-D) removal by Cu-Fe-layered double hydroxide from aqueous solution. **Applied Surface Science.** 280: 67-73.
- Nones, J., Riella, H. G., Poli, A., Trentin, A. G., and Kuhnen, N. C. (2015). Thermal treatment of bentonite reduces aflatoxin b1 adsorption and affects stem cell death. **Material Science and Engineering.** 55: 530-537.
- Zadaka, D., Nir, S., Radian, A., and Mishael, Y. G. (2009). Atrazine removal from water by polycation-clay composites: effect of dissolved organic matter and comparison to activated carbon. **Water Research.** 43: 677-683.
- Zhang, C., Yan, J., Zhang, C., and Yang, Z. (2012). Enhanced adsorption of atrazine from aqueous solution by molecularly imprinted TiO₂ film. **Solid State Sciences.** 14: 777-781.

CHAPTER V

THE INFLUENCE OF ALKALI ACTIVATION ON BENTONITE AND MODIFIED BENTONITE FOR ADSORPTION OF PESTICIDES

5.1 Abstract

The adsorption of the pesticides (atrazine, diuron, 2,4-D and paraquat) on a alkali-bentonite activated with 0.25 and 0.5 M NaOH at various activation times was studied using batch experiments. The techniques of XRD, XRF, FTIR, BET, SEM and particle size analysis were used to investigate an effect of alkali treatments on physicochemical properties, structure and morphology of bentonite for adsorption of the pesticides. The adsorption results show that the adsorption capacity of paraquat is higher than that of atrazine, diuron and 2,4-D. The paraquat adsorption capacity depends on negative charge, hydrophilicity (low $\text{SiO}_2/\text{Al}_2\text{O}_3$) of the surface of bentonite. Therefore, the alkali concentration and activation time affect the paraquat adsorption.

5.2 Introduction

Bentonite is composed of diverse mineral substances, including quartz, cristobalite, feldspars, and several varieties of clay mineral. The major component of bentonite is montmorillonite, a dioctahedral smectite. Montmorillonite is a porous clay mineral consisting of a 2:1-layered structure, with alternating layers of exchangeable cations. The layers consist octahedral alumina sheets that are sandwiched by two tetrahedral silica sheets. Substituting Al^{3+} for Si^{4+} in the silica tetrahedral sheets and Mg^{2+} for Al^{3+} in the alumina octahedral sheets produces a net negative charge, which is usually balanced by adsorbed cations. These cations are easily replaced by either organic or inorganic cations, accounts for the unique hydrophilic, tumescent, and adsorption properties of montmorillonite (Park et al., 2016). Bentonite minerals have complex surface morphologies and provide a unique combination of properties, including thixotropic gel formation with water, good water adsorption capacity, large surface area, a layered structure and high cation exchange capability (CEC) (Choo and Bai, 2016; Murray, 2006). The bentonite has been widely used as adsorbent for removing pesticide in solution. The hydrophilicity and hydrophobicity have been received increasing attention due to its highly correlation with the adsorption properties of bentonite. Bentonite can change its surface hydrophilicity and hydrophobicity property with their $\text{SiO}_2/\text{Al}_2\text{O}_3$ ratio. Bentonite with lower $\text{SiO}_2/\text{Al}_2\text{O}_3$ ratio and hydrophilicity can be used for removal of cationic pesticide such as paraquat. The desilication can be accomplished by alkali treatment using NaOH (Abelló et al., 2009; Matias et al., 2011) or organic hydroxides. Thus, we are interested in modification of bentonite by alkali to develop a simple and effective way for adsorption cationic pesticide.

5.3 Material and Methods

5.3.1 Materials

Bentonite (B) was purchased from Thai Nippon Chemical Industry Co., Ltd. Reagent grade of atrazine (2-chlo-4-ethylamino-6-isopropylamine-5-triaine) , diuron (1,2-dimethyl-3,5-diphenylpyrazolium methyl sulfate) , 2,4-D (2,4-dichlorophenoxy acetic acid), paraquat (1,1'-dimethyl-4,4-bipyridinium dichloride), NaOH were obtained from Sigma.

5.3.2 Preparation of Modified Bentonite

Bentonite was sieved with 63 μm mesh and dried overnight at 110°C before using in the modification. The alkali-activated bentonite samples were obtained according to the following procedure, 4 g of bentonite was suspended in 100 mL NaOH at 0.25 and 0.5 M at 100°C for various activation time (x), (B_NaOH0.25_x and B_NaOH0.5_x). Next, the mixture was centrifuged and washed with deionised-water, then dried in an oven overnight at 110°C. The samples were stored in a desiccator

5.3.3 Characterization

The chemical compositions of the major elements in bentonite and modified bentonite were determined by energy dispersive. The interlayer spacings of the samples were determined by X-Ray diffraction patterns obtained from back-pressed powder samples recorded on a Bruker, D5005 Cu $K\alpha$ radiation, scanning from 5°–50° at a rate of 0.05°/s at 35 mV and 35 mA. The framework and OH groups were confirmed by FT-IR spectroscopy (Spectrum GX, Perkin-Elmer) as KBr discs, over the range of 4000–400 cm^{-1} . Specific surface and pore size distributions were evaluated by nitrogen gas adsorption at -196°C using automated volumetric equipment (Autosorb 1-Quantachrome). The particle size distributions (PDS) of all samples were

analysed by a Horiba laser-scattering particle-size-distribution analyser (LA-950) . Scanning electron micrographs (SEM) were taken on a ZEISS, model AURIGA. The samples were deposited on a sample holder with an adhesive carbon foil and sputtered with gold. Atrazine, diuron, 2,4-D and paraquat concentrations were determined using UV-visible spectrophotometry at 223, 247, 283 and 257 nm, respectively (T80+ UV-Vis spectrophotometer PG instruments).

5.3.4 Batch Adsorption

All adsorbents were dried overnight at 110°C prior to commencing the adsorption study. The adsorption experiments were performed by a batch adsorption procedure, using 20 mg of bentonite or alkali-bentonite added to 10 mL of pesticide solution, and then kept in a shaker bath at 30°C for 24 h. The stock solution was prepared in methanol solutions and finally methanol concentrations were less than 0.5% (v/v) to avoid co-solvent effects (Xiang Li, 2016). Suspensions were centrifuged at 3500 rpm then filtered. Either pesticides concentration in filtrates was determined by UV-Vis spectroscopy.

5.4 Results and Discussion

5.4.1 Characterization of Bentonite and Modified Bentonite

5.4.1.1 Chemical composition

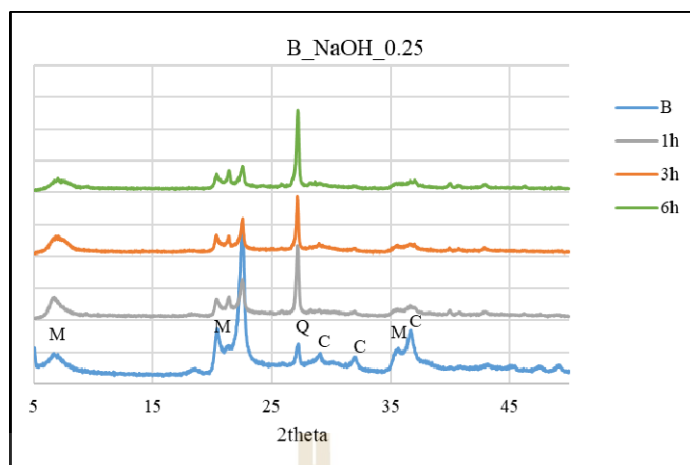
The compositions of bentonite and the modified bentonite with alkali (B_NaOH) at concentrations of 0.25, 0.5M and at various times are shown in **Table 5.1**. It indicates that SiO₂/Al₂O₃ ratio of all B_NaOH decreases from 8.29 to 6.15 except B_OH0.5_6h that increases to 13.93. The XRF values of SiO₂/Al₂O₃ ratio for the alkali bentonite confirm the desilication effects (Yong W, et. al. 2015). In addition, it was found that Na₂O content in the B_NaOH samples obviously increases and the increase in Na₂O is attributed to the residual reaction products of NaOH with bentonite.

Table 5.1 Chemical composition for bentonite and modified bentonite samples.

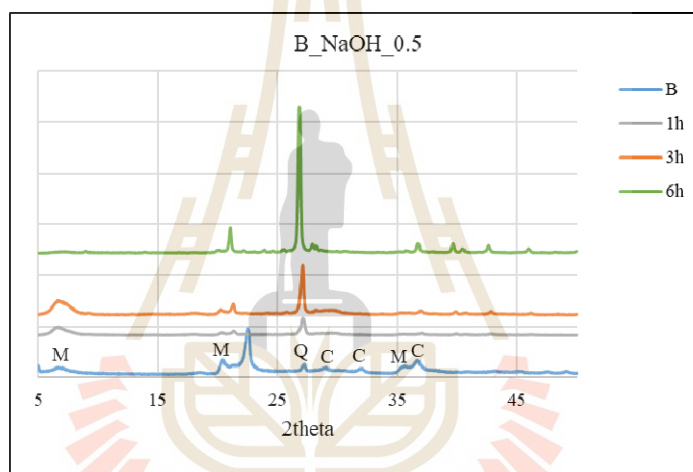
Sample	Chemical (%weight)									SiO ₂ /
	Na ₂ O	MgO	Al ₂ O ₃	SiO ₂	K ₂ O	CaO	TiO ₂	MnO	Fe ₂ O ₃	Al ₂ O ₃
Bentonite	0.079	0.607	9.472	78.543	1.703	2.813	0.788	0.045	4.239	8.29
B_NaOH0.25_1h	7.91	5.54	9.85	72.64	0.50	0.99	0.90	0.03	1.63	7.37
B_NaOH0.25_3h	10.58	5.08	11.22	69.04	0.46	0.97	0.69	0.03	1.91	6.15
B_NaOH0.25_6h	10.76	4.94	9.33	70.86	0.49	0.91	0.94	0.03	1.72	7.59
B_NaOH0.5_1h	10.19	4.04	9.10	71.75	0.55	0.88	1.46	0.04	1.99	7.88
B_NaOH0.5_3h	11.57	4.82	10.52	68.34	0.61	0.89	1.30	0.03	1.89	6.49
B_NaOH0.5_6h	9.33	3.56	5.58	77.78	0.62	0.65	1.51	0.021	0.941	13.93

5.4.1.2 XRD analysis

The XRD patterns of bentonite and alkali-activated bentonite samples were shown in **Figure 5.1(a)** and **(b)**. The bentonite shows characteristic diffraction peaks at $2\theta = 6.30, 19.77$ and 34.98 . Quartz (Q) and critobalite (C) impurities are observed in the patterns, the d_{001} reflection of bentonite at $2\theta = 6.30$ corresponds to d -spacing = 14.02 \AA . Alkali activation with mild concentration at various times was effect on the diffraction peaks of B_NaOH. The d_{001} reflection of B_NaOH0.25 shifts slightly from $2\theta = 6.30$ to $6.61, 6.34$ and 7.27 and basal spaces correspondingly shift from 14.02 to $13.36, 13.91$ and 12.15 \AA for reaction times at 1, 3 and 6 h, respectively. When concentration was increased to 0.5 M, the basal space changes from 14.02 to $13.62, 13.21$ and 12.25 \AA for activation times at 1, 3 and 6 h, respectively. Moreover, the intensity of the characteristic peak of montmorillonite (M) decreases but the peak of quartz (Q) increases with increasing activation times. The results suggest that the crystal structure of bentonite was partly changed after treated with NaOH solution.



(a)



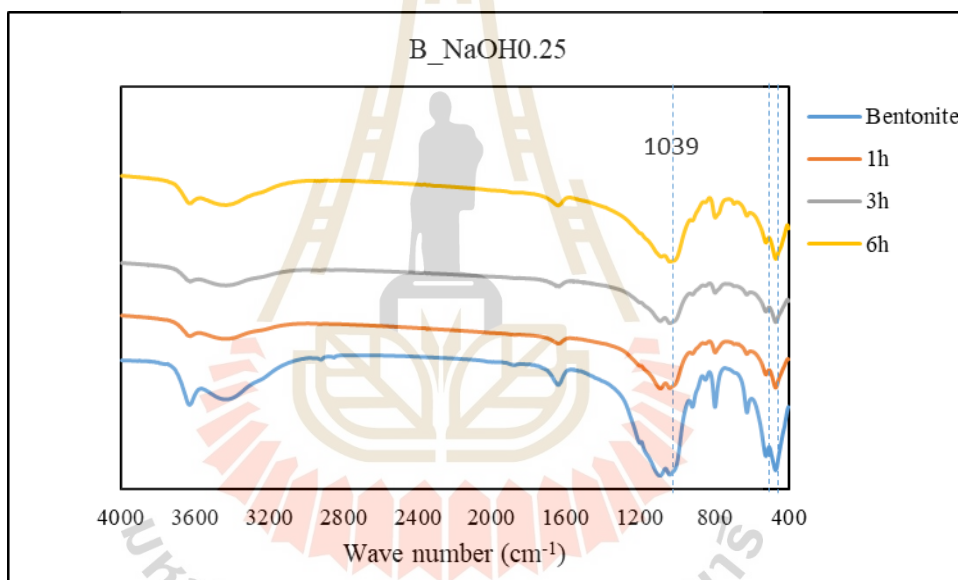
(b)

Figure 5.1 XRD patterns for bentonite and modified bentonite with 0.25M (a) and 0.5M NaOH (b) at various activation times. (Q = quartz; M = montmorillonite; C = cristobalite.)

5.4.1.3 FTIR analysis

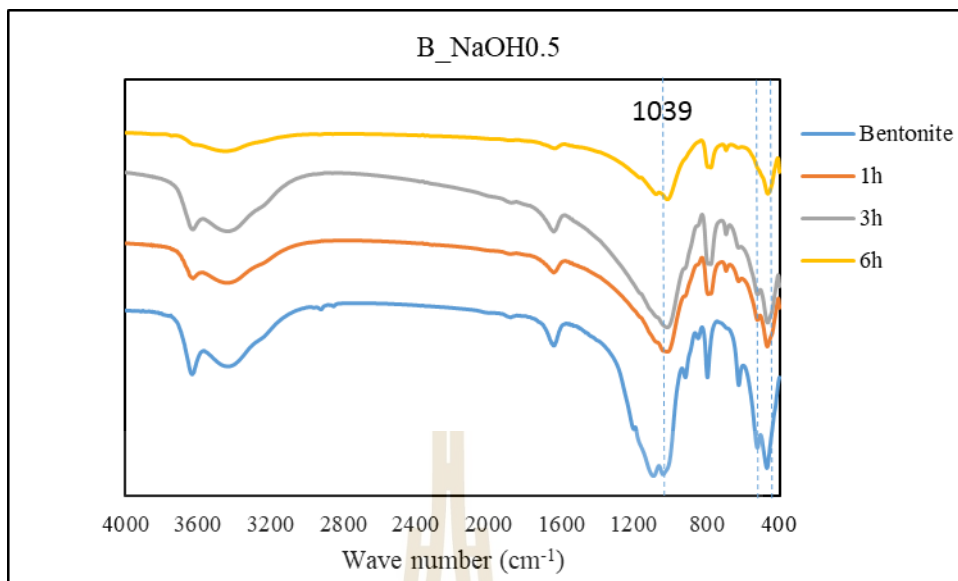
The FTIR spectrum (**Figure 5.2(a) and (b)**) was dominated by a Si-O-Si stretching band at 1039 cm^{-1} , with various intensities and shoulders. In the activated samples spectra, when concentration of NaOH was increased, the peak

position of Si-O-Si band progressively shifted to lower wavenumber. This phenomenon was likewise attributed to a decrease in $\text{SiO}_2/\text{Al}_2\text{O}_3$ ratio with increasing concentration of NaOH corresponding to XRF results (Table 5.1). Two bands at 520 and 469 cm^{-1} correspond to bending vibrations of Al-O-Si and Si-O-Si, respectively (Eren and Afsin, 2008). After treated with NaOH solution, these intensities of the bands decrease with increasing NaOH concentration, indicating the gradual removal of silica from the bentonite.



(a)

Figure 5.2 FT-IR spectra of bentonite and modified bentonite with 0.25M (a) and 0.5M NaOH (b) at various activation times.



(b)

Figure 5.2 (Continued) FT-IR spectra of bentonite and modified bentonite with 0.25M (a) and 0.5M NaOH (b) at various activation times.

5.4.1.4 Textural properties study

With high NaOH concentration has also a great influence on the specific surface area and pore volume of bentonite as summarized in **Table 5.2**. The BET surface area of the alkali-bentonite samples are apparently lower than that of bentonite, except B_NaOH0.5_3h with higher than bentonite. The pore volume of alkali-bentonite is larger than that of bentonite. Additionally, all of B_NaOH0.5 samples have smaller particle sizes than bentonite and B_NaOH0.25 and the mean particle sizes are shown in **Table 5.2**.

The zeta potential was determined to observe the changes in the surface charge of bentonite particles. The zeta potential of bentonite was -31.7 mV which increases slightly to -26.5, -30.3 and -30 mV for B_NaOH0.25_1h, B_NaOH0.25_3h, and B_NaOH0.5_1h, respectively, but decreases slightly to -32.9 for B_NaOH0.5_3h

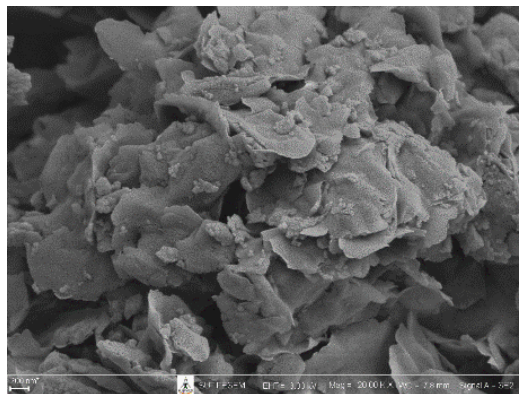
indicating that the sample of B_NaOH0.5_3h contains more amount of negative charge on the surface.

Table 5.2 Surface area, mean pore diameter, particle size and zeta potential of the bentonite and modified bentonite samples

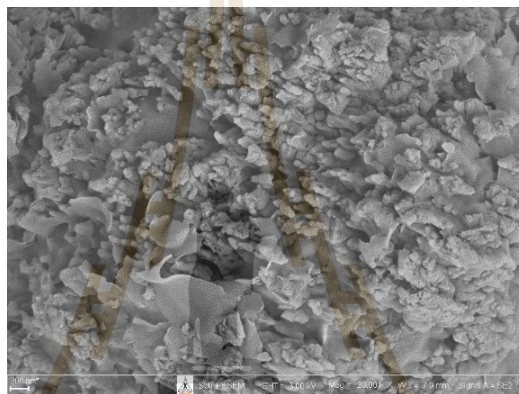
Main Characteristics	B	B_NaOH0.25			B_NaOH0.5		
		1 h.	3 h.	6h.	1h.	3h.	6h.
		Specific surface area (m ² /g)	31.76	32.70	27.02	24.80	19.20
Pore volume (cm ³ g ⁻¹)	0.1246	0.2348	0.1739	0.1401	0.2295	0.2152	0.2298
Mean particle size (μm)	7.15	8.28	8.06	9.33	6.92	6.14	6.24
Zeta potential (mV)	-31.7	-26.5	-30.3	0.33	-30.5	-32.9	-11.2

5.4.1.5 Surface morphology

The influence of 0.5 M NaOH activation on the morphology of bentonite at various times was observed by SEM (**Figure 5.3(a)-(c)**). As can be seen that, the bentonite exhibits a typical layered structure with a smooth surface and leafy appearance. After modification with 0.5 M NaOH at 3 hours (**Figure 5.3(b)**), some layer structures were broken and aggregated. Moreover, the alkali activation at 0.5M NaOH for 6 hours (**Figure 5.3(c)**), it shows a closely packed texture and exists a crystal of the adsorbent which corresponds to XRD patterns in **Figure 5.1(b)**.



(a)



(b)



(c)

Figure 5.3 SEM micrographs of bentonite (a) and modified bentonite with 0.5M NaOH 3 h (b) 0.5M NaOH 6 h (c)

5.4.2 Effect of alkali-activation on adsorption of pesticides.

Figure 5.4 shows the quantities of the pesticide adsorbed on the alkali-bentonite. The figure shows that the alkali-bentonite can adsorb paraquat more than atrazine, diuron and 2,4-D. The high adsorption of paraquat (PQ^{2+}) is described that the attraction of positive charge of paraquat and high negatively charged surface of B_NaOH0.25_3h and B_NaOH0.5_3h (see **Table 5.2**). While, 2,4-D is present in anion form resulting in repulsion between the negative charge on alkali-bentonite surface and the anion of 2,4-D. Moreover, SiO_2/Al_2O_3 of the alkali-bentonite is lower than that of bentonite (**Table 5.1**), indicating that hydrophilic properties of alkali-bentonite is lower than bentonite. Thus, the adsorptions of atrazine and diuron are very low because they prefer to hydrophobic site on the surface.

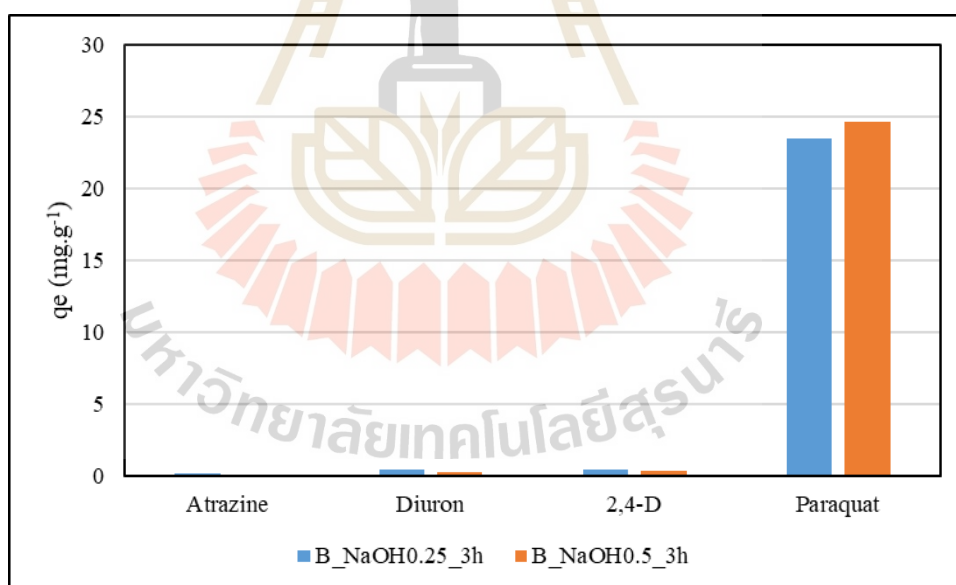


Figure 5.4 Effect of NaOH concentration with activation time of 3 hours on adsorption capacity of pesticide (50 ppm) at $pH 6 \pm 0.5$.

Figure 5.5 shows the quantities of PQ^{2+} adsorbed on the alkali-bentonite at 0.25 and 0.5 M NaOH for various activation times. It was found that the high adsorption of PQ^{2+} appeared in the sample of B_NaOH0.5_3h and the lowest adsorption of PQ^{2+} is in B_NaOH0.5_6h. The high amount of adsorbed PQ^{2+} on B_NaOH0.5_3h corresponds to the high negatively charged surface with zeta potential of -32.9mV, high surface area ($43.10 \text{ m}^2 \cdot \text{g}^{-1}$), small particle size ($6.14 \mu\text{m}$) and lower ratio of $\text{SiO}_2/\text{Al}_2\text{O}_3$ (6.49) increasing hydrophilic property more than B_NaOH0.5_6h sample.

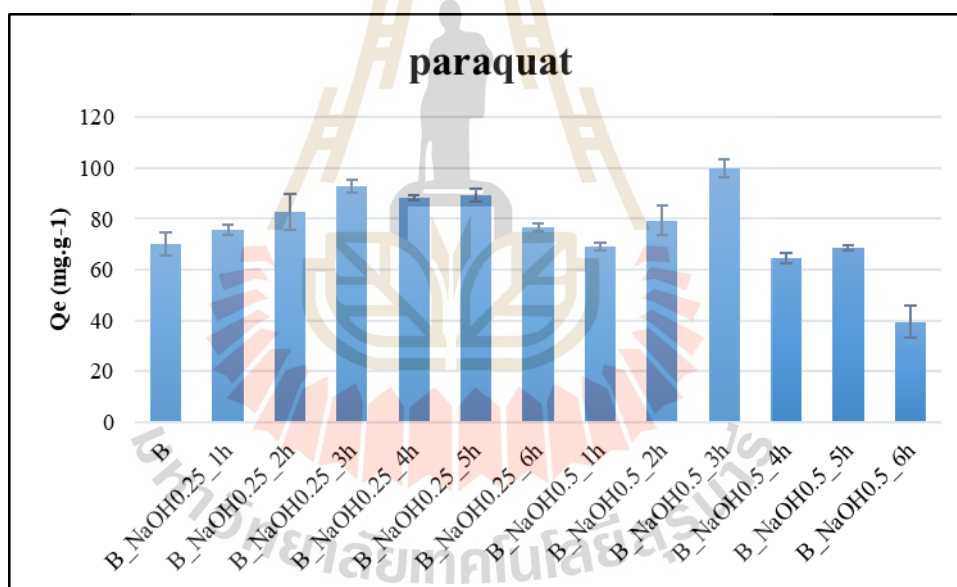


Figure 5.5 Effect of NaOH concentration at various activation times on adsorption capacity of paraquat (200 ppm) at $\text{pH } 6 \pm 0.5$.

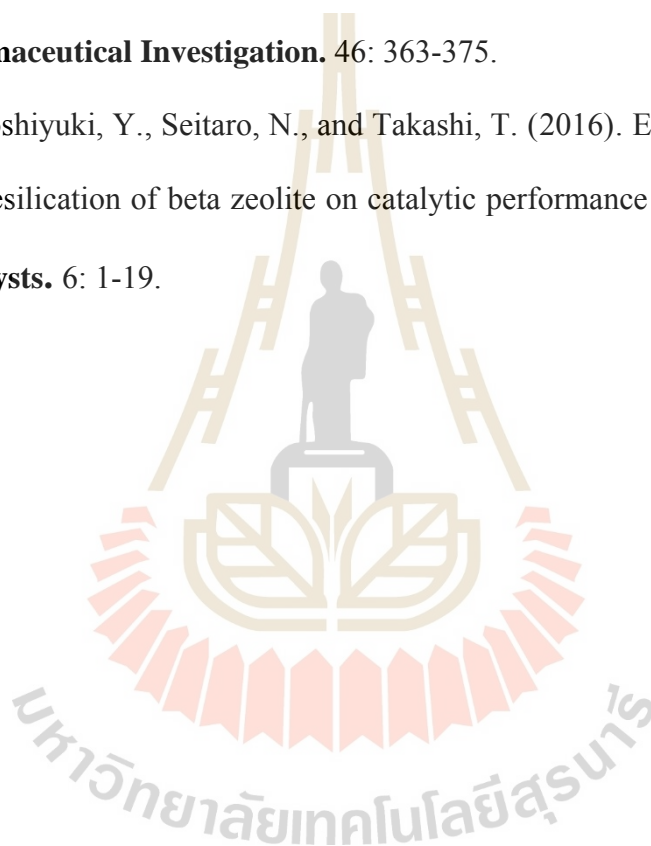
5.5 Conclusion

The effect of alkali treatment on the textural and structural properties of bentonite shows some physical changes clearly which affects in the potential adsorption capability. The results of these experiments indicate that the highest adsorption of PQ^{2+} appears in the sample of B_NaOH0.5_3h despite the alkali treatment applied to the bentonite. The amount of adsorbed PQ^{2+} on B_NaOH0.5_3h corresponds to the high negatively charged surface, high surface area, small particle size and low SiO_2/Al_2O_3 .

5.6 Reference

- Abelló, S., Bonilla, A., and Pérez-Ramírez, J. (2009). Mesoporous ZSM-5 zeolite catalysts prepared by desilication with organichydroxides and comparison with NaOH leaching, **Applied Catalysis A: General**. 364: 191-198.
- Choo, K. Y., and Bai, K. (2016). The effect of the mineralogical composition of various bentonites on CEC values determined by three different analytical methods. **Applied Clay Science**. 126: 153-159.
- Eren, E., and Afsin, B. (2008). An investigation of Cu(II) adsorption by raw and acid-activated bentonite: a combined potentiometric, thermodynamic, XRD, IR, DTA study. **Journal of Hazardous Materials**. 151: 682-691.
- Matias P., Couto C. S., Graça I., Lopes J. M., Carvalho A. P., and Ribeiro F. R. (2011). Desilication of a ton zeolite with NaOH: influence on porosity, acidity and catalytic properties, **Applied Catalysis. A Gen**. 399: 100-109.

- Paria, S., and Khilar, K. C. (2004). A review on experimental studies of surfactant adsorption at the hydrophilic solid–water interface. **Advances in Colloid and Interface Science**. 110(3): 75-95.
- Park, J-H., Shin, H-J., Kim, M. H., Kim, J-S., Kang, N., Lee, J-Y., Kim, K-T., Lee, J. I., and Kim, D-D. (2016). Application of montmorillonite in bentonite as a pharmaceutical excipient in drug delivery systems. **Journal of Pharmaceutical Investigation**. 46: 363-375.
- Yong, W., Toshiyuki, Y., Seitaro, N., and Takashi, T. (2016). Effect of dealumination and desilication of beta zeolite on catalytic performance in n-hexane cracking. **Catalysts**. 6: 1-19.

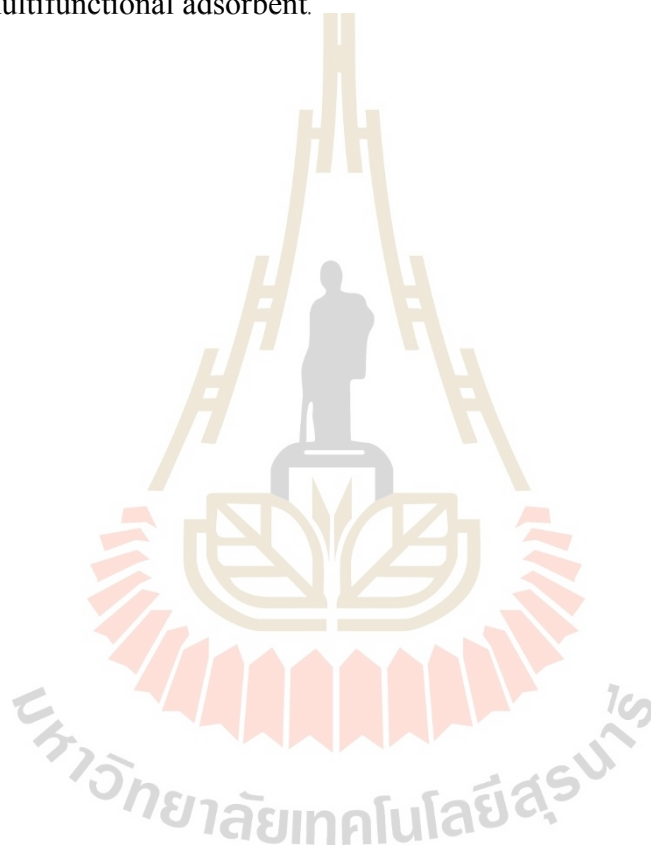


CHAPTER VI

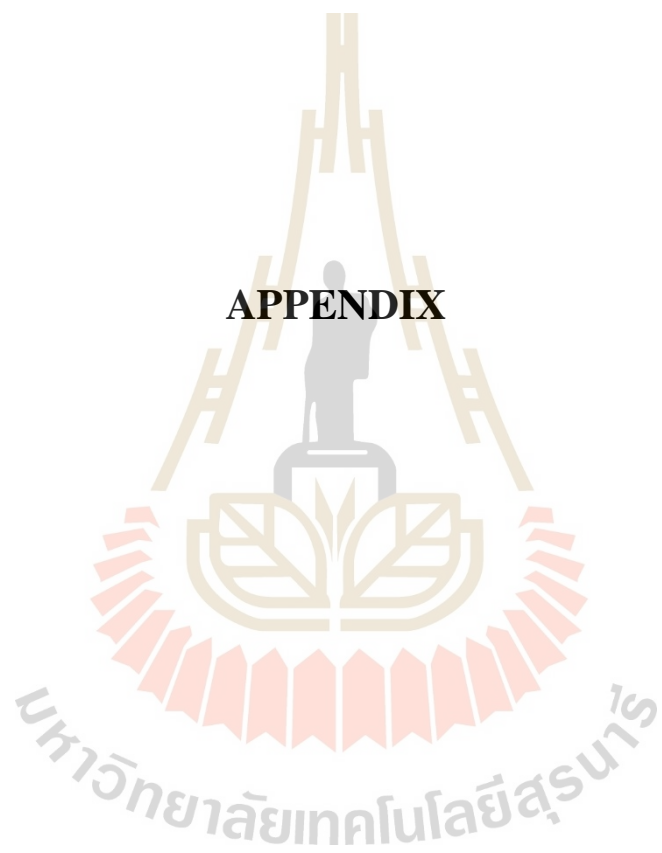
CONCLUSION

Modified bentonite with different method was investigated. The modified bentonite consisted of acid heat surfactant and alkali for pesticides adsorption. The pesticides were atrazine, diuron, 2,4-D and paraquat in the solution. The experimental of the surface modification by combination with acid and heat, it was found that the sequence of treatments has a strong effect on atrazine adsorption. Modified bentonite exhibits atrazine removal efficiency greater than bentonite; the BC₅₀₀A_{0.5} sample provides the maximal adsorption capacity at pH 6.0±0.5 as a result of it containing high active Al Lewis-acid sites, and Si-OH and Si-OH₂⁺ groups present on edges and faces. Moreover, BC₅₀₀A_{0.5} was found to be an effective as multifunctional adsorbent for the simultaneous pesticides removal from aqueous solution. In the case of bentonite and organo-bentonite (HDTMA-bentonite and SDS-bentonite), The increase in concentration of HDTMA can improve hydrophobic properties to remove the diuron and atrazine from aqueous solution. While, the 2,4-D adsorption capacity due to the positive head group of HDTMA bilayer able to interact with the negative charge of 2,4-D. For the SDS concentration loading does not affect the PQ²⁺ adsorption. In addition, the alkali-bentonites were able to treat with 0.25M and 0.5M NaOH at 1, 2, 3, 4, 5 and 6 hours. The bentonite was modified with 0.5M for 3 hours that suitable for removal of paraquat from aqueous solution when compare with bentonite. Because of

increase the negative charge of zeta potential (-32.9mV), high surface area ($43.10 \text{ m}^2 \cdot \text{g}^{-1}$), small particle size ($6.14 \text{ }\mu\text{m}$) and small $\text{SiO}_2/\text{Al}_2\text{O}_3$ (6.49) increase hydrophilic property for paraquat adsorption. Thermal and acid treatments, organo-bentonite and alkali-bentonite to enhance the adsorption performance of the adsorbent offer a number of benefits as low costs, easy implementation and low chemical consumption, including for using as multifunctional adsorbent.



APPENDIX



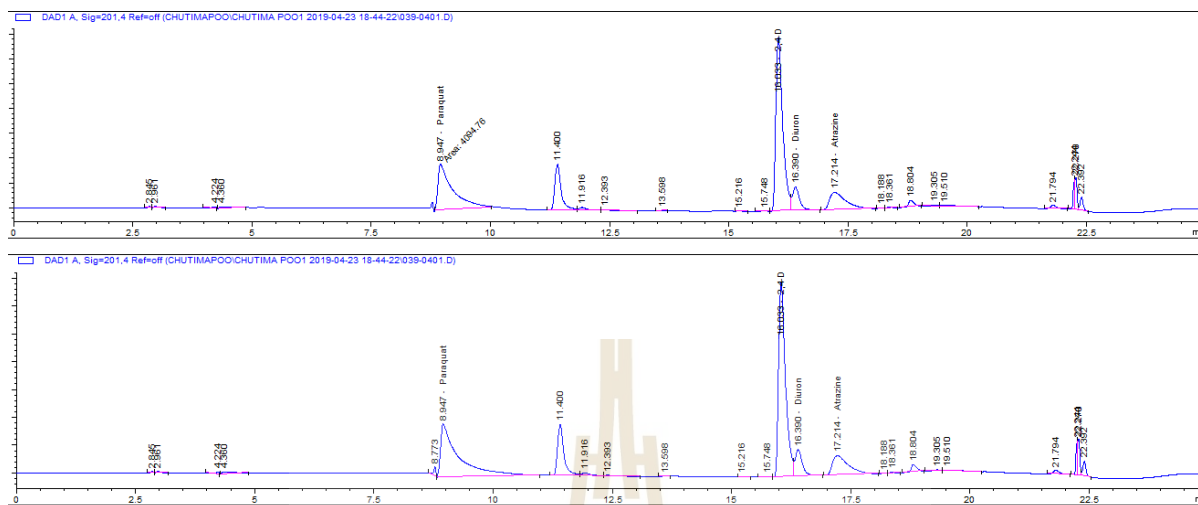


Figure A1 HPLC chromatograms of mixing standards of paraquat, 2,4-D, diuron and atrazine in 50 ppm.

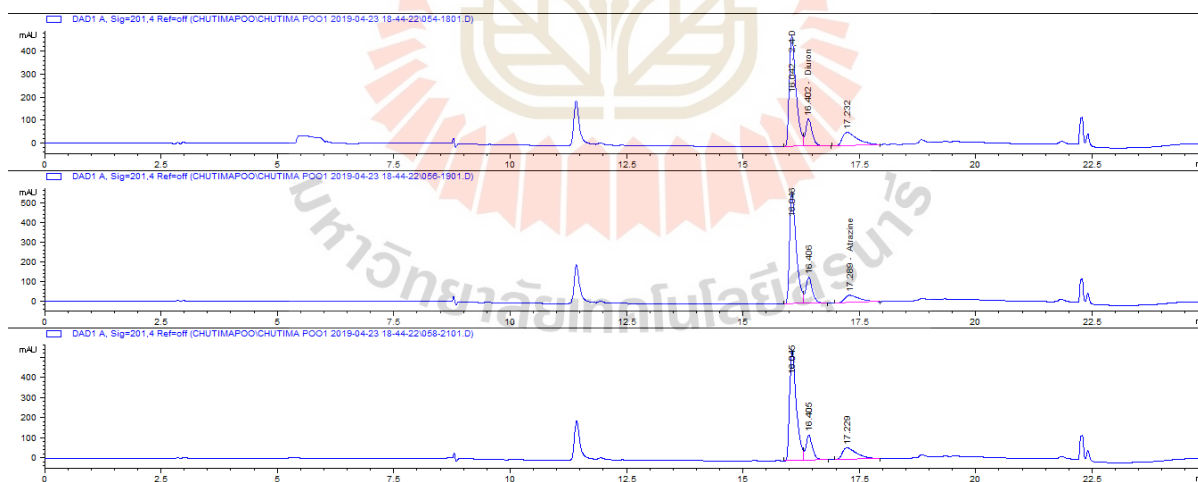


Figure A2 HPLC chromatograms of bentonite adsorption of paraquat, 2,4-D, diuron and atrazine in mixing pesticides solution at 50 ppm.

CURRICULUM VITAE

Name Mrs. Chutima Pluangklang **Date of Birth** October 08, 1976

Place of Birth Nakhon Ratchasima, Thailand

Education;

1999 Bachelor of Science (Chemistry), B.Sc. (Chemistry) Kasetsart
University, Bangkok, Thailand

2006 Master of Science (Chemistry), M.Sc. (Chemistry)
Suranaree University of Technology, Nakhon Ratchasima, Thailand

Grants and Fellowships; The Government Officers Development Scholarship,
funded by National Science and Technology Agency (NSTDA), for financial support.

Position and Place of Work; Lecturer at Faculty of Science and Technology,
Nakhon Ratchasima Rajabhat University, Nakhon Ratchasima, Thailand

Presentation

2015 Poster presentation "AMAM 2015" Italy June, 7-12, 2015

2019 Poster presentation "PACCON 2019", Bangkok, Thailand
February 7-8, 2019,